# SUBTASK 2.2 – FINE PARTICULATE ($PM_{2.5}$) CHARACTERIZATION AND SOURCE APPORTIONMENT

Final Report

*For the period of April 15, 1998, through November 30, 2004*

*Prepared for:*

AAD Document Control

U.S. Department of Energy
National Energy Technology Laboratory
PO Box 10940
Pittsburgh, PA 15236-0940

DOE Cooperative Agreement No. DE-FC26-98FT40320
Performance Monitor: Sara Pletcher

*Prepared by:*

Steven A. Benson
Charlene R. Crocker
John R. Gallagher
Alena Kubatova
Ye Zhuang
Kevin D. Galbreath
Kurt E. Eylands
Robert R. Jensen
Jason D. Laumb
Donald P. McCollor
Stanley J. Miller
Michelle M. Olderbak
Brian S. Helmowski

Energy & Environmental Research Center
University of North Dakota
PO Box 9018
Grand Forks, ND 58203-9018

05-EERC-01-04 January 2005

## DOE DISCLAIMER

This report was prepared as an account of work sponsored by an agency of the United States Government. Neither the United States Government, nor any agency thereof, nor any of their employees makes any warranty, express or implied, or assumes any legal liability or responsibility for the accuracy, completeness, or usefulness of any information, apparatus, product, or process disclosed or represents that its use would not infringe privately owned rights. Reference herein to any specific commercial product, process, or service by trade name, trademark, manufacturer, or otherwise does not necessarily constitute or imply its endorsement, recommendation, or favoring by the United States Government or any agency thereof. The views and opinions of authors expressed herein do not necessarily state or reflect those of the United States Government or any agency thereof.

This report is available to the public from the National Technical Information Service, U.S. Department of Commerce, 5285 Port Royal Road, Springfield, VA 22161; phone orders accepted at (703) 487-4650.

## ACKNOWLEDGMENT

This report was prepared with the support of the U.S. Department of Energy (DOE) National Energy Technology Laboratory Cooperative Agreement No. DE-FC26-98FT40320. However, any opinions, findings, conclusions, or recommendations expressed herein are those of the authors(s) and do not necessarily reflect the views of DOE.

## EERC DISCLAIMER

LEGAL NOTICE. This research report was prepared by the Energy & Environmental Research Center (EERC), an agency of the University of North Dakota, as an account of work sponsored by the U.S. Department of Energy. Because of the research nature of the work performed, neither the EERC nor any of its employees makes any warranty, express or implied, or assumes any legal liability or responsibility for the accuracy, completeness, or usefulness of any information, apparatus, product, or process disclosed, or represents that its use would not infringe privately owned rights. Reference herein to any specific commercial product, process, or service by trade name, trademark, manufacturer, or otherwise does not necessarily constitute or imply its endorsement or recommendation by the EERC.

## SUBTASK 2.2 – FINE PARTICULATE ($PM_{2.5}$) CHARACTERIZATION AND SOURCE APPORTIONMENT


### ABSTRACT

Particulate matter (PM) in the air is of considerable environmental interest because of research correlating exposure of ambient levels of fine particulate matter ($PM_{2.5}$) with acute respiratory and cardiovascular distress. The PM of interest consists of two forms—primary PM emitted directly from a source and secondary PM formed in the atmosphere. PM may be organic (soot, polycyclic aromatic hydrocarbons), inorganic (metals, sulfates, nitrates), or combinations of both organic and inorganic constituents. The overall of goal of the $PM_{2.5}$ program at the Energy & Environmental Research Center is to develop advanced sampling and analysis methodologies for PM that can be used for source apportionment and assist in health studies. Specific objectives include 1) developing extraction methods and toxicology tests to identify and evaluate the organic fraction of common air PM, 2) developing characterization methods to evaluate and source apportion the inorganic composition of PM, 3) performing toxicological assays of select PM samples to correlate the results with live animal studies, 4) characterizing and determining the sources of indoor air particle in a research facility, and 5) determining the impact of candle burning on indoor air quality. This work has been carried out in three activities.

In Activity 1, subcritical water was used for the extraction and fractionation of organic atmospheric particulate. Two types of carbonaceous aerosol, diesel exhaust particulate (a relatively nonpolar matrix) and wood smoke particulate (a polar matrix), were sequentially extracted using subcritical water at temperatures ranging from 25° to 300°C. The importance of each fraction was evaluated using two bacterial culture systems—the Polytox™ respiration test and the genotoxicity SOS-Chromotest—and two mammalian systems—the in vitro cytotoxicity test and the hepatic mitochondrial respiration test. The results from the toxicity tests were related to the composition of individual fractions.

In Activity 2, several particulate monitoring and collection devices, automated scanning electron microscopy, and cluster analysis were used to characterize particulate collected from one urban and three rural sampling sites. The analyses showed contributions of vegetation and fugitive dust from gravel roads and agriculture to the ambient $PM_{2.5}$ present at all locations. Samples collected at sites downwind of high-temperature combustion facilities also contained fine, spherical iron–silica and calcium aluminosilicate particles indicative of combustion fly ash. Particle morphology was key to separating such particles from the ubiquitous carbonate-based fugitive dust and soil clays. In toxicological assays performed on bacteriophage deoxyribonucleic acid (DNA) exposed to coarse and fine lignite-derived ash, both ashes showed significant activity in catalyzing DNA strand breakage.

In Activity 3, particle size and mass loading instruments were used to characterize the $PM_{2.5}$ content of indoor air in several areas of a research facility and of burning candles. Enrichments of sulfur, iron, silicon, and calcium in indoor aerosols were observed in the large submicron fraction. The PM levels in indoor air are influenced by indoor activities and the outdoor environment. One of those indoor activities, burning paraffin or soy wax candles,

contributes high levels (at least $10^8$ times) of fine particulate (soot) to the area immediately around the candle. The candle type—shape, additive, formulation—influences the emissions, which are from vaporization and condensation of volatile wax compounds as well as pyrolysis products.

## TABLE OF CONTENTS

LIST OF FIGURES ..... iv

LIST OF TABLES ..... x

NOMENCLATURE ..... xi

EXECUTIVE SUMMARY ..... xii

ACTIVITY 1 – FRACTIONATION OF ORGANICS FROM AIR PARTICULATES WITH SUBCRITICAL WATER ..... 1
- Introduction ..... 1
  - Evaluation of Toxicity of Agricultural Soils ..... 2
- Experimental ..... 2
  - Sample Material ..... 2
  - Subcritical Water Fractionation ..... 2
    - Fractionation of Common PM Samples ..... 2
    - Application of Subcritical Water Extraction–Fractionation to Ambient Aerosol Samples ..... 3
    - Subcritical Water Fractionation and Comparison to Solvent Extraction in Relation to Composition ..... 3
  - Toxicity Tests ..... 3
    - Polytox™ ..... 3
    - Cytotoxicity Test ..... 4
    - SOS-Chromotest ..... 4
    - Mitochondrial Respiration Assay ..... 5
  - Chemical Characterization ..... 5
    - Elemental Analysis ..... 5
    - Gas Chromatographic Analysis ..... 6
- Results and Discussion ..... 6
  - Toxicity of Wood Smoke Particulate ..... 6
  - Toxicity of Diesel Exhaust Particulate ..... 7
  - Characterization and Possible Relationship to Toxicity Results ..... 10
    - Elemental Analysis ..... 11
  - GC–MS and GC–FID Analysis ..... 13
  - Metal Analysis ..... 13
- Application of Subcritical Water Fractionation to Ambient Aerosol Samples ..... 15
- Application of Subcritical Water Fractionation to Pesticide-Contaminated Soil ..... 15
  - Cytotoxicity of Pesticides ..... 15
  - Comparison of Cytotoxicity in Extracts Obtained by Subcritical Water and Organic Solvent Extraction ..... 15

Continued. . .

**TABLE OF CONTENTS (continued)**


Conclusions ..... 17
References ..... 20

ACTIVITY 2 – SAMPLING AND ANALYSIS OF FINE PARTICULATE MATTER ($PM_{2.5}$) ..... 22
Activity 2.1 – Characterization of the Inorganic Fraction ..... 22
Objectives ..... 22
Experimental ..... 22
Burkard Sampler ..... 22
Fine Particulate Matter Sampling ..... 23
TEOM–ACCU ..... 23
SAS ..... 23
APS–SMPS ..... 24
Analytical Scanning Electron Microscopy Methods ..... 24
Multivariate Analysis ..... 26
Evaluation of APS–SMPS to Measure Atmospheric $PM_{2.5}$ ..... 26
Sample Collection Media ..... 27
Sampling Site Descriptions ..... 27
North Dakota Urban Site (Site 4) ..... 27
Minnesota Farm Site (Site 3) ..... 28
North Dakota Farm Site (Site 1) ..... 28
North Dakota Ranch Site (Site 2) ..... 29
Dispersion Modeling ..... 29
Results and Discussion ..... 30
SEM Analytical Methods ..... 30
Evaluation of APS–SMPS to Measure Atmospheric $PM_{2.5}$ ..... 31
Grand Forks (Site 4) ..... 31
Minnesota Farm Site (Site 3) ..... 33
Comparison of SAS, TEOM, and APS Measurements ..... 33
Comparison of ACCU and Burkard Data ..... 34
Weather and PM Loading ..... 39
North Dakota Farm Site (Site 1) ..... 39
Comparison of ACCU and Burkard Data ..... 39
Weather Conditions ..... 41
North Dakota Ranch Site (Site 2) ..... 42
Weather Conditions ..... 42
Dispersion Modeling ..... 44
Ternary Diagram Analysis ..... 45
Northwesterly Wind Conditions ..... 46
Southerly Wind Conditions ..... 47


Continued. . .

**TABLE OF CONTENTS (continued)**


Easterly Wind Conditions ..... 51
Results from the Magnetic Sampler ..... 51
Comparison of Particulate Matter Compositions from Sampling Sites 1–4 ..... 53
North Dakota Site 4 Data ..... 55
Minnesota Site 3 Data ..... 55
North Dakota Site 1 Data ..... 55
Unclassified Particles ..... 57
Conclusions ..... 59
References ..... 59
Bibliography ..... 60
Activity 2.2 – DNA Breakage Catalyzed by Coal-Derived Air Particulates ..... 61
Introduction ..... 61
Methods ..... 61
Results ..... 62
References ..... 63

ACTIVITY 3 – INDOOR AIR QUALITY ..... 64
Activity 3.1 – Characterization of Indoor Air Quality ..... 64
Introduction ..... 64
Objective ..... 65
Experimental ..... 65
Results and Discussion ..... 65
APS and SMPS Measurement ..... 65
TEOM Measurement ..... 69
Chemical and Morphological Analyses ..... 71
Conclusions ..... 74
References ..... 74
Activity 3.2 – Source of Indoor Air Pollution—Burning Candles ..... 75
Introduction ..... 75
Objectives ..... 76
Experimental ..... 76
Candle Selection ..... 76
Experiment Setup ..... 76
Sampling and Chemical Analysis ..... 78
Results and Discussion ..... 79
Particle Emissions and Size Distributions ..... 79
Chemical Analysis on Candle Emissions ..... 84
Morphological Analysis ..... 88
Conclusions ..... 91
References ..... 91

## LIST OF FIGURES


I-1 The results from bacterial toxicity tests performed on wood smoke particulate fractions obtained sequentially at 25°–300°C. a) Bacterial respiration (Polytox™) 5% of each extract, b) Genotoxicity (0.5%) ....7

I-2 The results from toxicity tests performed on wood smoke particulate fractions obtained sequentially at 25°–300°C. a) Cytotoxicity 1% of each extract compared to acrolein, b) Mitochondrial respiration (5%) compared to effect of DMSO ....8

I-3 The results from bacterial toxicity tests performed on diesel exhaust particulate fractions obtained sequentially at 25°–300°C. a) Bacterial respiration (Polytox™) 5% of each extract, b) Genotoxicity (0.5%) ....9

I-4 The results from bacterial toxicity tests performed on diesel exhaust particulate fractions obtained sequentially at 25°–300ºC. a) Cytotoxicity 1% of each extract compared to acrolein, b) Mitochondrial respiration (5%) compared to the effect of DMSO ....10

I-5 CHN and sulfur determination on diesel exhaust and wood smoke particulate fractions extracted sequentially with subcritical water at 25°–300°C ....11

I-6 Determination of extracted mass, total organic carbon, carbon, and estimates of organic compound mass of wood smoke and diesel exhaust particulate fractions extracted sequentially with subcritical water at 25°–300°C ....12

I-7 Concentrations of wood smoke particulate organics in subcritical water extracts collected sequentially at 25°–300°C ....13

I-8 Determination of metals in diesel exhaust particulate using ICP–MS ....14

I-9 Comparison of extraction efficiencies of pesticides using organic solvent extraction and subcritical water fractionation....16

I-10 SWF of pesticides from soil (2 g) ....17

I-11 Mass of material and pesticides extracted from soil using subcritical water fractionation followed by solvent extraction of residue, and using organic solvent extraction directly ....18

I-12 Cytotoxicity (% control cell viability of mammalian COS cells) of pesticides....18


Continued. . .

## LIST OF FIGURES (continued)


I-13 Comparison of the cytotoxicity in soil extracts (2 g) obtained with SWF followed by solvent extraction of residue, and organic solvent (methylene chloride/acetone [2:1]) extraction. Standard deviations are based on quadruplicate experiments. Top: Cytotoxicity in relation to the mass of material extracted in assay. Bottom: Cytotoxicity in relation to the mass of pesticides extracted in assay ..... 19

II-1 $PM_{2.5}$ sampling locations and major point sources ..... 28

II-2 Comparison of $PM_{2.5}$ to $PM_{10}$ fraction collected at the Energy & Environmental Research Center, August 29–31, 1999 ..... 30

II-3 SEM characterization of the $PM_{10}$ and $PM_{2.5}$ fractions ..... 31

II-4 SEM characterization of the $PM_{10}$ and $PM_{2.5}$ fractions at Site 4 (Grand Forks urban site) ..... 32

II-5 SAS, TEOM, and APS $PM_{2.5}$ loadings at Site 3 (Minnesota farm), May 24 to June 17, 2000 ..... 33

II-6 APS particle size distribution at Site 3 (Minnesota farm), May 17, 2000 ..... 34

II-7 SEM characterization of Burkard sample data collected at Site 3 (Minnesota farm) under a light northeasterly wind, May–June 2000, where the second pie chart shows the results of the cluster analysis on the unclassified fraction ..... 35

II-8 Classification of particles a) >2.5 µm and b) <2.5 µm collected at Site 3 (Minnesota farm), May 24–30, 2000 ..... 35

II-9 Mineral phases from ACCU filter samples collected at Site 3 (Minnesota farm), May–June 2000 ..... 37

II-10 Nitrate frequency distribution from SEM characterization of ACCU filter samples collected at Site 3 (Minnesota farm), May–June 2000 ..... 38

II-11 Sulfate frequency distribution from SEM characterization of ACCU filter samples collected at Site 3 (Minnesota farm), May–June 2000 ..... 38

II-12 Particle concentration and wind direction for two time periods (with sustained winds ≥6 mph [10 kph]) at Site 3 (Minnesota farm) ..... 40


Continued. . .

## LIST OF FIGURES (continued)


II-13 SAS, TEOM, and APS $PM_{2.5}$ loadings at Site 1 (North Dakota farm), August 9–29, 2000 ..... 40

II-14 Comparison of mass concentration of ambient air $PM_{2.5}$ at Sites 1 and 3 during 1 week of sampling, August and May 2000, respectively ..... 41

II-15 Classification of particles a) >2.5 µm and b) <2.5 µm collected at Site 1 (North Dakota farm), August 2000 ..... 42

II-16 SAS, TEOM, and APS $PM_{2.5}$ loadings at Site 2 (North Dakota ranch), August 29 to September 13, 2001 ..... 43

II-17 Chemical classification of $PM_{2.5}$ from ACCU samples collected at Site 2 (North Dakota ranch) ..... 43

II-18 Dispersion modeling results for August 8, 7–10 PM, at Site 1 ..... 44

II-19 The ratio of aluminum and silicon to alkali metals in the a) Burkard and b) ACCU samples collected from noon to noon, August 15–17, 2000, at Site 1 when the wind was from the north-northwest ..... 46

II-20 The ratio of silicon, aluminum, and iron in a) Burkard and b) ACCU samples collected from noon to noon, August 15–17, 2000, at Site 1, when the wind was from the north-northwest ..... 47

II-21 SEM micrograph of Burkard sample collected between noon and noon, August 15–17, from Site 1, when the wind was from the north-northwest ..... 48

II-22 The ratio of calcium, sulfur, and sodium in a) Burkard and b) ACCU samples collected from noon to noon, August 15–17, 2000, at Site 1, when the wind was from the north-northwest ..... 48

II-23 The ratio of silicon, aluminum, and iron in a) Burkard and b) ACCU samples collected from noon to noon, August 9–11, 2000, at Site 1, when the wind was from the south ..... 49

II-24 SEM micrograph of Burkard, top, and ACCU, bottom, sample, collected from noon to noon, August 9–11, 2000, at Site 1, when the wind was from the south ..... 50


Continued. . .

## LIST OF FIGURES (continued)


II-25 The ratio of calcium, sulfur, and sodium in a) Burkard and b) ACCU samples collected from noon to noon, August 9–11, 2000, at Site 1, when the wind was from the south ....51

II-26 The ratio of silicon, aluminum, and iron in Burkard samples collected from 3:00 to 23:00 on August 21, 2000, when the wind was from the east ....52

II-27 The ratio of calcium, sulfur, and sodium in Burkard samples collected from 3:00 to 23:00 on August 21, 2000, when the wind was from the east ....52

II-28 SEM micrograph of Burkard sample collected from 3:00 to 23:00 on August 21, 2000, when the wind was from the east ....53

II-29 SEM micrograph of the magnetic sampler substrate collected from Site 1 on August 8–10, 2000, when the wind was generally from the south ....54

II-30 Particle type categories determined for Site 3 (Minnesota farm, Week 2) using cluster analysis ....56

II-31 Particle type categories determined for Site 1 (North Dakota farm, Week 1) using cluster analysis ....56

II-32 Chemical classification of the ACCU $PM_{2.5}$ fraction from Site 3 ....58

II-33 Chemical classification of the ACCU $PM_{2.5}$ fraction from Site 1 ....58

III-1 Particle size distribution in the lobby — APS and SMPS results ....66

III-2 Particle size distribution in the office area — APS and SMPS results ....66

III-3 Particle size distribution in the demonstration facility — APS and SMPS results ....67

III-4 Particle size distribution in the laboratory — APS and SMPS results ....67

III-5 Particle size distribution in the hallway — APS and SMPS results ....68

III-6 Particle size distribution in the welding area — APS and SMPS results ....68

III-7 $PM_{1.0}$ mass concentration in the shipping/receiving room ....69

III-8 $PM_{1.0}$ mass concentration in the analytical research laboratory ....70


Continued. . .

## LIST OF FIGURES (continued)

III-9 Mass concentration of $PM_{1.0}$ in the welding area .....70

III-10 Elemental distribution in the welding area .....71

III-11 Elemental distribution in the shipping/receiving room.....72

III-12 Elemental distribution in the Analytical Research Laboratory.....72

III-13 SEM images of particles collected in the Analytical Research Laboratory.....73

III-14 SEM image of particles collected in the shipping/receiving room .....73

III-15 SEM image of particles collected in the welding area.....74

III-16 Picture showing the different shaped candles tested.....77

III-17 Schematic of the experimental apparatus .....78

III-18 Picture showing the experimental apparatus and sampling system .....78

III-19 Particle emissions from pillar candles .....80

III-20 Particle emissions from jar candles.....80

III-21 Particle emissions from votive candles.....81

III-22 Particle size distributions for paraffin wax candle emissions.....82

III-23 Particle size distributions for soybean wax candle emissions .....82

III-24 Impact of burning candles on ambient environment.....83

III-25 Picture showing black fume from a burning candle .....85

III-26 Picture showing black fume from a burning candle .....85

III-27 Organic compound emissions from soybean wax candles without color and fragrance ...86

III-28 Organic compound emissions from soybean wax candles with color and fragrance .....87

III-29 Organic compound emissions from paraffin candles with color and fragrance .....87

Continued. . .

## LIST OF FIGURES (continued)

III-30 Alkane distributions by carbon number for paraffin candles and their emissions.....88

III-31 Alkane distributions in particle emissions from a heavy-duty diesel truck.....89

III-32 Alkane distribution by carbon number for paraffin and soybean wax candle emissions ..89

III-33 SEM showing dense accumulation of fine particles on the filter .....90

III-34 TEM image (150×) of diesel soot.....90

## LIST OF TABLES


I-1 Mass Extracted Using Subcritical Water Fractionation of Airborne Particulate Samples (1 quarter) Collected in Pittsburgh....15

I-2 Solubility of Pesticides in Ambient Water....17

II-1 Daily $PM_{2.5}$ Mass Loadings at Site 4, Grand Forks....32

II-2 Mean Composition of the Eight Significant Groups as Defined by Cluster Analysis of the Farm Site Data....36

II-3 Average Composition of Significant Clusters....37

II-4 Anion Analysis of Rainwater Collected at Sites 1 and 3, Summer 2000....39

II-5 SEM Analysis of Particles Presented in Figure II-29 Collected from the Magnetic Sampler at Site 1....54

II-6 Cluster Analysis Results of Unknowns from Selected Burkard Sample Data Sets....57

II-7 Percent DNA Breakage Induced by Cyclone #1 Ash....63

II-8 Percent DNA Breakage Induced by Filter #115 Ash....63

III-1 Particle Size Distributions by SMPS and APS at Various Locations....69

III-2 Summary of the Tested Candles and Emissions from Candle Burning....77

III-3 Summary of Burning Rate of Different Candles under Stable Combustion....79

III-4 Organic Species Detected in Paraffin and Soybean Wax Candles....86

## NOMENCLATURE

| | |
|---|---|
| ACCU | automatic cartridge collection unit |
| ADP | adenosine diphosphate |
| AP | alkaline phosphatase |
| APS | aerodynamic particle sizer |
| ASEM | automated scanning electron microscopy |
| CHN | carbon, hydrogen, nitrogen |
| CPC | condensation particle counter |
| DMSO | dimethyl sulfoxide |
| DNA | deoxyribonucleic acid |
| EERC | Energy & Environmental Research Center |
| EPA | U.S. Environmental Prote-ction Agency |
| FID | flame ionization detection |
| GC | gas chromatograph; gas chromatography |
| HYSPLIT | Hybrid Single-Particle Lagrangian Integrated Trajectory model |
| ICP | inductively coupled plasma |
| L | lysine |
| MS | mass spectrometer; mass spectrometry |
| NCA | National Candle Association |
| NIST | National Institute of Standards and Technology |
| NQO | nitroquinoline oxide |
| OC | organic carbonaceous |
| ONPG | o-nitrophenyl-ß-D-galactopyranoside |
| PAH | polycyclic aromatic hydrocarbons |
| PM | particulate matter |
| $PM_{2.5}$ | fine particulate matter |
| SAS | sequential air sampler |
| SEM | scanning electron microscopy |
| SMPS | scanning mobility particle sizer |
| SWF | subcritical water fractionation |
| TEOM | tapered electronic oscillating microbalance |
| TOC | total organic carbon |
| TSP | total suspended particulate |
| UCM | unidentified complex mixture |

## SUBTASK 2.2 – FINE PARTICULATE ($PM_{2.5}$) CHARACTERIZATION AND SOURCE APPORTIONMENT

### EXECUTIVE SUMMARY

Particulate matter (PM) in the air is of considerable environmental interest because of research studies correlating exposure of ambient levels of fine particulate matter ($PM_{2.5}$) with acute respiratory and cardiovascular distress. The PM of interest consists of two forms—primary PM emitted directly from a source and secondary PM formed in the atmosphere. PM may be organic (soot, polycyclic aromatic hydrocarbons [PAHs]), inorganic (metals, sulfates, nitrates), or combinations of both organic and inorganic constituents.

Currently, PM mass is the only parameter correlated with respiratory and cardiovascular distress. Presently, it is not known which particles are the bad actors, although theories related to particle size and composition exist. In spite of this lack of knowledge, PM emissions, especially those for PM less than 2.5 μm in diameter ($PM_{2.5}$), face increased regulation within the United States. Sources of $PM_{2.5}$ emissions include, but are not limited to, oil- and coal-fired power plants; gasoline- and diesel-fueled motor vehicles; fugitive dust from roads, agriculture, and industrial operations; metal smelters and steel mills; mining, quarrying, and aggregate handling; natural emissions from vegetation and uncontrolled fires; cooking and heating with wood stoves and fireplaces; and volcanic eruptions.

The overall of goal of the $PM_{2.5}$ program at the Energy & Environmental Research Center (EERC) is to develop advanced sampling and analysis methodologies for PM that can be used for source apportionment and assist in health studies. These techniques can be used to determine sources of $PM_{2.5}$ in rural states such as North Dakota. Specific objectives include 1) developing extraction methods and toxicology tests to identify and evaluate the organic fraction of common air PM, 2) developing characterization methods to evaluate and source apportion the inorganic composition of PM, 3) performing toxicological assays of select PM samples to correlate the results with live animal studies, 4) characterizing and determining the sources of indoor air particle in EERC buildings, and 5) determining the impact of candle burning on indoor air quality. The specific objective is to characterize the soot emission from candle burning as a function of candle type and burning conditions

The research activities carried out under the EERC Base Cooperative Agreement Subtask 2.2 focused on the following areas: 1) Fractionation of Organics from Air Particulates with Subcritical Water, 2) Sampling and Analysis of PM – Characterization of the Inorganic Fraction, and 3) Characterization of Indoor Air Quality, including the effects of burning candles.

### ACTIVITY 1 – FRACTIONATION OF ORGANICS FROM AIR PARTICULATES WITH SUBCRITICAL WATER

The toxicity of aerosol particulate is mostly evaluated indirectly through correlation of aerosol composition with epidemiological studies and/or inhalation studies requiring a large

number of samples directly delivered to tested organisms (1–3). Because of faster evaluation (1–3 days) and low expenses, in vitro tests are often used for evaluation of different environmental matrices such as soils or waste waters (4). Several in vitro tests have been previously employed to express toxicity of aerosol particulate (5–7).

In this work, subcritical water (from 25° to 300°C) is used to fractionate two carbonaceous aerosols sequentially: diesel exhaust particulate (a relatively nonpolar matrix) and wood smoke particulate (a polar matrix). To evaluate the importance of each fraction, four different toxicity tests were performed. Effects on respiration were examined using bacterial culture (Polytox™) and rat hepatic mitochondria. The SOS-Chromotest was used to measure bacterial genotoxicity. Cytotoxicity to mammalian cells was analyzed using COS cells. Each test was first performed using concentrated water extracts, but because the cooled concentrated water extracts precipitated, the tests were also performed on dried extracts, which were dissolved in dimethyl sulfoxide (DMSO). Both tests gave similar trends, but the response was more pronounced in DMSO-dissolved extracts. Therefore, all data presented are based on the use of DMSO. The data obtained were related to composition of extracts, which was determined on the basis of carbon, hydrogen, nitrogen (CHN) and sulfur analysis, total organic carbon (TOC), gas chromatography–mass spectrometry (GC–MS) analysis, and diesel exhaust particulate analysis of metals.

In addition, the developed method was applied to evaluate toxicity of another environmental matrix—soil contaminated with pesticides. Pesticides are expected to be a major contributor to toxicity in agricultural soils. When determining the contamination of soil or ground water caused by agricultural use, chemical analysis targeted specifically for pesticides is performed. This approach automatically assumes that pesticides are the only contributor to total soil toxicity and omits possible pollution by pesticide degradation products or their metabolites.

To evaluate whether pesticides are the only contributor to the total toxicity of soils, the toxicity of different components of the soil must be evaluated. As was shown for air particulate, subcritical water is a suitable tool for the fractionation on the polarity bases. Subcritical water fractionation (SWF) was applied to pesticide-contaminated soil and compared to organic solvent extraction, which extracts mainly pesticides. The subcritical water fractions and organic solvent extracts were evaluated with respect to their cytotoxicity, content of pesticides, and mass of material extracted.

### Toxicity of Wood Smoke Particulate

The toxicity tests were performed on the same proportion of each temperature extract. This approach allowed comparison of the contribution of each water fraction to the total toxicity of the whole sample. Results obtained with different toxicity tests are obviously specific to different classes of compounds. The data on Polytox™ show the low sensitivity of this test. The tests on extracts dissolved in water, which were performed with larger fractions of samples, (20% and 40%), showed inhibition to 20% of normal bacterial respiration of 25° and 50°C fractions (polar). For the second bacterial test, the SOS-Chromotest, two sets of data were obtained: 1) the alkaline phosphatase activity representing the total protein synthesis, which shows that fractions collected at 100° and 150°C have the highest toxicity; and 2) the genotoxic response, which is expressed as a formation of the ß-galactosidase enzyme; for wood particulate extracts, no

genotoxic response was observed. It is known that many compounds, such as PAHs, are genotoxic after enzymatic metabolic activation, when arylhydroxylase in the liver metabolizes PAHs into hydroxylated compounds, which are water-soluble and toxic. Therefore, tests also were performed with rat liver microsomal S9; however, no increase in genotoxicity was observed after activation. Each test was validated on test compounds, m-cresol for the Polytox™ and 4-nitroquinoline oxide for the genotoxicity test. Similarly to Polytox™, the cytotoxicity test using mammalian COS cells showed higher toxicity of more polar fractions; however, it is important to note that the extracted mass was higher in polar fractions.

The results from the test on rat liver mitochondrial respiration show uncoupling activity of higher temperature (200°–300°C) extracts (State 4). In addition, the extracts of 150° and 200°C blocked adenosine diphosphate (ADP)-stimulated respiration (State 3).

**Toxicity of Diesel Exhaust Particulate**

Both the water fraction obtained at 25°C (polar materials), which was dried and dissolved in DMSO, and the concentrated water showed significant inhibition of bacterial respiration. In contrast to wood smoke particulate, significant genotoxicity was observed for fractions extracted between 100° and 250°C. For those temperatures, the protein synthesis also was inhibited.

The cytotoxicity of diesel exhaust (nonpolar matrix) showed increasing toxicity with increasing extraction temperature. This trend is opposite to the cytotoxicity of wood smoke particulate (polar matrix) fractions and may correspond with the difference of sample polarities.

Mitochondrial respiration significantly increased for the fractions collected above 100°C; this may correspond to the extracts uncoupling activity (State 4). The same fractions also had blocked State 3 respiration. Interestingly, the 25°C fraction for which the inhibition of bacterial respiration was observed did not show uncoupling activity but did block ADP-stimulated respiration (State 3).

***Characterization and Possible Relationship to Toxicity Results***

Detailed characterization is needed to explain the toxicity of different fractions. Therefore, elemental analyses for CHN and S were performed, the TOC was determined, the extracts were analyzed using GC–MS, and the diesel exhaust particulate was characterized for metals.

In the elemental analysis, the gravimetric data show the most polar water (25°C) extracted the highest mass of particulate. The total extracted particulate with subcritical water extraction (25°–300°C) was 42 and 34 wt% for wood smoke particulate and diesel exhaust particulate, respectively. The CHN and S composition corresponded to 40–60 wt% of the extracted mass for each fraction. For most of the wood smoke particulate water fractions, the estimated total organic compound mass corresponds to (or exceeds) the amount extracted. For diesel exhaust, the estimated total organic compound mass is lower than the total extracted, probably because of the presence of inorganic compounds, especially in the most polar (25°C) fraction.

The most selective extraction was observed for sulfur. Increased sulfur content was found in both samples of the fraction collected at 25°C. The initial concentration of sulfur in diesel exhaust particulate was 40 mg/g. In the lowest-temperature fractions (which were the most toxic), 75% of the sulfur was recovered.

The identification of individual components in each fraction was performed using GC–MS. GC–flame ionization detection was used for tentative quantification. Although GC is limited to the determination of mainly nonpolar or slightly polar compounds present in samples, we observed increased concentrations of lignin pyrolysis products such as syringol and quaiacol derivatives, phenols, and benzenediols in low-temperature fractions from wood smoke particulate. Interestingly, a high quantity of levoglucosan, a typical marker of wood burning, was found in water extracts but was not observed in acetone extracts. It is important to note that in using GC–MS, we were able to analyze with only about 24% of the total extracted mass. GC–MS analysis of diesel exhaust was not as informative as that of wood smoke particulate, because the GC-elutable fraction of diesel exhaust consists mainly of alkanes and PAHs. When using GC–MS in selected ion recording mode, selective extraction of nitropyrene at temperature 150° and 200°C was observed. The presence of nitroaromatics would explain genotoxicity of the same diesel exhaust extracts.

Inductively coupled plasma–MS metal analysis showed high concentrations of zinc, iron, magnesium, and manganese in the most polar fraction (25°C). All of these elements were probably present in the form of sulfates, which are soluble in water.

### Application of Subcritical Water Fractionation to Pesticide-Contaminated Soil

Both techniques—organic solvent extraction and SWF (sum of all fractions)—extracted a comparable mass of pesticides. Therefore, if toxicity in the soil corresponds only to pesticides, the toxicity of the extract obtained with subcritical water (total) should correspond to the toxicity showed by organic solvent extraction. Detailed determination of pesticides in each subcritical water fraction showed that the majority of the pesticides were extracted in the most polar fraction of 25°C. This corresponds to the high solubility of most pesticides.

To determine whether pesticides alone or if other material also are responsible for the toxicity of extracts, the cytotoxicity was compared to the concentration of material and pesticides extracted with each method. The toxicity of the material extracted by subcritical water seems to be lower than that of organic solvent, but it is important to note that the total mass extracted by water is 10 times higher than that of solvent. Thus because of the presence of unidentified compounds (in addition to pesticides), the total toxicity of water extracts is higher than that of organic solvent. This is confirmed by detailed investigation of relations between pesticides present in the water fractions and cytotoxicity observed. The cytotoxicity of the fraction collected at 175°C, containing mainly pendimethalin (a common lawn weed killer) and trifluralin (an agricultural herbicide), corresponds to the cytotoxicity of standard pesticides. A similar trend would be expected for the fraction collected at 225°C, also containing pendimethalin and trifluralin. In contrast to the 175°C fraction, the cytotoxicity of 225°C in dependence on pesticide content is significantly higher, although the concentration of pesticides in this fraction was slightly lower. The higher cytotoxicity of 225°C can be explained by the presence of additional

cytotoxicity components. Similar to the 175°C fraction, the cytotoxicity of 125°C may be attributed to pesticide present in this fraction. The polar fractions collected at 25° and 75°C did not show significant toxicity, although most of the water-soluble pesticides were extracted in the 25°C fraction. The relatively low response might be the result of the low concentration of pesticides. Further investigation is needed to confirm this assumption.

**Conclusions**

The selective fractionation of wood smoke and diesel exhaust particulate demonstrated the potential of subcritical water for toxicity studies of wide-range polarity components in PM, as well as other environmental matrices such as soils. As expected, not only nonpolar compounds were responsible for the toxicity of PM, but also less-studied polar components contributed at least the same extent to total toxicity.

The project resulted in the following conclusions:

- Subcritical water selectively extracts organic compounds ranging from polar to nonpolar.
- High toxicity was found in the polar fractions, which are not expected to be extracted by organic solvents.
- GC–MS characterization of wood smoke particulate showed phenols, benzenediols, and levoglucosan extracted preferentially in lower-temperature fractions.
- Higher content of sulfur, magnesium, iron, and zinc was found in the lowest-temperature fraction (the most polar) of diesel exhaust particulate.
- Standard methods employing organic solvents do not characterize the polar fractions of aerosol particulate, which are important from a toxicological point of view.
- Tests studying leachates (water extracts at ambient temperature) might omit toxicologically important polar fractions extracted above 25°C.

This work has shown that different classes of compounds may contribute to the total toxicity of PM. Nevertheless, the current study employed surrogate samples of atmospheric particulates and general toxicity tests. Therefore, future work will involve SWF analysis of ambient atmospheric particulate and toxicity tests more closely approximating the exposure of human respiratory system to these pollutants. Moreover, characterization of carbonaceous particulate should focus on polar species using other analytical techniques.

## ACTIVITY 2 – SAMPLING AND ANALYSIS OF FINE PARTICULATE MATTER ($PM_{2.5}$)

### Activity 2.1 – Characterization of the Inorganic Fraction

Specific objectives for the research under Activity 2.1 included developing automated scanning electron microscopy (ASEM) analysis methods to elucidate key physical and chemical information, developing source apportionment methods, extensively characterizing samples collected, and developing a scientifically sound $PM_{2.5}$ database. The primary activities undertaken were to 1) collect and characterize $PM_{2.5}$ samples using instrumentation in the sampling trailer, 2) develop and improve ASEM characterization techniques, and 3) provide detailed characterization information for the samples collected.

#### *Experimental*

Six instruments were assembled in a sampling trailer and optimized for data analysis prior to field sampling and data collection of ambient $PM_{2.5}$ characterization. They include a Burkard Spore Trap Sampler for collection of total suspended particulate (TSP), a tapered electronic oscillating microbalance (TEOM) for mass loading of fine particulate with an automatic cartridge collection unit (ACCU) for sample collection, a sequential air sampler (SAS) as a federal reference monitor of fine particulate, an aerodynamic particle sizer (APS) and a scanning mobility particle sizer (SMPS) for real-time particle sizing measurements. The trailer also included instrumentation to track and record weather data.

Scanning electron microscopy (SEM) methods were developed for the characterization and source apportionment of the ambient-air PM. For the Burkard samples, analyses were taken across the tape, providing hourly data for each 24-hour period. The 20-mm-wide carbon tape from the Burkard sampler was cut into 48-mm-long pieces, with each piece representing a 24-hour period. Starting times were known and the carbon tapes were cut to represent midnight to midnight sampling periods. These 24-hour strips were then mounted on a standard petrographic slide and inserted directly into the SEM for analysis without further sample preparation. An analogous SEM technique was developed for analysis of the ACCU filter samples. Cluster analysis was performed on the particle chemical compositions to classify them into chemical groupings. Eight major chemical categories have been identified and used to classify $PM_{2.5}$. These are quartz, feldspar, clays (e.g., kaolinite, chlorite, muscovite, biotite, and illite), Na–K salts (NaCl and KCl), carbonates (calcite, dolomite, ankerite, siderite), iron-rich (e.g., pyrite, magnetite, ilmenite, and hematite), sulfur-rich (e.g., anhydrite and gypsum), and unclassified (chemically complex particles such as mixed clays, clay-coated mineral grains, and/ or organic compounds).

$PM_{2.5}$ emission point sources and ACCU sampling sites are indicated in Figure ES-1. Ambient PM samples were collected under atmospheric conditions continuously for 18–60 days at one urban and three rural sites. A potato processing plant, a concrete fabrication plant, a railroad yard, and other light industry were located in the vicinity of the winter sampling (December 1999–January 2000) at the urban site in Grand Forks, North Dakota (Site 4). Lack of normal snow cover along with heavy truck traffic on nearby unpaved roads resulted in significant

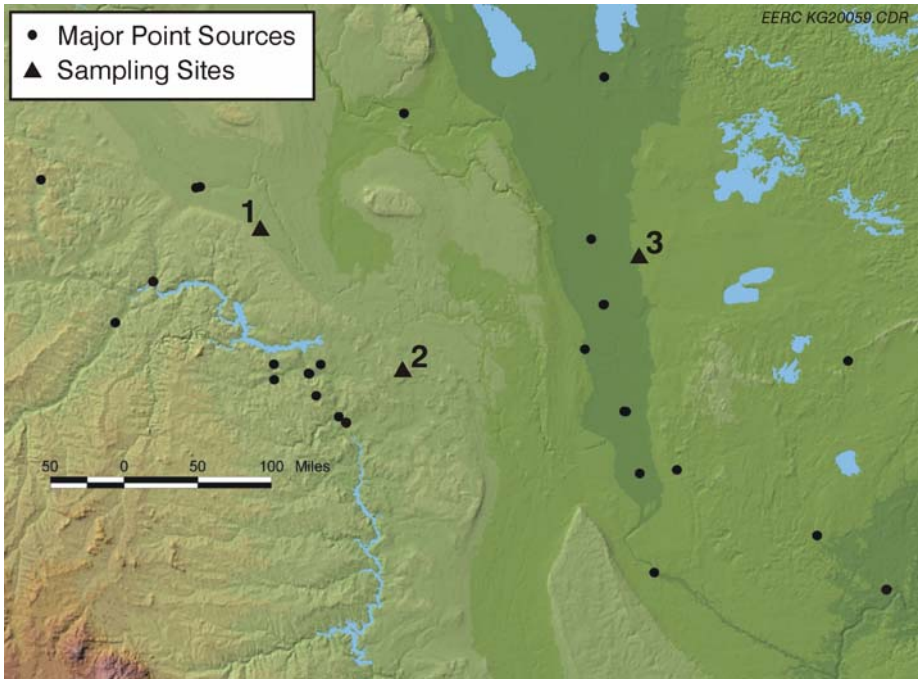


Figure ES-1. $PM_{2.5}$ sampling locations and major point sources.

wind-blown soil and road dust at the site. Sampling at the easternmost site (Site 3) was performed during a period of spring tillage and planting (May 18–June 15, 2000). This site is remote from large population centers, industrial activity, and thermal power plants. The westernmost site (Site 1) is similarly in an agricultural region, with sampling performed in late summer (August 8–25, 2000) during the grain harvest. This site is remote from large population centers and industrial activity; however, several large (500-$MW_e$) coal-fired power plants and a large coal gasification facility are within 110–150 km of the site. Land use in the central southernmost site (Site 2) is dominated by ranching. A well-traveled paved and an infrequently traveled gravel road exist within approximately 60 m of this sampling site. Sampling at this site was performed August 27–September 14, 2001. An oil refinery and several coal-fired power plants are located approximately 95 km west of Site 2. Potential sources of $PM_{2.5}$ at the sampling sites include diesel- and gasoline-fueled motor vehicles, fugitive dust from gravel roads and agriculture, vegetation and fires, an oil refinery, and coal-fired power plants.

### ***Results and Discussion***

#### *Grand Forks (Site 4)*

The monitoring activities at the Grand Forks site were, in part, shakedown tests. $PM_{2.5}$ particulate loadings were monitored using the SAS at Site 4. A comparison of the inorganic phase compositions of PM greater than and less than or equal to 2.5 µm ($>PM_{2.5}$ and $\leq PM_{2.5}$, respectively) collected from Site 4 showed that the compositions of the two size fractions are similar. The majority of particles in both size ranges are unclassified because they are mostly organic particles, such as spores, pollen, and topsoil. The clay, quartz, carbonate, and feldspar

particles probably represent dust derived from vehicular traffic on a nearby gravel road. The sulfur-rich particles are probably gypsum released from a concrete fabrication facility in the area.

*Minnesota Farm Site (Site 3)*

A comparison of $PM_{2.5}$ particulate loadings obtained from the SAS, TEOM, and APS at Site 3 show the same trends in $PM_{2.5}$ concentration, although the TEOM measurements are consistently higher than those from the SAS. The APS measurements also are consistently lower than the SAS values, which may be related to assumptions of particle density used to calculate a mass concentration.

A total of 16,605 and 13,324 individual particles from the Burkard and ACCU samples, respectively, collected at Site 3 were analyzed using ASEM. The Burkard samples provide time-resolved data in 1-hour increments, while the ACCU filter samples represent 72-hour intervals. Particle compositions obtained from the Burkard sampler during a 5-hour period when the wind was consistently light from the northeast were dominantly crustal material and generally larger than 2.5 µm in diameter. In contrast, 87% of the particles collected by the ACCU filter were classified as biologic in origin.

The mineral distribution of particles ≤2.5 µm generally follows the pattern of the larger particles where carbonate minerals are predominant in the classified fraction. The amount of unclassified particles in both size ranges is rather large, 51% of the particles >2.5 µm and 58% of the particles ≤2.5 µm. These data points in particular were evaluated using cluster analysis, which showed that the majority of the unclassified analyses were mostly mixed clays that have variable amounts of Ca, K, Fe; Na and Si around 30 wt%; and Al around 10 wt%. Further reductions were applied to these data by checking all of the analyses for stoichiometric relationships between various elements to identify possible sulfate, nitrate, and phosphate phases. These results show that several of these phases may exist, with the sulfate predominating. The ACCU filter sample contains more sulfur-rich phases, mostly gypsum–anhydrite ($CaSO_4$) and thenardite ($Na_2SO_4$).

*North Dakota Farm Site (Site 1)*

A comparison of $PM_{2.5}$ particulate loadings obtained from the SAS, TEOM, and APS at Site 1 showed the same trends between the mass loading and single-particle counting techniques. The PM mass measurements were found to be higher in North Dakota than in Minnesota. Analysis of ACCU samples indicated approximately 15% of the more than 10,000 particles sampled at this site may be attributed to particles from combustion sources.

The results of the mineral classification of samples collected at Site 1 using the Burkard spore sampler for the >2.5-µm and the <2.5-µm size fractions showed that the differences in the types of materials are larger quantities of feldspar materials in the larger sizes and the larger quantity of unclassified materials in the submicron-size fraction.

Anion analysis of rainwater from Sites 1 and 3 is presented in Table ES-1. Site 1 rainwater had higher incidence of all five anions evaluated. The Site 1 water was especially high in sulfates

**Table ES-1. Anion Analysis of Rainwater Collected at Sites 1 and 3, Summer 2000**

| Analyte | Site 1 | Site 3 |
|---|---|---|
| Chlorine, Cl | 1.5 | 1.3 |
| Bromine, Br | 1.2 | Not detected |
| Nitrate, $NO_3$ | 5.7 | 1.3 |
| Phosphate, $PO_4$ | 2.2 | Not detected |
| Sulfate, $SO_4$ | 5.93 | 2.8 |

nitrates, and phosphorus, some of which could have leached from soil and plant particles disturbed during harvest.

*North Dakota Ranch Site (Site 2)*

A comparison $PM_{2.5}$ particulate loadings obtained from the SAS and TEOM at Site 2 shows generally consistent but higher loadings for the TEOM than the SAS. The PM mass measurements at Site 2 were much lower than at Site 1. The TEOM daily mean concentration for Site 2 is 9.6 vs. 15 $\mu g/m^3$ at Site 1. Most (79%) of the $PM_{2.5}$ consisted of unclassified and organic components. The particles in these classification categories are mostly spores, pollen, soil, and fugitive dust. The remaining 13%–21% of $PM_{2.5}$ collected at the sites was inorganic-rich. The clays, quartz, carbonates, and feldspars are primarily associated with fugitive dust from nearby gravel roads and fields. The alkali-salt content of all three samples is consistent, suggesting a regional, and perhaps natural, source for this particle type. $PM_{2.5}$ samples from Sites 1 and 3 are compositionally similar. $PM_{2.5}$ from Site 2, however, contains a greater proportion of sulfur-rich particles, presumably composed of secondary sulfate compounds. Combustion-derived particles (fly ash) were not significant PM components at this site, with only three instances from about 1,200 particles that were analyzed.

*Dispersion Modeling*

The monitoring results from the North Dakota farm and ranch Sites 1 and 2 were drastically different—in particle loading, in composition, and in appearance. Site 1 sampling results indicate high amounts of fly ash that predominantly were attributable to a combustion process. Emission from the coal-fired power plant northwest of the sampling site is the likely source of these materials. Dispersion modeling results indicated time periods at Sites 1 and 2 when emissions could potentially be contributing to the surface ambient air sample composition. With respect to Site 1, these periods have a dispersive movement from the northwest towards the southeast where the sampling site was located. The power generation region near Site 2 could also have influenced the PM composition at Site 1 during periods from south to northerly dispersion. Dispersion model results at Ranch Site 2 indicated the probable influence of coal-fired power generation activity in the area west of the sampling site. Time periods of west-to-east dispersion would result in an effect on sampling results from sources.

Since the Site 1 Burkard and ACCU samples were collected under a variety of wind directions, analyses collected during times of northwesterly, southerly, and easterly winds were compared for chemical composition and appearance to determine whether wind direction had a

measurable effect on PM composition. Ternary diagrams, essentially three-dimensional histograms, compare the concentration of three elements in a sample relative to each other, with the center of the diagram representing equal portions of each element in the material analyzed. As with any frequency diagram, the vertical axis represents the number of particles in each bin, i.e., containing each ratio of the elements represented at the vertices. Elemental groupings were selected to represent combinations of mineral elements typical of fly ash and/or fugitive dust particles.

Figure ES-2A shows the ternary diagram of the Si–Al–Fe ratios from the Burkard sample collected noon to noon August 15–17, 2000, under a northwesterly wind; this diagram shows quartz and clay groupings of particles. It also shows a strong contingent of SiFe particles along the Fe–Si axis. While present in both sample types, it has greater frequency of occurrence in the ACCU sample collected during the same time period (Figure ES-2B).

Fe–Al-silicates and Fe–Si compounds are potential signatures of fly ash. Pure Fe could be rust; pure Si could be sand. However, compounds rich in both Fe and Si indicate the presence of fly ash particles in the ambient sample. The ACCU sample, in particular, had a high frequency of particles of this type. The Burkard sample ternary indicated some Fe–Si particles, but more Fe–Al-silicates, Al–Si, and Si were present. The Fe–Al-silicates indicate fly ash particles. In contrast, Al–Si can arise from either fly ash and/or clay particles from fugitive dust.

More analyses consistent with fly ash particles were observed in the ACCU than in the Burkard sample. This can be explained by air current–particle settling. As in an aquatic stream, the coarse particle fraction in the atmosphere will settle faster than the fine fraction. Since the

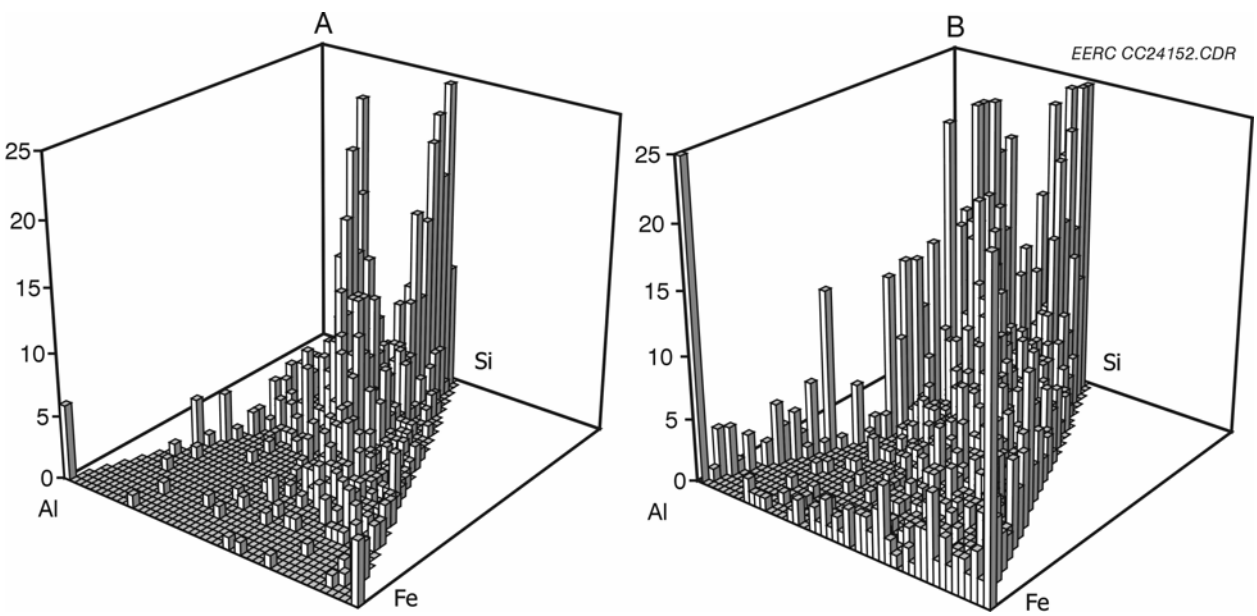


Figure ES-2. The ratio of silicon, aluminum, and iron in a) Burkard and b) ACCU samples collected from noon to noon, August 15–17, 2000, at Site 1, when the wind was from the north-northwest.

ACCU collects only the $PM_{2.5}$ fraction, we can infer that the sampling site is a long distance from the possible high-temperature combustion sources, and more of the coarse particle fraction has settled out of the ambient air before reaching the sampling site.

Confirming the presence of fly ash particles is the spherical morphology indicative of the particle passing through a high-temperature combustion process. This is seen in Figure ES-3, where the spherical fly ash particles are easily visible among angular dust and organic materials in the SEM micrograph of the Burkard sample collected during this time period. The $PM_{2.5}$ mass concentration during this sampling time was 10.9 $\mu g/m^3$ and the total accumulated mass was 63.9 µg.

Na and Ca sulfates can be combustion by-products or fertilizers. The Burkard sample appeared to have small amounts of $CaSO_4$, but the primary material present had higher Na–Ca content and low S content. These would likely represent clay particles. In contrast, the ternary diagram of the ACCU sample indicated a relatively larger number of particles of $CaSO_4$ and $Na_2SO_4$. Because these particles are finer, they are consistent with combustion-generated PM.

The ternary diagram of the Si–Al–Fe ratios from the Burkard and ACCU samples collected under a southerly wind from noon to noon August 9–11, 2000, shows quartz and clay groupings of particles. Compared to the samples collected during a northwesterly wind, the Burkard sample collected when the wind was from the south contained primarily Al–Si particles (aluminosilicates), which are common compositions in both fly ash and crustal material. Likewise, the ACCU sample contained a larger portion of Al–Si particles. However, particles

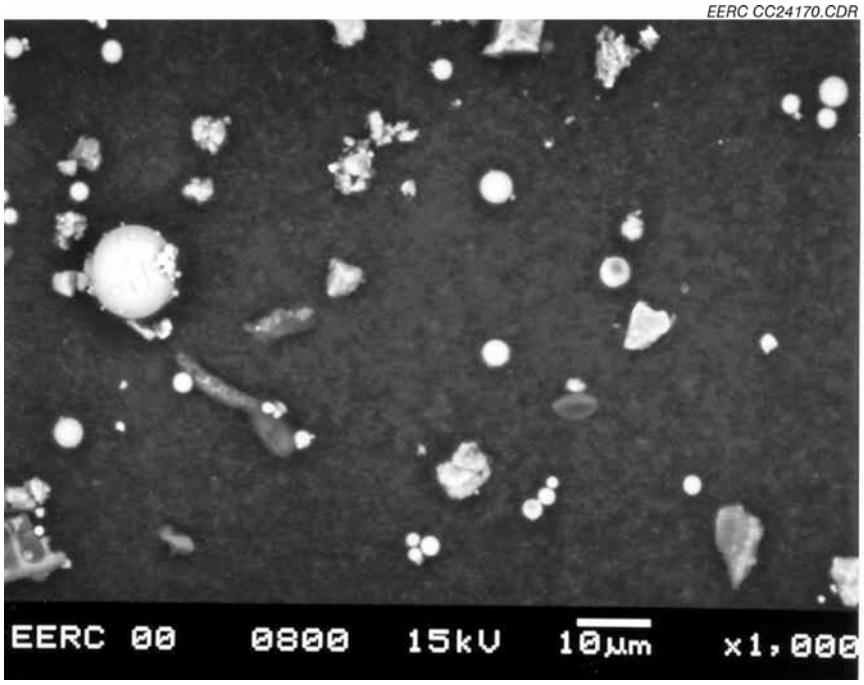


Figure ES-3. SEM micrograph of Burkard sample collected between noon and noon, August 15–17, from Site 1, when the wind was from the north-northwest.

rich in Fe–Al–Si were present, suggesting that a certain level of fly ash was present in the sample. In this case, the Burkard sampler had a greater frequency of occurrence than the ACCU samples. Microscopic inspection of the samples collected during the southerly wind period revealed large and small agglomerated spherical particles present with angular forms. The Burkard sample image includes organic matter visible at the bottom of the micrograph. The $PM_{2.5}$ mass concentration during this sampling time was 23 $\mu g/m^3$ and the total accumulated mass was 148 µg.

The Ca–S–Na ratios for these Burkard and ACCU samples indicate that the Burkard sample collected under a south wind contained more $CaSO_4$ and Ca–Na-rich particles suggestive of clay particles. A comparison of the ternary diagram from the northwest wind and the south wind Burkard samples indicate that more Ca–Na–S particles were collected from the south than from the northwest. While TSP was not measured quantitatively, the TEOM total mass measurement for the $PM_{2.5}$ fraction during each period suggests that the total particle loading for the southerly wind period was greater (150 vs. 62 µg total mass at the loading rate of 13 LPM). A comparison of the ternary diagram from the northwest wind and the south wind ACCU samples indicates a lower particle loading in the ambient air from the south with respect to particles containing Ca, Na, and S. The ACCU sample collected under a south wind also contained lower concentrations of $CaSO_4$ than the sample collected under a northwest wind and fewer $CaSO_4$ and Ca–Na-rich particles than the larger size fraction.

The ternary diagram for the Burkard sample collected under an easterly wind on August 21, 2000, from 3:00 to 23:00 is presented in Figure ES-4. This represents 42% of the

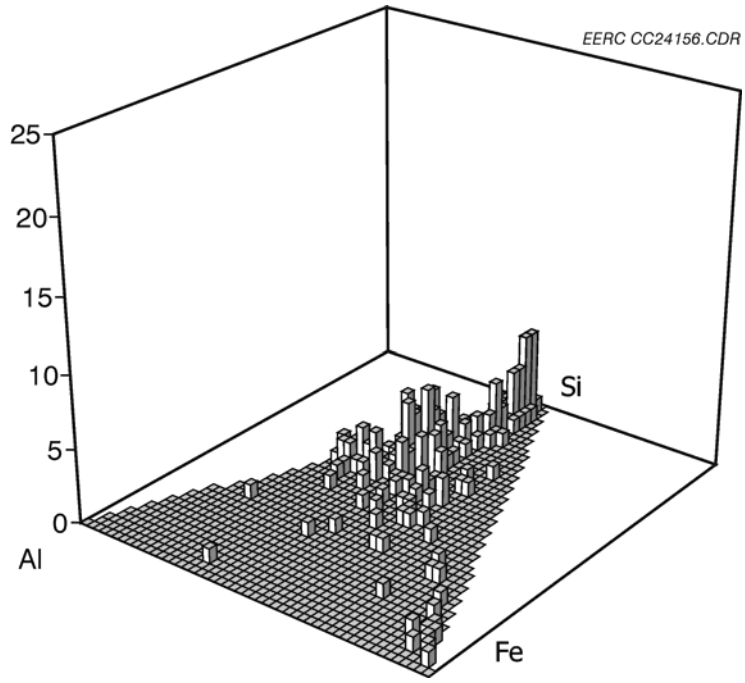


Figure ES-4. The ratio of silicon, aluminum, and iron in Burkard samples collected from 3:00 to 23:00 on August 21, 2000, when the wind was from the east.

period evaluated for the two previous wind directions, so one might expect the frequencies to be lower. However, as the figure indicates, the TSP loading during this time period was comparatively very low with respect to particles containing Al, Fe, and Si. The pattern is consistent with some Fe aluminosilicate fly ash along with crustal materials. Likewise, the ternary diagram illustrating the Ca–S–Na ratio show low particle frequency and the highest incidence of calcium-rich materials and Na–Ca-rich particles with very low S content, suggestive of clays. Little $NaSO_4$ or $CaSO_4$ was present. Figure ES-5 shows a micrograph of the Burkard sample collected during this time period, containing fewer particles and which are non-spherical, indicative of crustal materials, i.e., no fly ash was present. There is no corresponding ACCU sample because the sampling timeframe from the east was limited, and each ACCU sample overlapped with wind conditions from either the NW or S. The $PM_{2.5}$ mass concentration during this sampling time was 6.1 $\mu g/m^3$ and the total accumulated mass was 9.0 µg.

*Results from the Magnetic Sampler*

Particles of nearly pure metallic Fe, which are often agglomerated with Al–Si particles, are a definitive signature of fly ash produced from high-temperature combustion. Such material is attracted to, and therefore can be collected easily with, a magnet. A magnetic sampler containing a polycarbonate-coated filter membrane used to collect samples in the ACCU was mounted upside down under the Burkard sampler platform as a screening tool for fly ash particles at Site 1. Most of the particles collected were spherical and contained mostly Fe with some O, indicative of high-temperature combustion products.

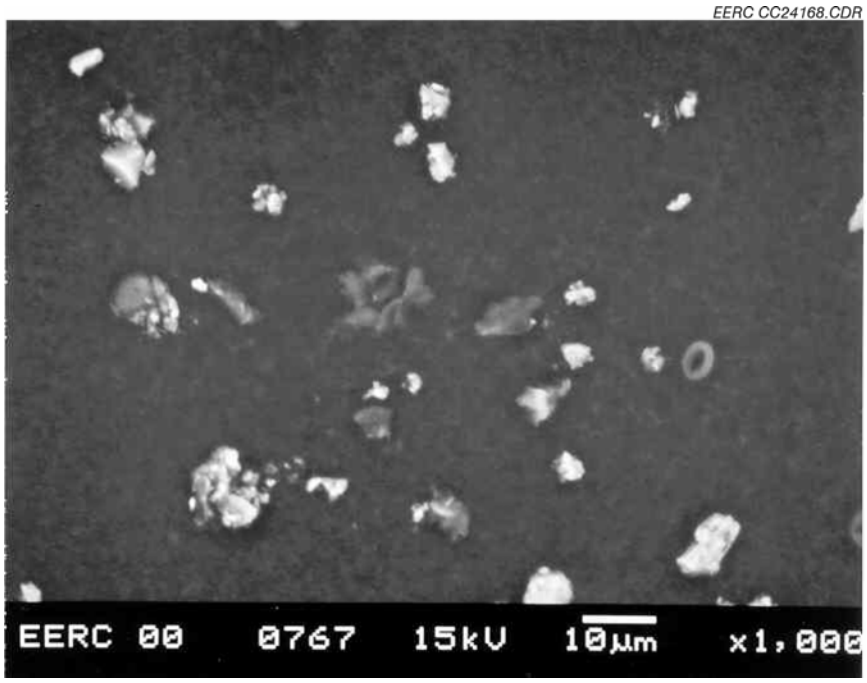


Figure ES-5. SEM micrograph of Burkard sample collected from 3:00 to 23:00 on August 21, 2000, when the wind was from the east.

### *Conclusions*

Comparison of SAS, TEOM, and APS showed the same trends in particle concentration. The differences measured by these instruments likely are the result of the way each instrument measures $PM_{2.5}$. If particle densities could be measured, the mass loading would be more comparable. This anomaly reinforces the need for more than one sampler to obtain a complete picture of $PM_{2.5}$.

The characteristics of particles collected with the ACCU and Burkard samplers showed significant differences. The Burkard sampler collects particles >0.5 µm; these particles consist of crustal materials such as clays and road dust. The ACCU sampler collects particulate <2.5 µm, including low-density organic particles and sulfates and nitrates. Both sampling techniques combined with computer-controlled SEM analysis provided better representation of the PM, and facilitated the tracking of PM sources.

Dispersion modeling results indicate that the prevailing westerly and northwesterly winds during the sampling campaigns may have contributed primary and secondary combustion $PM_{2.5}$ to the samples collected at Sites 1 and 2. $PM_{2.5}$ collected on the membrane filters generally ranged from <0.4 to 1 µm in diameter. About 79%–87% of the $PM_{2.5}$ consists of unclassified and organic components. The particles in these classifications are mostly spores, pollen, soil, and fugitive dust. The remaining 13%–21% of $PM_{2.5}$ collected is inorganic-rich. The clays, quartz, carbonates, and feldspars are primarily associated with fugitive dust from nearby gravel roads and fields. The alkali-salt content of all three samples is consistent, suggesting a regional, and perhaps natural, source for this particle type. $PM_{2.5}$ samples from Sites 1 and 3 are compositionally similar. $PM_{2.5}$ from Site 2, however, contains a greater proportion of sulfur-rich particles, probably composed of secondary sulfate compounds.

### Activity 2.2 – DNA Breakage Catalyzed by Coal-Derived Air Particulates

Based on evidence presented in the scientific literature, at least one mechanism of toxicity by respirable particles is through the formation of reactive oxygen species. There is some evidence that these reactive oxygen species can damage deoxyribonucleic acid (DNA) (damaged DNA is a potential mechanism for cancer). We evaluated the potential for coal-derived fly ash to catalyze reactive oxygen species DNA strand breakage. Two ash samples obtained from the combustion of Beulah lignite in the conversion and environmental process simulator at the EERC provided a contrast of a larger size fraction (Cyclone #1), and a smaller size (Filter 115). The assay used is essentially that of Lund and Aust (8); it incubates the sample with bacteriophage DNA in the presence and absence of chelators and other chemicals. This DNA is a closed-circular superhelical DNA molecule; when it is cleaved, the superhelix unwinds, resulting in a relaxed molecule. The samples are separated on an agarose gel by electrophoresis. Although the molecular weight of the superhelical and relaxed forms are equal, the superhelical form migrates more quickly in the gel because of its apparent smaller size. All samples were compared by expressing each as a percentage of the control DNA (i.e., DNA treated under identical conditions minus ash) and subtracted from 100% to give the percentage of DNA with single-stranded breaks. Inhibition of DNA breakage was determined with the iron chelator deferoxamine mesylate, or by a competing $OH^{\cdot}$ scavenger (mannitol).

The tests included several treatments. Ascorbic acid can reduce the oxidation state of metals. Citric acid is a chelator that can increase the solubility of transition metals, resulting in increased activity. Deferoxamine mesylate is a specific chelator of iron and can decrease its availability. Mannitol, a sugar alcohol, is added as a scavenger of hydroxyl radicals.

***Results***

Cyclone #1 ash catalyzed much higher strand breakage with ascorbic acid, suggesting that the reduction of metals was important. The addition of citric acid did not increase strand breakage, suggesting that metals were sufficiently soluble with chelation. The presence of deferoxamine mesylate decreased strand breakage, suggesting that iron was important in catalyzing strand breakage. The addition of mannitol did not decrease strand breakage, suggesting that hydroxyl radicals were not the breakage mechanism.

Filter 115 ash showed a different pattern than was observed for the larger particle-size ash. As with the Cyclone ash, the presence of ascorbic acid increased strand breakage. However, the addition of citric acid showed a much larger effect in increasing strand breakage. This suggests that chelation was important in solubilizing metals. The addition of deferoxamine mesylate decreased strand breakage, as was observed with the Cyclone #1 ash; however, the decrease in breakage was less than for the Cyclone #1 ash. The addition of mannitol completely halted strand breakage in the Filter ash, but not in the Cyclone #1 ash. This suggests that hydroxyl radical formation was the chief mechanism of strand breakage in this sample.

Both ashes showed significant activity in catalyzing DNA strand breakage. But the mechanism of strand breakage differed between the two samples. These differences could be the result of the types of metals, the soluble concentrations of the metals, or both. More work is necessary to evaluate the effects of other conditions on catalysis of strand breakage. Additionally, it would be valuable to compare the composition and solubility of the two samples.

## ACTIVITY 3 – INDOOR AIR QUALITY

Because people spend 85% of their time indoors (9), it is widely recognized that a significant portion of total personal exposure to ambient PM occurs in indoor environments. Ambient PM is a complex mixture of particle sizes and types from many sources. Studies (10, 11) show that the indoor particles not only came from outside, but the indoor activities, such as cooking, space heating, office machines, ventilation, etc., also can generate submicrometer-size particles. As a result of these indoor sources, indoor particle concentrations are often higher than ambient concentrations (12).

Despite the public health implications of indoor particle exposures, few studies have characterized sources of indoor $PM_{2.5}$. It is important, therefore, to quantify the major sources of indoor exposure, as well as the particle size and chemical composition distributions. Also, there are virtually no data on the effectiveness of air cleaning in reducing indoor exposures to $PM_{2.5}$ (13). It is important to evaluate control technology for indoor exposure.

Candles are a fast-growing industry that may have an effect on the health of the average American. The National Candle Association reports $2 billion worth of candles are sold annually. Kline and Company did a study that illustrated 7 out of 10 homes regularly burn candles. With these numbers, the potential effect on the U.S. population is significant.

Several air pollutants are released into the ambient environment during candle burning, such as metallic species (lead, zinc, or tin), volatile organic compounds (acetaldehyde, formaldehyde, polyaromatic hydrocarbons, etc.), and PM (soot). Lead poisoning was the initial concern with burning candles, and studies performed by Van Alphen (14) and Nriagu and Kim (15) showed high level of lead (~13.1 $\mu g/m^3$) while candles with metal-core wicks were burned. Several carcinogenic organic compounds have been detected in candle emissions. Experimental data by Lau et al. (16) showed that the emissions could be higher than the U.S. Environmental Protection Agency's excess cancer-risk level under certain scenarios.

Soot emissions from burning candles are another concern for human health and have drawn increased attention in recent years. A significant amount of ultrafine soot is generated during candle burning. The generated ultrafine particles are easily deposited in the pulmonary region (17), penetrate the epithelium and reach interstitial sites (18) in the lungs. Finally, the ultrafine particles are biologically more reactive than larger sized particles and thus elicit effects at lower concentrations (19). Candle soot production increases when the candle wax is supplied to the wick is greater than can be burned effectively. This can occur when wicks are too long or the waxes melt and vaporize too quickly. Few studies have analyzed the composition of candle emissions or evaluated emission rates and maximum concentration.

### Activity 3.1 – Characterization of Indoor Air Quality

The objective of this activity was to characterize indoor air particle concentration, size distribution, and composition. A SMPS and an APS were used to screen particle concentrations and size distributions at several locations in the EERC buildings: office area, hallway, lobby, demonstration facility, laboratory, and welding area. A TEOM–ACCU system measured and collected $PM_{1.0}$ at three different locations: the shipping/receiving room, an analytical laboratory, and a welding area. The sampling time was varied from 250 to 400 hr, depending on the sampling location. The collected samples were analyzed for chemical composition by SEM, which was also used to investigate particle morphology.

#### *Results and Discussion*

A summary of the indoor particle size distributions (from 0.02 to 20 μm) is listed in Table ES-2. As expected, most of the PM in indoor environment is in the submicron range (more than 95% of particles based on number concentration).

The lobby area had the lowest particle number concentration because of a new ventilation system and a lack of human activity. Most of the office area is maintained at a reasonably low particle concentration level, ranging from $4.0 \times 10^3$ to $7.0 \times 10^3$ particles/cm$^3$. Higher particle concentration (7942 particles/cm$^3$) at the EERC demonstration facility resulted in a high particle number concentration of $1.1 \times 10^4$ in the hallway connecting it to the office area because of

**Table ES-2. Particle Size Distributions by SMPS and APS at Various Locations**

| Location | Total Number Concentration, particles/cm$^3$ | Geometric Mean Diameter, µm |
|---|---|---|
| Lobby | 3814 | 0.083 |
| Office Room | 4062–7093 | 0.096–0.085 |
| Demonstration Facility | 7942 | 0.137 |
| Laboratory | 9006 | 0.10 |
| Hallway (next to the demonstration facility) | $1.1 \times 10^4$ | 0.094 |
| Welding Area | $5.1 \times 10^4$ | 0.173 |

entrainment caused by frequent door opening. A particle concentration of $5.1 \times 10^4$ (the highest value is $9.3 \times 10^6$ particles/cm$^3$) was measured in the welding area during welding.

Based on the TEOM–ACCU system, the mass concentration of $PM_{1.0}$ in the Analytical Research Laboratory mainly fluctuated in the range of 2–12 µg/m$^3$ with an average value of 5.85 µg/m$^3$ and a standard deviation of 2.07. The highest concentration was 19.6 µg/m$^3$. Sulfur was the dominant element. The $PM_{1.0}$ mass concentration in the shipping/receiving room averaged 4.37 µg/m$^3$, with a standard deviation of 1.80, lower than the $PM_{1.0}$ level obtained in the Analytical Research Laboratory. The results are somewhat surprising because the Analytical Research Laboratory had a new filtration system. Again, sulfur was the dominant element. The PM in both locations are single particles and probably come from the outdoor environment The $PM_{1.0}$ mass concentration in the welding area ranged from 0.4 µg/m$^3$ to 1.52 mg/m$^3$ during the 400-hour sampling period. The widely varying and high concentrations during welding indicated that the ventilation system does not protect operators from the metallic fumes generated by their welding. Iron from the metallic fumes generated by welding was the dominant element. SEM analysis also indicated that a significant number of the particles in the welding area are in the nanometer range and were generated by welding.

#### *Conclusions*

Particulate sampling shows that most particles in indoor environments are in the submicron range. High enrichments of sulfur, iron, silicon, and calcium in indoor aerosols were observed. PM levels in indoor environments are influenced by indoor activities and outdoor environment.

### Activity 3.2 – Source of Indoor Air Pollution—Burning Candles

The goal of this study was to evaluate the impact of candle burning on indoor air quality by characterizing soot emissions from candles as a function of candle type. Because emissions from burning candles vary as functions of wax formulation, additives (pigment, fragrance), and shape (jar, pillar, votive), nine different candle types were selected to test their emissions. A summary of the selected candles is listed in Table ES-3. The diameters of the jar and pillar candles are in the range of 60–80 mm, while the votive candles usually are 35 mm in diameter.

**Table ES-3. Summary of the Tested Candles and Emissions from Candle Burning**

| Formulation | Color | Fragrance | Shape | Candle Number | Particle Emission, particles/g candle | Mass Emission, mg/g candle |
|---|---|---|---|---|---|---|
| | | | Jar | 1-A | $4.0 \times 10^{11}$–$1.3 \times 10^{13}$ | 0.159–0.998 |
| Paraffin | Yes | Yes | Pillar | 1-B | $1.53 \times 10^{12}$ | NA |
| | | | Votive | 1-C | $1.6 \times 10^{12}$ | 0.203 |
| | | | Jar | 2-A | $6.4 \times 10^{11}$ | NA |
| Soy Wax | Yes | Yes | Pillar | 2-B* | NA* | NA |
| | | | Votive | 2-C | $1.9 \times 10^{12}$ | 0.145 |
| | | | Jar | 3-A* | NA* | NA |
| Paraffin | No | No | Pillar | 3-B | $2.17 \times 10^{12}$ | 0.08 |
| | | | Votive | 3-C | $4.2 \times 10^{12}$ | 0.113 |
| | | | Jar | 4-A | $4.1 \times 10^{14}$ | 0.014 |
| Soy Wax | No | No | Pillar | 4-B* | NA* | NA |
| | | | Votive | 4-C | $3.0 \times 10^{12}$ | 0.087 |

* Unavailable due to candle manufacturer limitations.

A plexiglass chamber with a volume of 0.34 $m^3$ provided the controlled conditions for examination of the candle emissions. A condensation particle counter (CPC) measured particle emissions as a function of time, and an SMPS measured particle size distributions. Burning rates were monitored gravimetrically. Two prebaked quartz fiber filters in series ensured complete capture of PM and condensable organic compounds. The front filter collected essentially 100% of the PM and some adsorbed gas-phase materials. The backup filter was exposed to gas-phase materials, some of which adsorbed on the clean surface. Both filters were extracted with hexane followed by benzene/2-propanol. The extracts were filtered and split into two fractions for nonpolar organic compound analysis by GC, and for polar organic compound analysis. SEM provided the morphological analysis.

### *Results and Discussion*

The burning rates for the jar and pillar candles were in the range of 0.08–0.095 g/min; rates in the range of 0.05–0.06 g/min were observed for the votive candles. Particle emissions per gram of burning candle, both number and mass basis, were calculated based on the burn rates, particle concentrations in the exhaust, and exhaust flow rates; the results are listed in Table ES-3.

Temporal variations in particle number concentration in the exhaust were measured by CPC for jar, pillar, and votive candles. Particulate emissions for paraffin pillar candles with and without additives showed no significant impact of pigment and fragrance on particle emissions. Two soy wax jar candles (with and without additives) also were examined for their particle emissions under the same environment as the paraffin jar candle tests. The results, however, showed that the soy wax jar candle without any additives (pigment and fragrance) started with an extremely high particle emission, almost 2 orders of magnitude higher than the soy wax jar candles with additives (pigment and fragrance). The candle additives, instead of enhancing, impeded particle emissions from the soy wax jar candles. The soft soybean wax candle probably vaporized faster and produced more soot when burned than the hard-wax paraffin candles. By

comparing the mass and number concentration data for both paraffin and soy wax candles, it is clear that the particulate produced in soy wax candles either has a much smaller size or has a lighter density than the particle from paraffin candles. Paraffin jar candles appear to be as clean as, if not cleaner than, soy wax candles.

In the pillar and jar candle tests, the flames were stable, and so were the particle emissions. In the votive candle tests, however, the candle flame flickered more than the pillar and jar candle flames. Initially, with a steady supply of wax to wick, the flickered flame was stable. The continuously released heat melted the votive candle to form a wax pool with a much-reduced flame, resulting in a decreased burning rate and less heat released. Also, the natural air convection surrounding the flame was disturbed when the air was drawn across the votive edge. The disturbed air had a more obvious impact on the stability of the flame with a reduced size, causing more flickering. Therefore, particle emissions from burning votive candles fluctuated. The SMPS data indicated that significant amounts of nanometer particles were generated during burning regardless of wax formulation, additive, and shape of candle.

Most paraffin and soy wax candles had approximately the same level of particle emissions, except for the soy wax jar candles without additives, which were nearly 100 times higher. From a mass-based emission perspective, however, candles with color and fragrance have higher mass emission rates than candles without color and fragrance. Since most candles have similar particle size distributions, the discrepancy between the number and mass-based particle emissions suggests that denser particulates were generated from the colored and fragranced candles than the candles without color nor fragrance.

To further illustrate the impact of burning candle on PM level indoors, particle concentrations in the testing chamber under no candle burning were measured as a function of time with and without a HEPA filter, respectively. Without a HEPA filter trapping particles flowing into the test chamber, particle concentration in the chamber was maintained at $5.1 \times 10^3$ particles/cm$^3$, and gradually decreased to 0 particles/cm$^3$ when the HEPA filter was used. After a particle-free environment was obtained, the candles were ignited while the particle-free air continuously flowed through the chamber. The air flow rate had to be increased dramatically (an increased air-exchange rate of 36/hr) to dilute the particle concentration in the exhaust below the CPC measurement limit. Even under high dilution, the particle concentration jumped to $1.1 \times 10^6$ particles/cm$^3$.

The test candles were extracted and analyzed by GC to determine organic species present. Table ES-4 summarizes the organic compound class detected in paraffin and soy wax candles.

**Table ES-4. Organic Species Detected in Paraffin and Soybean Wax Candles**

| | |
|---|---|
| Paraffin Candle with Additive | Alkane (including straight chain and branched alkanes), ester, and UCM |
| Soybean Wax Candle Without Additive | Alkane (including branched and cyclo alkanes), alkanoic acid, ester, UCM |
| Soybean Wax Candle with Additive | Alkane, alkanoic acid, ester, UCM[1] |

[1] UCM: Unidentified complex mixture.

Extractable and elutable fractions of the PM and vapor samples from candle burning also were identified and further quantified by GC–MS. The analytical results suggest that most of the organic compounds in the PM and vapor emissions from candle burning consist of candle components. The predominant alkanes in the paraffin candle emission are most likely the result of direct vaporization of alkane wax material and subsequent condensation into the particle phase. The presence of ester in the soy wax emission (the dominant component) was also due to volatilization. Other compounds found in the emissions are pyrolysis products. Higher levels of organic acid were detected in the emission from the soy wax candle with additive, which is probably caused by the pigments and fragrances in the candles. No PAHs were detected. Neither paraffin nor soy wax candles contain identified alkenes, but low levels of alkenes were found in their emissions, in the range of $C_{11}$–$C_{17}$. The measured alkenes are most likely derived from alkanes that are thermally altered.

The morphological analysis of the particle sample using SEM revealed huge amounts of fine particles (much less than 1 μm) on the filter. These fine particles were generated from burning candles by volatilization and condensation. These airborne fine particles were likely agglomerated with each other to form clusters when they were captured on the filter. Although there was no significant amount of toxic materials found in the candle emissions, the ultrafine particles generated in candle burning present in high number with greater surface area than larger particles, and can reach the alveoli deep in the lungs with high deposition efficiency of 50% (17). The deposition of ultrafine particles in airway not only induce inflammatory response which may damage tissue surface but also may move rapidly into blood stream to trigger other effects. Since ultrafine particle may be more likely to interact with cells in the lungs than those larger particles, they may be harmful regardless of specific components, or they can be a carrier to ferry toxicants deep into the lungs.

### *Conclusions*

Various candles in terms of formulation (paraffin and soy wax), additives (with and without color and fragrance), and shape (jar, pillar, and votive) were tested in a controlled environment to examine their emissions. Experimental data show that burning always released significant amounts of fine particles (less than 1 μm): $10^{12}$–$10^{13}$ particles/g — paraffin candle, and $10^{11}$–$10^{14}$ particles/g — soy wax candle. Both jar and pillar type candles had stable particle emissions, while votive candles had a fluctuated pattern because of the turbulent air flow surrounding the flame.

Chemical analysis showed that most emissions are from vaporization and condensation of volatile wax compound combined with thermally altered by-product. Although no PAH was detected in both particle and vapor emissions from paraffin and soybean wax candles, the generation of significant amounts of ultrafine particles may still be of concern to human health.

## REFERENCES

1. Hannigan, M.P.; Cass, G.R.; Penman, B.W.; Crespi, C.L.; Lafleur, A.L.; Busby, W.F. Jr.; Thilly, W.G. *Environ. Sci. Technol.* **1997**, *31*, 438.

2. Moolgavkar, S.H.; Luebeck E.G. *Epidemiology*. **1996**, *7*, 420.

3. Squadrito, G.L.; Cueto, R.; Dellinger, B.; Pryor, W.A. *Free Rad. Biol. & Med.* **2001**, *31*, 9.

4. Bitton, G.; Koopman, B. *Rev. Environ. Contam. Toxicol.* **1992**, *125*, 1.

5. Oanh, N.T.K.; Nghiem, L.H.; Phyu, Y.L. *Environ. Sci. Technol.* **2002**, *36*, 833.

6. Buschini, A; Cassoni, F.; Anceschi, E.; Pasini, L.; Poli, P.; Rosi C. *Chemosphere* **2001**, *44*, 1723.

7. Li, N.; Venkatesan, M.I.; Miguel, A.; Kaplan, R.; Gujuluva, C.; Alam, J.; Nel, A. *J. Immunol.* **2000**, *165*, 3393.

8. Lund, L.G.; Aust, A.E. Iron mobilization from crocodilite asbestos greatly enhances crocodilite-dependent formation of DNA single-strand breaks in φX174 RFI DNA. *Carcinogenesis*. **1992**, *13*, 637–642.

9. Long, C.M.; Suh, H.H.; Koutrakis, P. *J. Air Waste Manage. Assoc*. **2000**, *50*, 1236–1250.

10. Kamens, R.; Lee, C.T.; Weiner, R.; Leith, D. *Atmos. Environ*. **1991**, *25A*.

11. Wallace, L.A. *J. Air Waste Manage. Assoc.* **1996**, *46*, 98–126.

12. Veranth, J.M.; Smith, K.R.; Hu, A.A.; Lighty, J.S.; Aust, A.E. *Chem. Res. Toxicol.* **2000**, *13,* 382–389.

13. Tucker, W.G, *Fuel Processing Technology*, **2000**, 65, 379–392.

14. Van Alphen, M. Emission Testing and Inhalational Exposure-Based Risk Assessment for Candles Having Pb Metal Wick Cores. *Science of the Total Environment*, **1999**, *243/244*, 53–55.

15. Nriagu J.O.; Kim, M.J., Emission of Lead and Zinc from Candles with Metal-Core Wicks. *Science of the Total Environment* **2000**, *250*, 31–37.

16. Lau, C.; Fiedler, H.; Hutzinger, O.; Schwind, K.-H.; Hosseinpour, J. Levels of Selected Organic Compounds in Materials for Candle Production and Human Exposure to Candle Emissions. *Chemosphere*. **1997**, *34*, 1623–1630.

17. International Commission on Radiological Protection, Human Respiratory Tract Model for Radiological Protection, Report of Committee 2 of the ICRP, Oxford: Pergamon Press, 1994.

18. Seaton, A.; MacNee, W.; Donaldson, K.; Godden, D. Particulate Air Pollution and Acute Health Effect. *Lancet*, **1995**, *345*, 176–178.

19. Utell, M.J.; Frampton, M.W. Acute Health Effects of Air Pollution: The Ultrafine Particle Hypothesis. *Journal of Aerosol Medicine*, **2000**, *13* (4), 355–359.

# SUBTASK 2.2 – FINE PARTICULATE ($PM_{2.5}$) CHARACTERIZATION AND SOURCE APPORTIONMENT

## ACTIVITY 1 – FRACTIONATION OF ORGANICS FROM AIR PARTICULATES WITH SUBCRITICAL WATER

### Introduction

The toxic effects of fine particulate aerosols (particles smaller than 2.5 μm) are discussed in a number of studies (1, 2). In contrast to inorganic aerosols, which are well characterized, only 15%–50% of the organic carbonaceous (OC) particulate mass has been characterized. The characterized compounds are almost exclusively nonpolar (3). The limited knowledge on OC fractions is due to the use of organic solvents, which are able to extract only nonpolar or slightly polar organics. Moreover, with conventional solvent extraction, toxicity tests on OC are difficult to perform because the solvents employed are biologically toxic. Consequently, the toxicity of organic aerosols has been primarily studied for nonpolar OC (for example, polycyclic aromatic hydrocarbon [PAHs]), while the toxicity of significant polar fractions of OC is not known. These polar organics may also be important for mobilizing toxic metals from air particulates in biological systems by chelation reactions (4). Although not previously reported, subcritical water should have the ability to extract a broad range of polar to low-polarity OC from air particulate matter (PM), as well as to provide extracts in a solvent (water) that is directly useful for toxicological tests. At lower temperatures (e.g., 50°–100°C), water can extract polar compounds. At higher temperatures (e.g., to 250°C), the polarity of water decreases, and therefore, nonpolar compounds can be extracted (5, 6). Earlier studies have shown that compounds of different polarities such as phenols, PAHs, and alkanes could be sequentially extracted from a petroleum waste sludge by increasing subcritical water temperature (7).

The toxicity of aerosol particulate is mostly evaluated indirectly through correlation of aerosol composition with epidemiological studies and/or inhalation studies requiring large amounts of samples directly delivered to tested organisms (1, 8, 9). Because of faster evaluation (1–3 days) and low expenses, in vitro tests are often used for evaluation of different environmental matrices such as soils or waste waters (10). Several in vitro tests have been previously employed to express toxicity of aerosol particulate (11–13).

In this work, we have used subcritical water (from 25°–300°C) to sequentially fractionate two carbonaceous aerosols: diesel exhaust particulate (a relatively nonpolar matrix) and wood smoke particulate (a polar matrix). To evaluate the importance of each fraction, four different toxicity tests were performed. Effects on respiration were examined using bacterial culture (Polytox™) and rat hepatic mitochondria. The SOS-Chromotest was used to measure bacterial genotoxicity. Cytotoxicity to mammalian cells was analyzed using COS cells. The data obtained were related to composition of extracts, which was determined on the basis of carbon, hydrogen, nitrogen (CHN) and sulfur analysis, total organic carbon (TOC), gas chromatography–mass spectrometry (GC–MS) analysis, and diesel exhaust particulate analysis of metals.

### *Evaluation of Toxicity of Agricultural Soils*

In addition, the developed method was applied to evaluate toxicity of another environmental matrix such as soil contaminated with pesticides. Pesticides are expected to be a major contributor to the toxicity in agricultural soils. When determining the contamination of soil or ground water caused by agricultural use, chemical analysis targeted specifically for pesticides is performed. This approach automatically assumes that pesticides are the only contributor to total soil toxicity and omits possible pollution by pesticide degradation products or their metabolites.

To evaluate whether pesticides are the only contributor to the total toxicity of soils, the toxicity of different components of the soil must be evaluated. As was shown for air particulate, subcritical water is a suitable tool for the fractionation on the polarity bases. Subcritical water fractionation (SWF) was applied to pesticide-contaminated soil and compared to organic solvent extraction, which extracts mainly pesticides. The subcritical water fractions and organic solvent extracts were evaluated with respect to their cytotoxicity, content of pesticides, and mass of material extracted.

## Experimental

### *Sample Material*

Bulk diesel exhaust particulate was collected from the exhaust pipe of a diesel bus, homogenized and stored frozen until use. Bulk wood smoke particulate was collected from a chimney that vented an airtight wood stove burning a mix of hardwoods (14).

Samples of ambient PM were obtained from Assist. Prof. Allen Robinson (Carnegie Mellon University, Pittsburgh) and the subcritical fractionation method was successfully applied to those samples.

### *Subcritical Water Fractionation*

#### *Fractionation of Common PM Samples*

Subcritical water extraction was performed in an apparatus previously described in detail (15). The sequential extraction was performed at temperatures of 25°, 50°, 100°, 150°, 200°, 250°, and 300°C, holding each temperature for 30 min. The pressure was first held at 50 bar. At 250° and 300°C the pressure was increased to 100–150 bar to maintain the water in a liquid state. The extracts were collected into 5 mL of water into a preweighed collection vial (40 mL). To prevent loss of samples, the collection vial was cooled in an ice bath. After each extraction, the extraction system was washed with water heated from 25° to 325°C, and at 325°C with steam. The system was also washed in sequence with 5 mL of acetone, methylene chloride, and again acetone.

### *Application of Subcritical Water Extraction–Fractionation to Ambient Aerosol Samples*

Three different samples—an ambient aerosol sample from Pittsburgh area, an ambient aerosol sample influenced by coke emissions, and a sample collected in a Pittsburgh highway tunnel—were obtained from Prof. Allen Robinson, Carnegie Mellon University. Atmospheric samples for organic analyses are collected on 20 × 25 cm quartz filter using high volume throughput sampler. In contrast to previously tested samples—wood smoke and diesel exhaust particulate—which were available in powder form (as a bulk). Therefore, before the experiment on particulate samples, we tested subcritical water extraction of the blank filter to verify that no plugging would occur. Once the particulate was extracted using the subcritical water extraction technique, the in vitro toxicity tests were applied.

### *Subcritical Water Fractionation and Comparison to Solvent Extraction in Relation to Composition*

In order to evaluate the subcritical water extraction in comparison to standard organic solvent extraction, the soil sample heavily contaminated with pesticides (2 g) was extracted using two different methods:

a) Organic solvent extraction. The soil was sonicated for 18 h in methylene chloride–acetone (2:1).

b) SWF (25°–275°C). The sample was extracted at each temperature for 20 min at flow rate of 1 mL/min. The residue from the subcritical water extraction was further extracted using solvent extraction.

## ***Toxicity Tests***

Each toxicity test was first performed on concentrated water extracts. Because the concentrated water extracts precipitated, additional tests were performed on dried samples, which were redissolved in dimethyl sulfoxide (DMSO). For each toxicity test, no toxic effect of DMSO was observed. The highest concentration of DMSO per assay was 1%. All tests were performed on the same fraction of water extracts.

### *Polytox™*

The bacterial respiration test was performed with specialized bacterial cultures of Polytox™ (InterBio, The Woodlands, Texas). The freeze-dried culture was grown overnight at 37°C mixed in buffered solution (16). The culture was allowed to settle, then decanted and supernatant stored on ice and used for toxicity screening. The bacterial consumption of oxygen was measured with a biological oxygen monitor (YSI, Inc., Yellow Springs, Ohio). The DMSO (10 µL) samples did not influence the oxygen consumption/formation.

*Cytotoxicity Test*

The cytotoxicity test measured the inhibition of the viability of mammalian COS cells using MTT (microtiter) assay (17, 18). The cells were grown in tissue culture flasks (75 mL) in 12 mL of D-modified essential medium (DMEM) tissue culture medium with 10% fetal calf serum and 1% penicillin streptomycin in a thermostated $CO_2$ incubator. When the confluence of the cells achieved 90%–100%, the cells were removed from the flasks with 0.05% Trypsin (a proteolytic enzyme) and 0.53 mM EDTA•4Na (a chelating agent), counted, and diluted to obtain a concentration of 10,000 cells per 180 µL of tissue culture medium. The experiment was performed on 96-well microplates. On the first day, 180 µL of culture was introduced to each well, and on the second day 10 µL of sample diluted in tissue culture medium was added; the final concentration of DMSO in tissue culture (if used) was <1%. All samples were studied in quadruplicate with two blank controls and were incubated overnight. The toxicity was evaluated using MTT assay (17, 18). The results were analyzed at absorbance of 570 nm using an enzyme-linked immunosorbent assay (ELISA) plate reader (SpectraMax Plus 384, Molecular Devices).

Before the toxicity test, the pH of all samples was adjusted with 1M NaOH to 7.

*SOS-Chromotest*

The SOS-Chromotest is a bacterial genotoxicity test developed by Quilllardet et al (19) as an alternative to the Ames test (20).

An *Escherichia coli* strain PQ 37 (obtained from Pasteur Institute, France) containing a fusion gene of a ß-galactosidase (ß-Gal) gene (lacZ) with an SOS response gene (sfiA) was used in this assay. Activation of the SOS repair system by genotoxic agents is measured by photometric determination of the ß-Gal enzyme activity. The procedure for the miniaturized test was based on previously published procedures (21–23). A sample of overnight culture was diluted with 10 mL of L-arginine (LA) medium (20) and incubated at 37°C in a gyratory incubator until it reached optical density of $OD_{600}$ = 0.5, then 1 mL of culture was diluted with 9 mL of lysine (L) medium (20). For metabolically activated experiments, activity of bacteria used was 4× higher (24). The tester strain (100 µL) and 10 µL of samples were introduced into 2 mL polypropylene tubes, which were incubated with shaking for 2 hr at 37°C in a water bath. For the toxicity determination of each extract, eight tubes were prepared, two with L medium instead of the culture (blanks) and six with the culture. Half of the samples (blank + 3) were used for the determination of alkaline phosphatase (AP) activity and the other half for determination of ß-Gal activity.

ß-Gal assay was based on Miller's procedure (23). After incubation of the sample with the culture, 0.9 mL of ß-Gal buffer, 30 µL 0.1% SDS, and 50 µL chloroform were added, mixed, and incubated at 37°C for 5 min, than 200 µL of 0.4% o-nitrophenyl-ß-D-galactopyranoside (ONPG) (Aldrich) was added and the mixtures were incubated for 25–60 min (time sufficient for color development) with shaking at 37°C in a water bath. The conversion of ONPG was stopped by 200 µL of 4 M $NaNO_3$. The procedure for AP determination was similar to ß-Gal assay, only instead of the ß-Gal buffer, an AP buffer was used, and instead of ONPG, p-nitrophenyl phosphate disodium salt hexahydrate (pNPP-NA, Aldrich) was used. The reaction was stopped

after 10 min with 200 µL of 6 M NaOH. The extent of reaction was measured on a Spectrometer 65 DU (Beckman) at absorbance of 405 nm against a blank (tube containing all ingredients but bacteria). A similar procedure was followed for metabolically activated experiments, with rat liver mixture S9 (In Vitro Technologies, Baltimore, Maryland) added to the culture prior to the incubation with extracts (21, 24).

As with the cytotoxicity tests, the pH of these samples was adjusted with 1M NaOH.

*Mitochondrial Respiration Assay*

Liver tissue was isolated from adult male Harlan Sprague-Dawley rats using a modified procedure of Picklo and Montine (25). Isolation buffer consisted of mannitol (0.21 M), sucrose (70 mM), HEPES (an organic buffer) (5 mM), EGTA (an acid reagent) (1 mM), and bovine serum albumin (BSA 1 mg/mL) with a final pH of 7.4 at 4°C. Rats were deeply anesthetized and their livers removed and homogenized in a 10-fold excess (v/w) of buffer. Homogenates were centrifuged at 3000 g for 2 minutes (4°C) to pellet nuclei and cellular debris. The supernatant was then centrifuged at 12,000 g (4°C) for 10 minutes. The pellet was resuspended in 10 mL of homogenization buffer and centrifuged at 12,000 g (4°C) for 10 minutes. The pellet was resuspended in buffer (10 mL) without BSA and was centrifuged at 12,000 g (4°C) for 10 minutes. This final pellet was resuspended in 0.5 mL of buffer without EGTA. Protein concentration was measured using a protein assay reagent (BioRad) with BSA as the standard.

Respiration was measured using an oxygen electrode (YSI, Inc., Middleton, Wisconsin) and oxygen consumption chamber (Gilson) (25). Experiments were performed at 37°C. Assay media contained 125 mM KCl, 5 mM $MgCl_2$, 2 mM $KPO_4$, and 5 mM HEPES-KOH (pH 7.4). Complex I-linked substrate (5-mM glutamate) was used to stimulate State 4 respiration. State 3 respiration was measured for 2 minutes following adenosine diphosphate (ADP) (1 mM) addition.

***Chemical Characterization***

*Elemental Analysis*

CHN analyses were performed on wood smoke and diesel exhaust particulate water extracts of 500 and 200 mg, respectively. The extracts were dried under a stream of nitrogen and submitted to analysis. TOC analyses were performed directly on water extracts obtained by extraction of 100 mg of particulate using U.S. Environmental Protection Agency (EPA) Method 415.1. To obtain general information on total composition of wood smoke and diesel exhaust particulate, x-ray fluorescence spectrometry semiquantitative scans were performed on both particulate samples. Diesel exhaust particulate contained higher quantities of metals. Therefore, the extracts were analyzed using inductively coupled plasma mass spectrometry (ICP–MS) for selected metals.

### *Gas Chromatographic Analysis*

Prior to analysis, the water extracts were dried and redissolved in 200 µL of acetone. GC/MS analyses were performed using a Hewlett-Packard Model 5890 GC with a Hewlett-Packard Model 5972 GC–MS in the full-scan mode (45–500 m/z) with electron-impact ionization. Tentative quantifications were performed on GC with flame ionization detection (FID) on a Hewlett Packard Model 5890 Series II GC equipped with an autosampler. Quantitative analyses were based on the external calibration with compounds typical for diesel exhaust and wood smoke particulate such as PAHs, alkanes, syringol, and quaiacol derivatives. On both instruments, chromatographic separations were accomplished with a 30 m DB-5 column with a 0.25 mm I.D. and a 0.25 µm film thickness (J&W Scientific, Rancho Cordova, California) with injections in the splitless mode. The oven temperature was held at 40°C for 0.2 min followed by 10°C/min gradient to 320°C and then held for 20 min.

## Results and Discussion

Two common carbonaceous aerosols—diesel exhaust particulate (relatively nonpolar matrix) and wood smoke particulate (polar matrix)—were sequentially extracted using a range of subcritical water temperatures from 25° to 300°C. The toxicological importance of individual fractions was studied on four separate models: bacterial and mammalian cell respiration, mammalian cell cytotoxicity, and bacterial genotoxicity. Each test was first performed using concentrated water extracts, but because the cooled concentrated water extracts precipitated, the tests were also performed on dried extracts, which were dissolved in DMSO. Both tests gave similar trends, but the response was more pronounced in DMSO-dissolved extracts. Therefore, all data presented are based on the use of DMSO.

### ***Toxicity of Wood Smoke Particulate***

The toxicity tests were performed on the same proportion of each temperature extract. This approach allowed comparison of the contribution of each water fraction to the total toxicity of the whole sample. Results obtained with different toxicity tests are obviously specific to different classes of compounds. The data on Polytox™ show the low sensitivity of this test (Figure I-1a). The tests on extracts dissolved in water, which were performed with larger fractions of samples, (20% and 40%), showed inhibition to 20% of normal bacterial respiration of 25° and 50°C fractions (polar). For the second bacterial test, the SOS-Chromotest (Figure I-1b), two sets of data were obtained: 1) The AP activity representing the total protein synthesis, which shows that fractions collected at 100° and 150°C have the highest toxicity; and 2) the genotoxic response, which is expressed as a formation of β-galactosidase enzyme; for wood particulate extracts, no genotoxic response was observed. It is known that many compounds such as PAHs are genotoxic after enzymatic metabolic activation, when arylhydroxylase in the liver metabolizes PAHs into hydroxylated compounds, which are water-soluble and toxic. Therefore, tests also were performed with rat liver microsomal S9; however, no increase in genotoxicity was observed after activation. Each test was validated on test compounds, m-cresol for the Polytox™ and 4-nitroquinoline oxide (NQO) for the genotoxicity test. Similarly to Polytox™, the cytotoxicity test using mammalian COS cells (Figure I-2a) showed higher toxicity of more polar fractions; however, it is important to note that the extracted mass was higher in polar fractions.

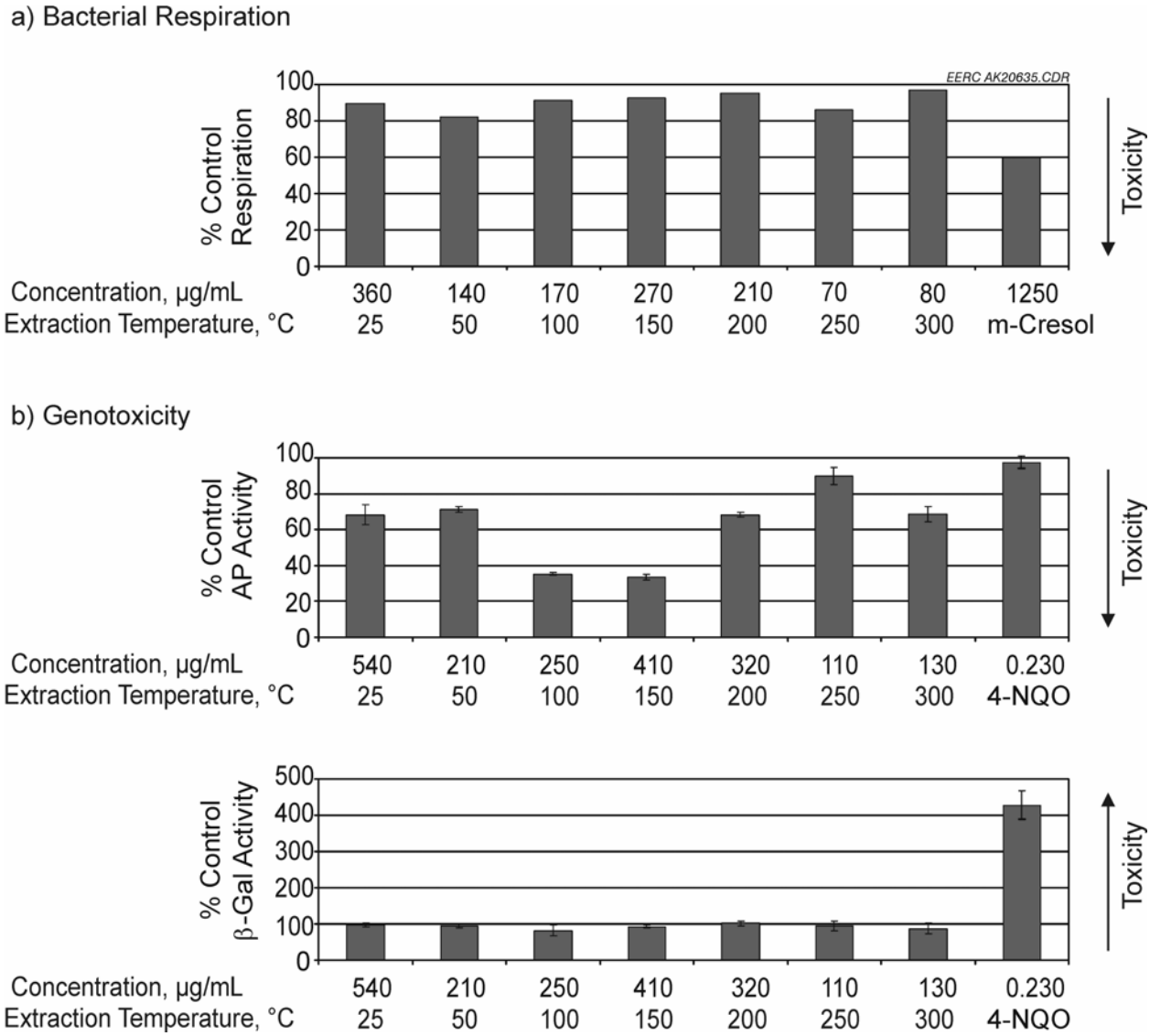


Figure I-1. The results from bacterial toxicity tests performed on wood smoke particulate fractions obtained sequentially at 25°–300°C. a) Bacterial respiration (Polytox™) 5% of each extract, b) Genotoxicity (0.5%).

The results from the test on rat liver mitochondrial respiration (Figure I-2b) show uncoupling activity of higher temperature (200°–300°C) extracts (State 4). In addition, the extracts of 150° and 200°C blocked ADP-stimulated respiration (State 3).

### *Toxicity of Diesel Exhaust Particulate*

The toxicity of diesel exhaust particulate water fractions is shown in Figures I-3 and I-4. Both the water fraction obtained at 25°C (polar materials), which was dried and dissolved in DMSO, and the concentrated water showed significant inhibition of bacterial respiration (Figure I-3a). In contrast to wood smoke particulate, significant genotoxicity was observed for

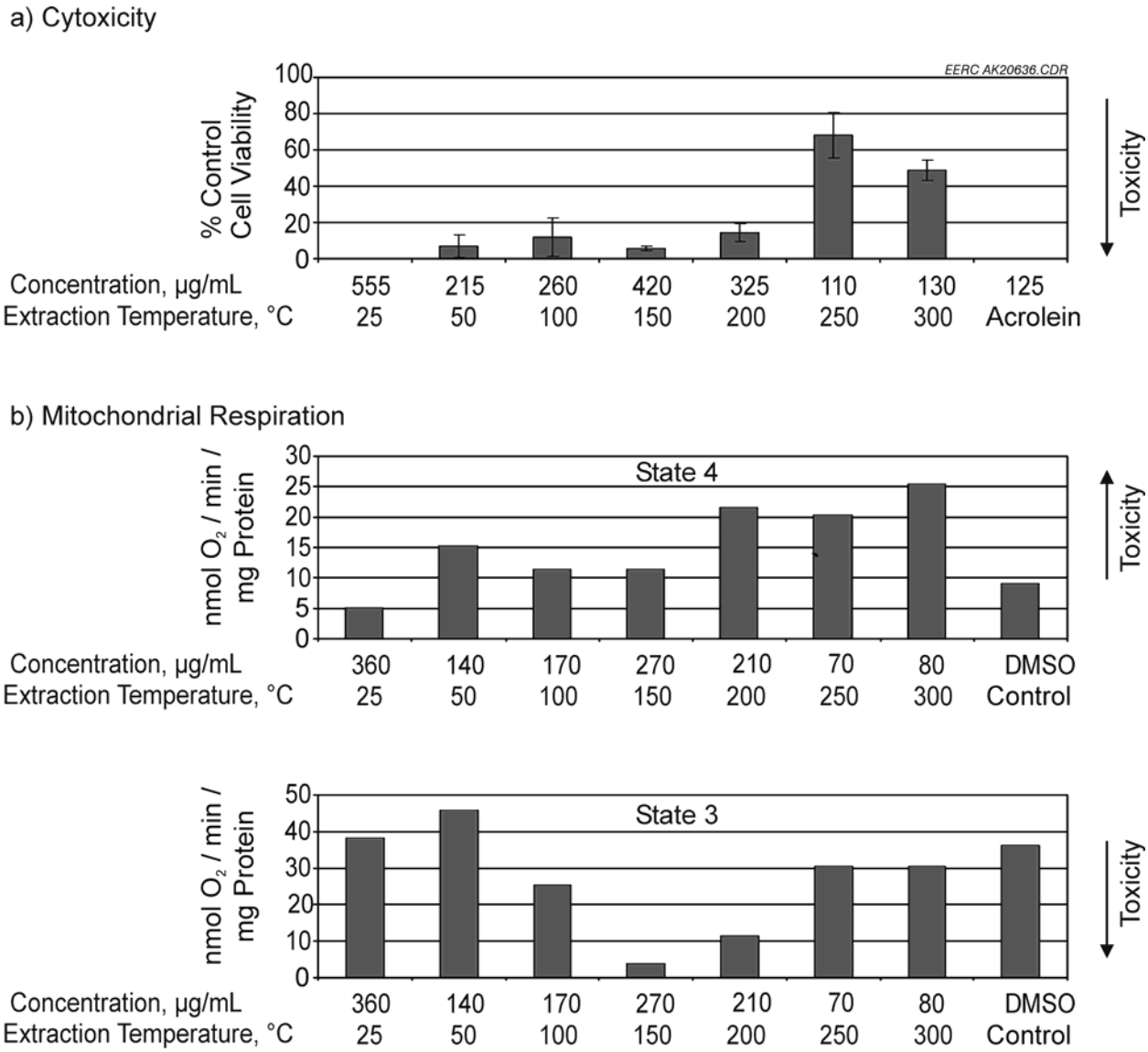


Figure I-2. The results from toxicity tests performed on wood smoke particulate fractions obtained sequentially at 25°–300°C. a) Cytotoxicity 1% of each extract compared to acrolein, b) Mitochondrial respiration (5%) compared to effect of DMSO.

fractions extracted between 100° and 250°C. For those temperatures, the protein synthesis also was inhibited (Figure I-3b).

The cytotoxicity of diesel exhaust (nonpolar matrix) showed increasing toxicity with increasing extraction temperature. This trend is opposite to the cytotoxicity (Figure I-4a) of wood smoke particulate (polar matrix) fractions (Figure I-2a) and may correspond with the difference of sample polarities.

Mitochondrial respiration significantly increased for the fractions collected above 100°C; this may correspond to the extracts uncoupling activity (state 4). The same fractions also had

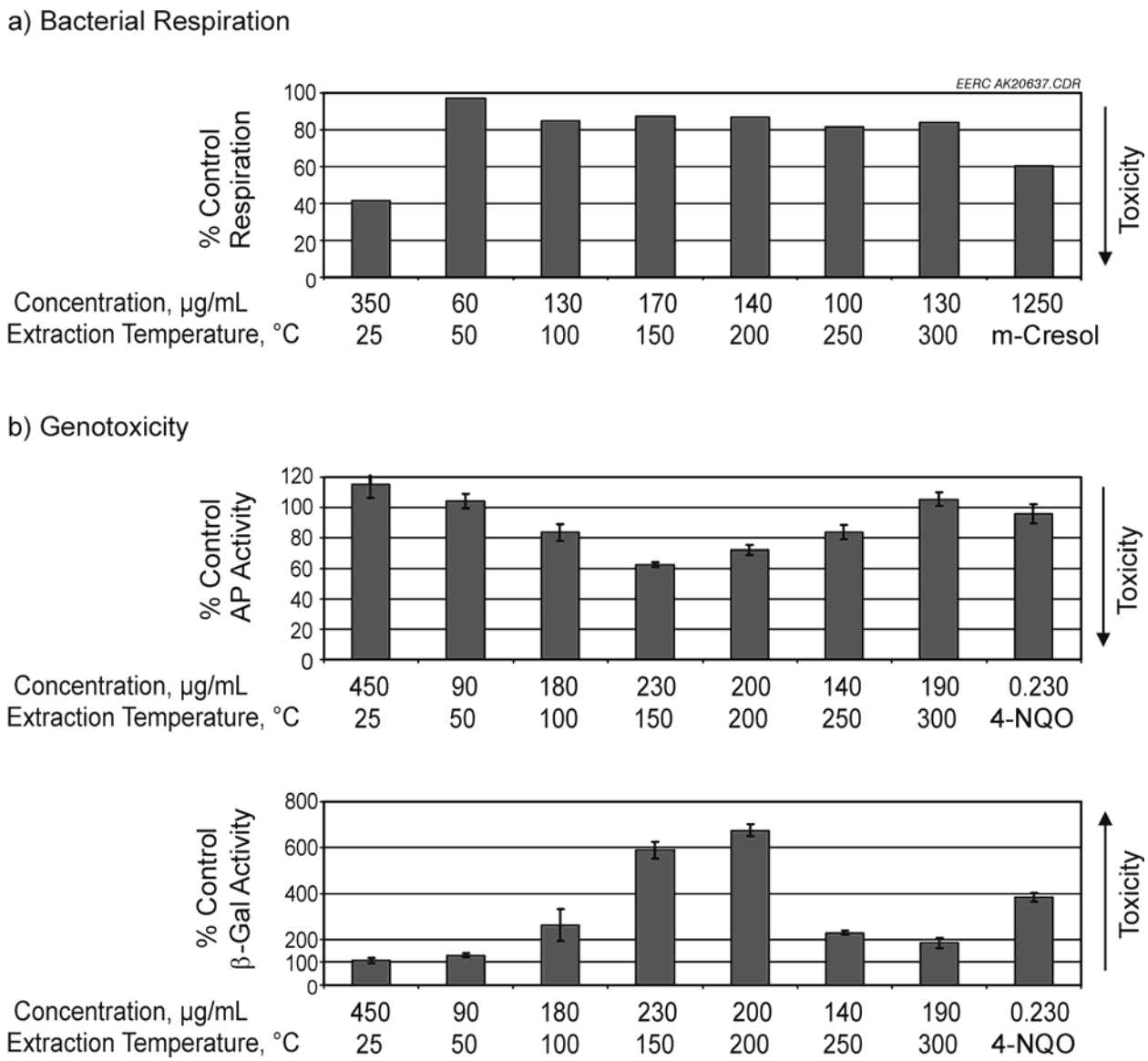


Figure I-3. The results from bacterial toxicity tests performed on diesel exhaust particulate fractions obtained sequentially at 25°–300°C. a) Bacterial respiration (Polytox™) 5% of each extract, b) Genotoxicity (0.5%). Each test was validated on test compounds, m-cresol for the Polytox™ and 4-NQO for the genotoxicity test.

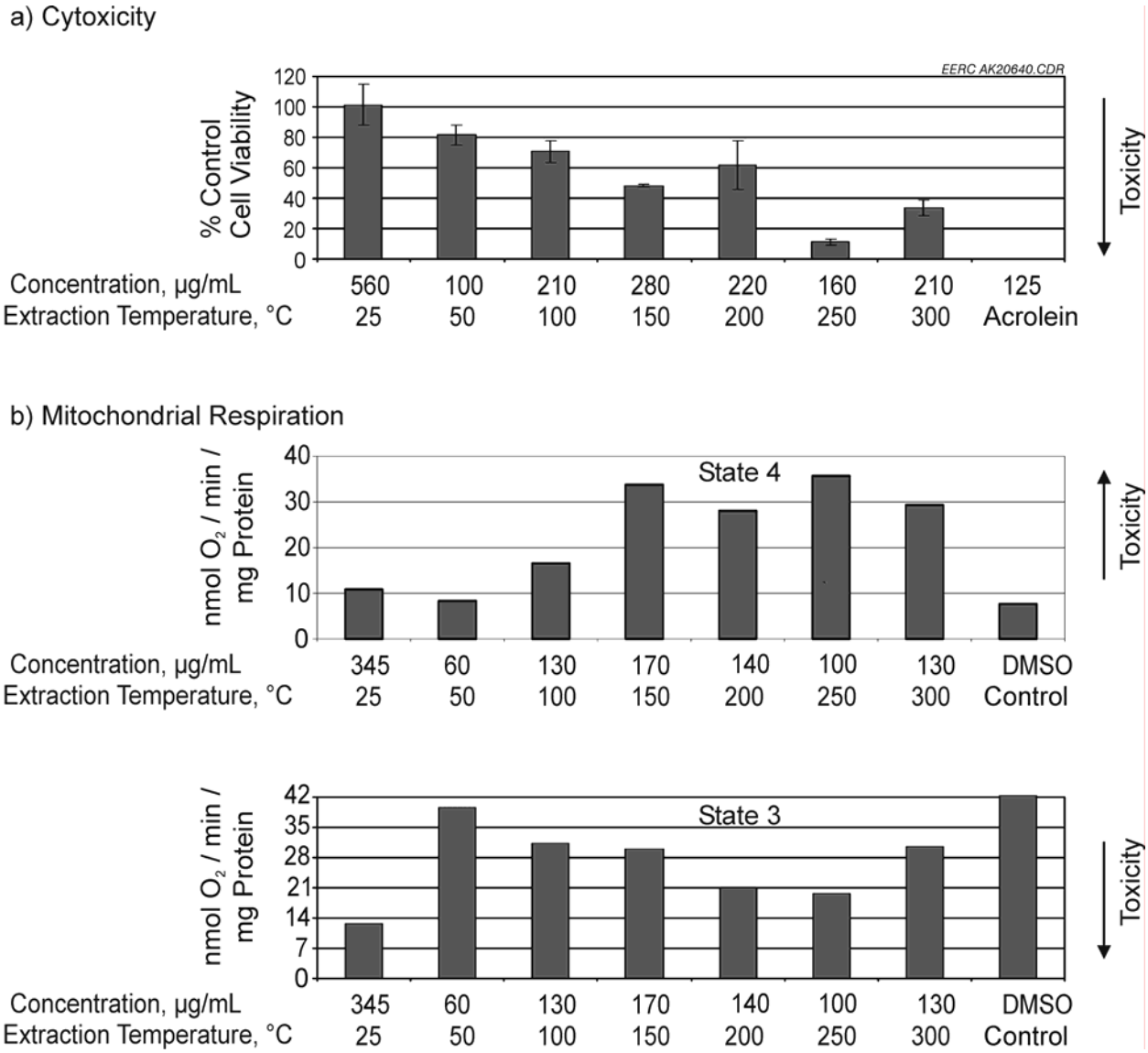


Figure I-4. The results from bacterial toxicity tests performed on diesel exhaust particulate fractions obtained sequentially at 25°–300ºC. a) Cytotoxicity 1% of each extract compared to acrolein, b) Mitochondrial respiration (5%) compared to the effect of DMSO.

blocked state 3 respiration. Interestingly, the 25°C fraction for which the inhibition of bacterial respiration was observed did not show uncoupling activity but did block ADP-stimulated respiration (state 3).

### *Characterization and Possible Relationship to Toxicity Results*

Detailed characterization is needed to explain the toxicity of different fractions. Therefore, elemental analyses for CHN and S were performed, the TOC was determined, the extracts were analyzed using GC–MS, and the diesel exhaust particulate was characterized for metals.

*Elemental Analysis*

The mass extracted, CHN, and sulfur contents for both PMs are shown in Figure I-5. The gravimetric data show the most polar water (25°C) extracted the highest mass of particulate. The total extracted particulate with subcritical water extraction (25°–300°C) was 42 and 34 wt% for wood smoke particulate and diesel exhaust particulate, respectively. Figure I-5 shows that the CHN and S composition corresponds to 40–60 wt% of the extracted mass for each fraction. To determine if the carbon extracted with water is mainly organic carbon (as opposed to carbonate or graphitic carbon), elemental carbon (total carbon) values were compared to TOC values in the water extracts (Figure I-6). Good agreement between elemental carbon and TOC values demonstrates that extracted carbon is essentially organic. Organic carbon determinations can be used to approximate the extracted mass of organic compounds, including oxygenated organics, by multiplying the TOC values by a factor estimated to include average oxygen content. The most common factor is 1.4, which corresponds mainly to aerosols in urban areas (26). Recently, it has been shown that for aerosols heavily impacted by wood smoke, a factor of 2.2–2.6 is more

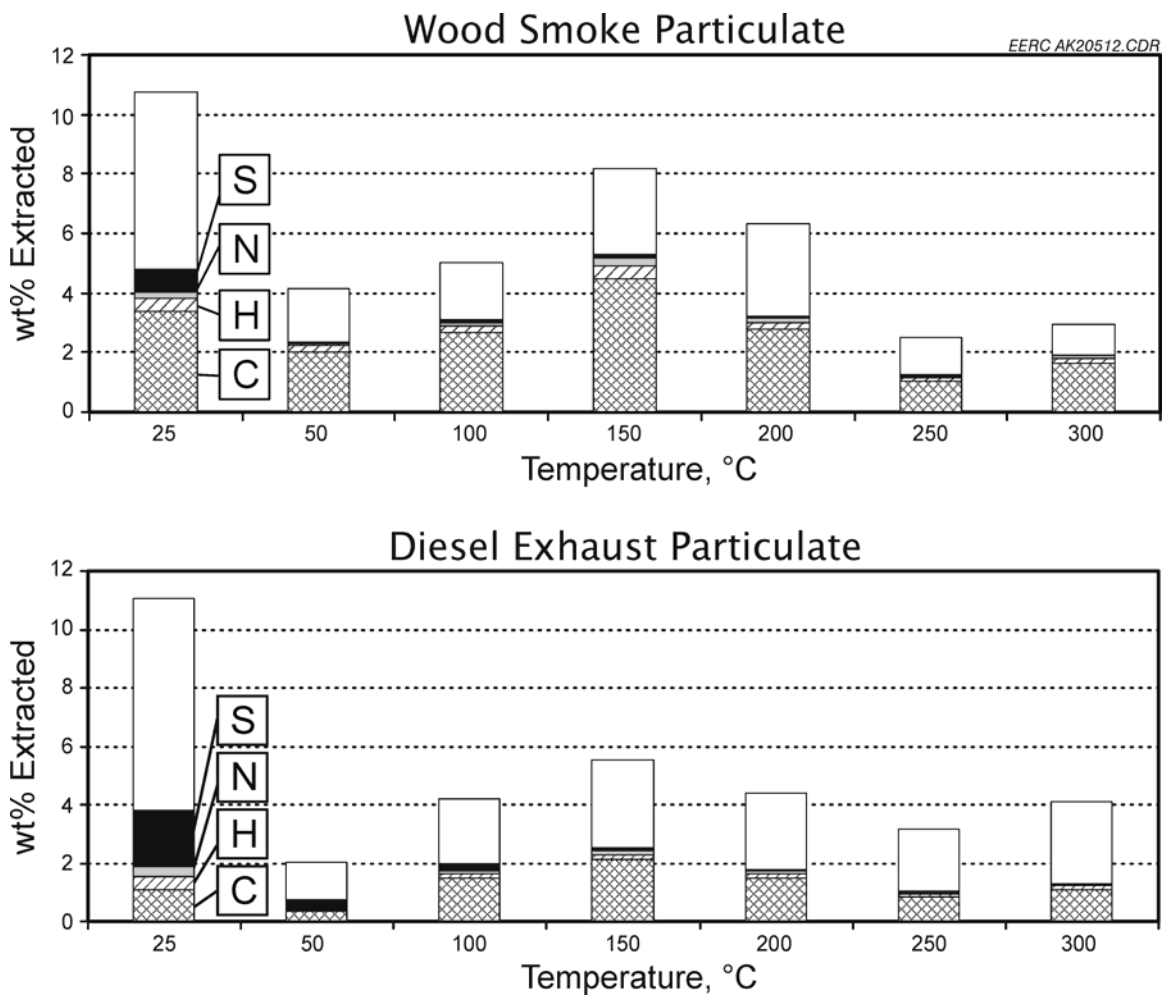


Figure I-5. CHN and sulfur determination on diesel exhaust and wood smoke particulate fractions extracted sequentially with subcritical water at 25°–300°C.

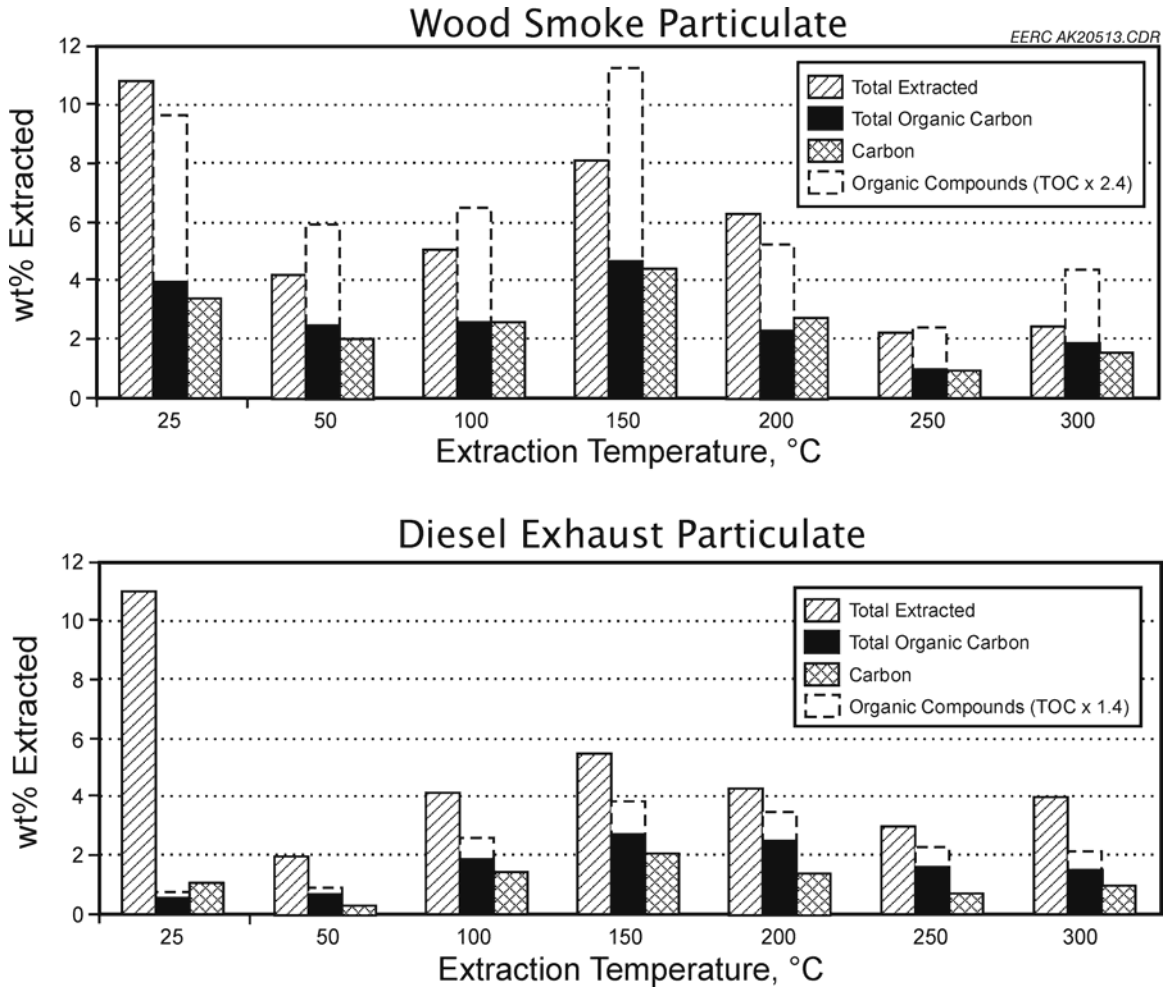


Figure I-6. Determination of extracted mass, total organic carbon, carbon, and estimates of organic compound mass of wood smoke and diesel exhaust particulate fractions extracted sequentially with subcritical water at 25°–300°C.

suitable (26). Therefore, for an estimation of total organics in wood smoke and diesel exhaust particulate, which includes oxygenates, we have used an average factor of 2.4 and 1.4, respectively. For most of the wood smoke particulate water fractions, the estimated total organic compound mass corresponds to (or exceeds) the amount extracted. For diesel exhaust, the estimated total organic compound mass is lower than the total extracted, probably because of the presence of inorganic compounds, especially in the most polar (25°C) fraction.

The most selective extraction was observed for sulfur (Figure I-5). Increased sulfur content was found in both samples of the fraction collected at 25°C. The initial concentration of sulfur in diesel exhaust particulate was 40 mg/g. In the lowest-temperature fractions (which were the most toxic), 75% of the sulfur was recovered.

### *GC–MS and GC–FID Analysis*

The identification of individual components in each fraction was performed using GC–MS. GC–FID was used for tentative quantification. Although GC is limited to the determination of mainly nonpolar or slightly polar compounds present in samples, we observed increased concentrations of lignin pyrolysis products such as syringol and quaiacol derivatives, phenols, and benzenediols in low-temperature fractions from wood smoke particulate (Figure I-7). Interestingly, a high quantity of levoglucosan, a typical marker of wood burning, was found in water extracts but was not observed in acetone extracts. It is important to note that in using GC–MS, we were able to analyze with only about 24% of the total extracted mass. GC–MS analysis of diesel exhaust was not as informative as that of wood smoke particulate, because the GC-elutable fraction of diesel exhaust consists mainly of alkanes and PAHs. When using GC–MS in selected ion recording mode, selective extraction of nitropyrene at temperature 150° and 200°C was observed. The presence of nitroaromatics would explain genotoxicity of the same diesel exhaust extracts.

### *Metal Analysis*

ICP–MS metal analysis showed high concentrations of zinc, iron, magnesium, and manganese in the most polar fraction (25°C) (Figure I-8). All of these elements were probably present in the form of sulfates, which are soluble in water. The presence of sulfates may correspond to increased concentration of sulfur (Figure I-5) and also to lower pH of 2.5. The

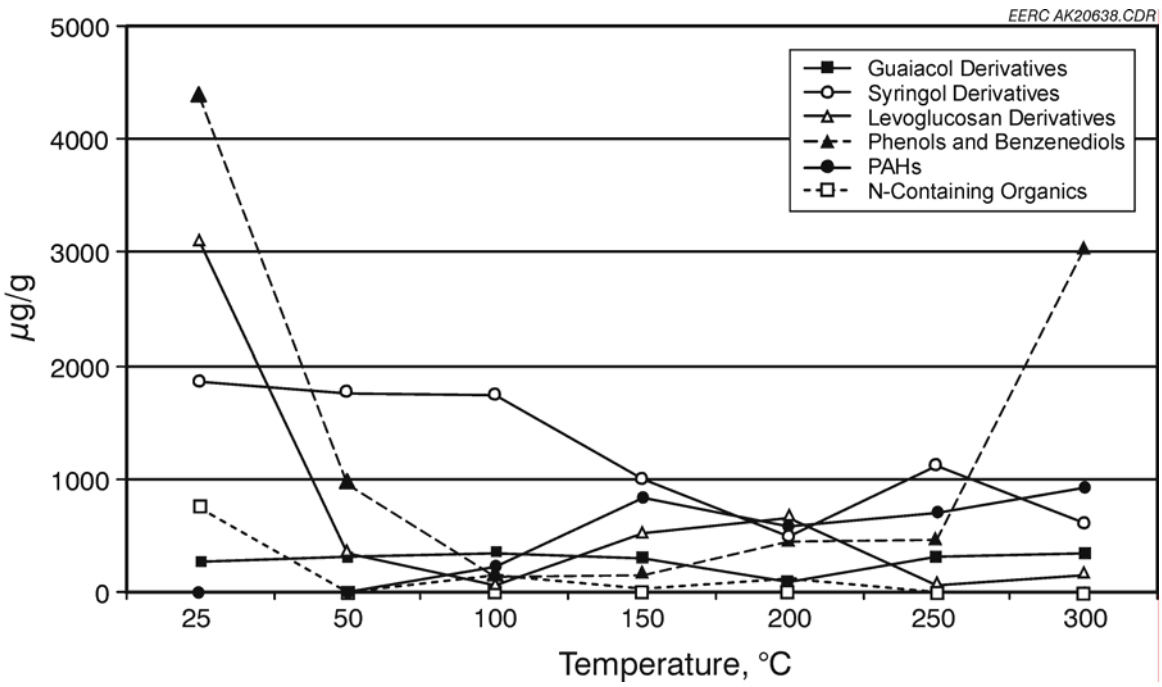


Figure I-7. Concentrations of wood smoke particulate organics in subcritical water extracts collected sequentially at 25°–300°C.

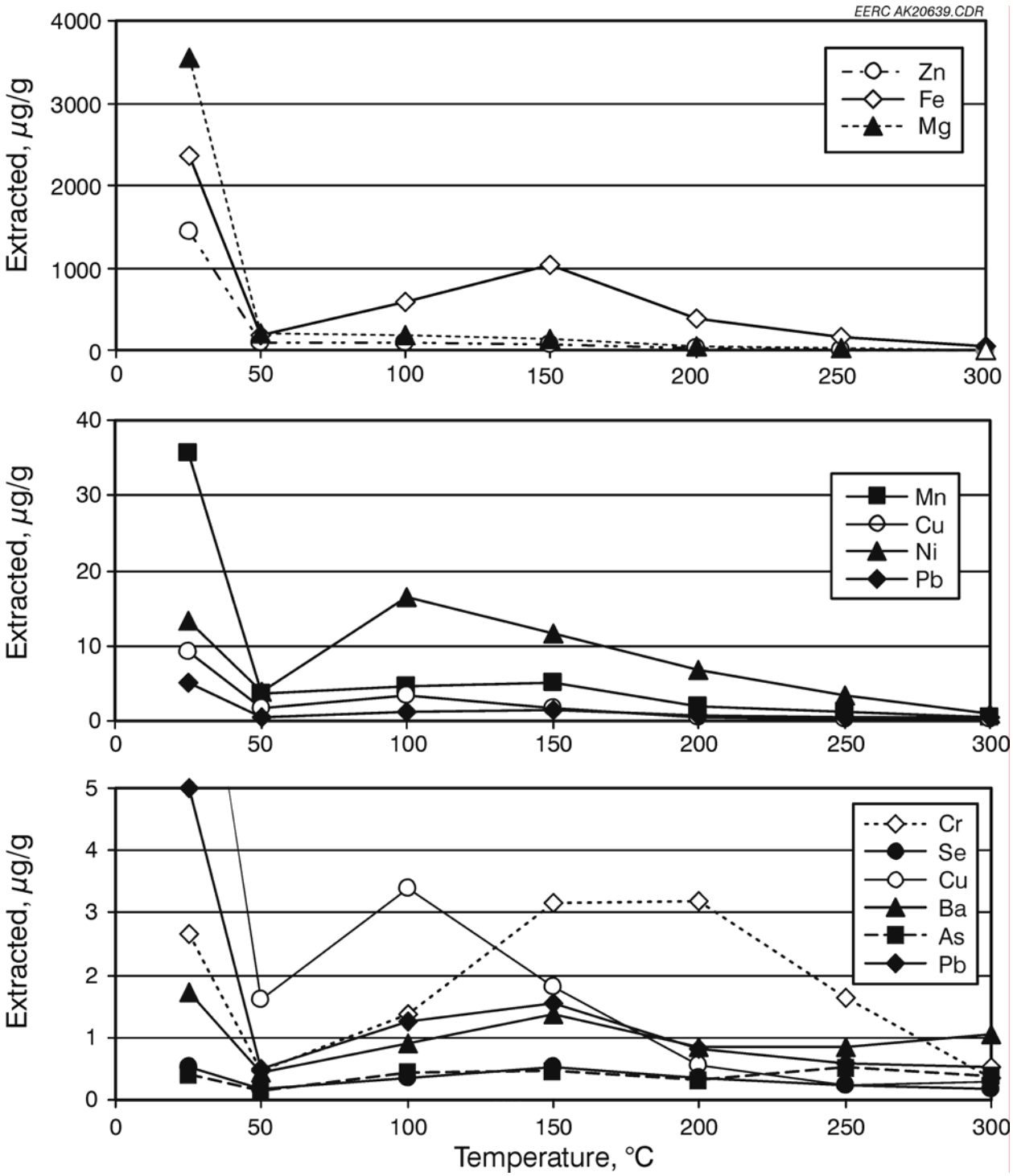


Figure I-8. Determination of metals in diesel exhaust particulate using ICP–MS.

increased recoveries of certain metals at different temperatures probably resulted from selective extraction of different metal species.

### Application of Subcritical Water Fractionation to Ambient Aerosol Samples

The SWF was successfully applied to ambient PM samples collected in Pittsburgh. The gravimetric determination (Table I-1) showed a significant mass of samples was extracted. Future study will be necessary to evaluate the toxicity of the fractions.

**Table I-1. Mass Extracted Using Subcritical Water Fractionation of Airborne Particulate Samples (1 quarter) Collected in Pittsburgh**

| | Subcritical Water Fractionation, °C | | | | | | |
|---|---|---|---|---|---|---|---|
| Sample | 25 | 50 | 100 | 150 | 200 | 250 | 300 |
| Ambient PM | 11.9 | 0.7 | 1.3 | 3.4 | 11.7 | 22.2 | 30.8 |
| PM Influenced by Coke Emissions | 13.5 | 0.8 | 1.3 | 6.2 | 9.7 | 31.3 | 56.1 |
| Highway Tunnel PM | 2 | 0.4 | 0.25 | 0.7 | 1.4 | 6.7 | 16.6 |

### Application of Subcritical Water Fractionation to Pesticide-Contaminated Soil

Both techniques—organic solvent extraction and SWF (sum of all fractions)—extracted a comparable mass of pesticides (Figure I-9). Therefore, if toxicity in the soil corresponds only to pesticides, toxicity of extract obtained with subcritical water (total) should correspond to the toxicity showed by organic solvent extraction. Detailed determination of pesticides in each subcritical water fraction showed that the majority of the pesticides were extracted in the most polar fraction of 25°C (Figure I-10). This corresponds to the high solubility of most pesticides (Table I-2). Pendimethalin and trifluralin, which are not well soluble at ambient temperatures, were extracted at temperatures of 175° and 225°C. Since components other than pesticides also can contribute to the toxicity of samples, we also determined the mass of material extracted by each method and presented it in contrast to the mass of pesticides (Figure I-11).

#### *Cytotoxicity of Pesticides*

In order to evaluate the cytotoxicity of each extract, the cytotoxicity of pure pesticide standards was determined to verify the suitability of the test. Figure I-12 shows that at concentration of 150 µg/ml (per assay) all pesticides affected viability of cells. Alachlor and trifluralin—both herbicides, often applied together—were the most toxic to the cells.

#### *Comparison of Cytotoxicity in Extracts Obtained by Subcritical Water and Organic Solvent Extraction*

For cytotoxicity tests, each soil extract (fraction) was dried and dissolved in DMSO and an aqueous buffer solution (0.5 % DMSO per assay). Figure I-13 shows the comparison of cytotoxicity results obtained by organic solvent extraction and SWF, followed by the organic solvent extraction of SWF residue.

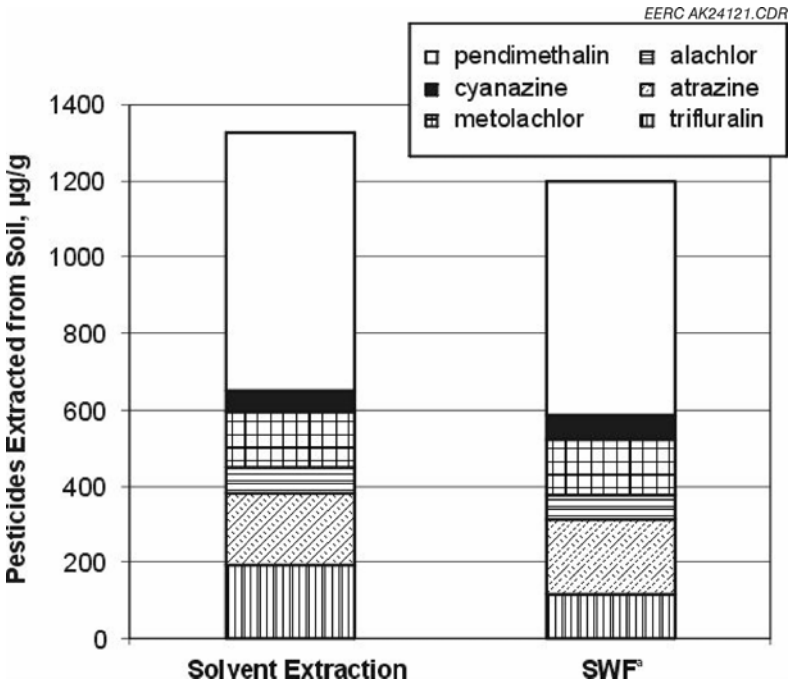


Figure I-9. Comparison of extraction efficiencies of pesticides using organic solvent extraction and subcritical water fractionation (a = total mass of pesticides calculated as a sum of pesticides present in all fractions).

To determine whether pesticides alone or if other material also are responsible for the toxicity of extracts, cytotoxicity is presented in relation to the concentration of material (Figure I-13a) and pesticides (Figure I-13b) extracted with each method. Because a significant portion of the organic solvent extract corresponds to pesticides present in soil samples (Figure I-11), the cytotoxicity found in the organic solvent extract can be related to those pesticides. This is supported by the similar cytotoxic response of organic solvent extract (Figure I-13b) and the cytotoxicity of pesticide standards (Figure I-12). The toxicity of the material extracted by subcritical water seems to be lower than of organic solvent (Figure I-13a), but it is important to note that total mass extracted by water is 10 times higher than that of solvent (Figure I-11). Thus because of the presence of unidentified compounds (in addition to pesticides), the total toxicity of water extracts is higher than that of organic solvent. This is confirmed by detailed investigation of relations between pesticides present in the water fractions (Figure I-10) and cytotoxicity observed. The cytotoxicity (Figure I-13) of the fraction collected at 175°C, containing mainly pendimethalin (a common lawn weed killer) and trifluralin (Figures I-10, I-11), corresponds to the cytotoxicity of standard pesticides (Figure I-12). A similar trend would be expected for the fraction collected at 225°C, also containing pendimethalin and trifluralin. In contrast to 175°C fraction, the cytotoxicity of 225°C in dependence on pesticide content is significantly higher, although the concentration of pesticides in this fraction was slightly lower (Figure I-10). The higher cytotoxicity of 225°C can be explained by the presence of additional cytotoxicity components. Similar to the 175°C fraction, the cytotoxicity of 125°C may be attributed to pesticide present in this fraction. The polar fraction collected at 25° and 75°C did not show significant toxicity, although most of the water-soluble pesticides were

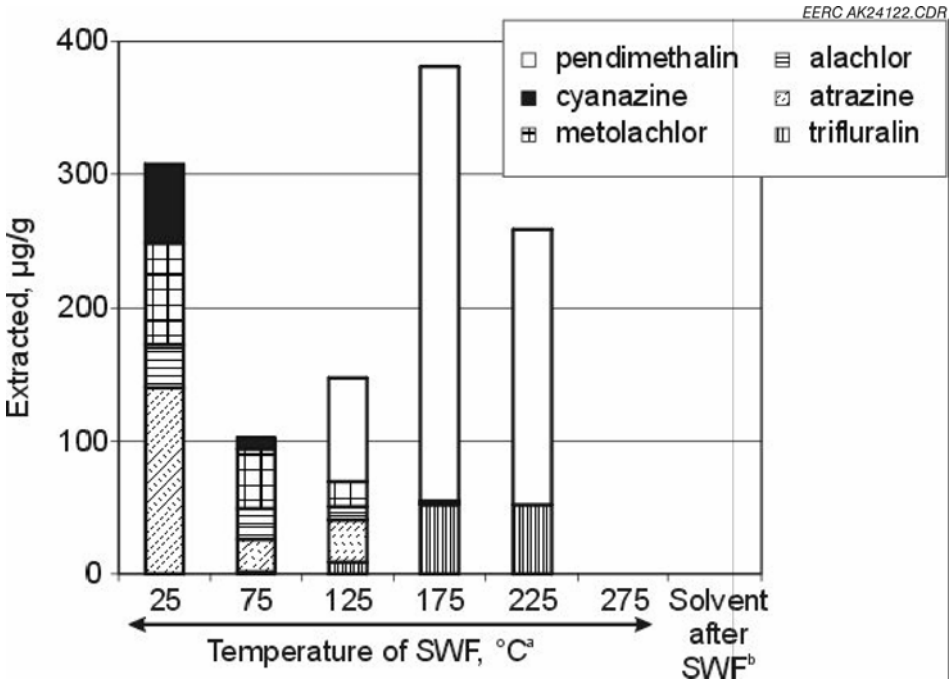


Figure I-10. SWF of pesticides from soil (2 g) (a = each fraction was collected for 20 min at 1 mL/min. b = After the SWF, the residue was sonicated for 18 h with mixture methylene chloride/acetone [2/1]).

**Table I-2. Solubility of Pesticides in Ambient Water**

| Pesticide | Solubility (25°C), µg/mL |
|---|---|
| Atrazine | 30 |
| Alachlor | 242 |
| Cyanazine | 171 |
| Metolachlor | 530 |
| Trifluralin | <1 |
| Pendimethalin | 0.30 |

extracted in the 25°C fraction. The relatively low response might be the result of the low concentration of pesticides (Figures I-12, I-13b). Further investigation is needed to confirm this assumption.

### Conclusions

The selective fractionation of wood smoke and diesel exhaust particulate demonstrated the potential of subcritical water for toxicity studies of wide-range polarity components in PM, as well as other environmental matrices such as soils. As expected, not only nonpolar compounds were responsible for the toxicity of PM, but also less-studied polar components contributed at least the same extent to total toxicity.

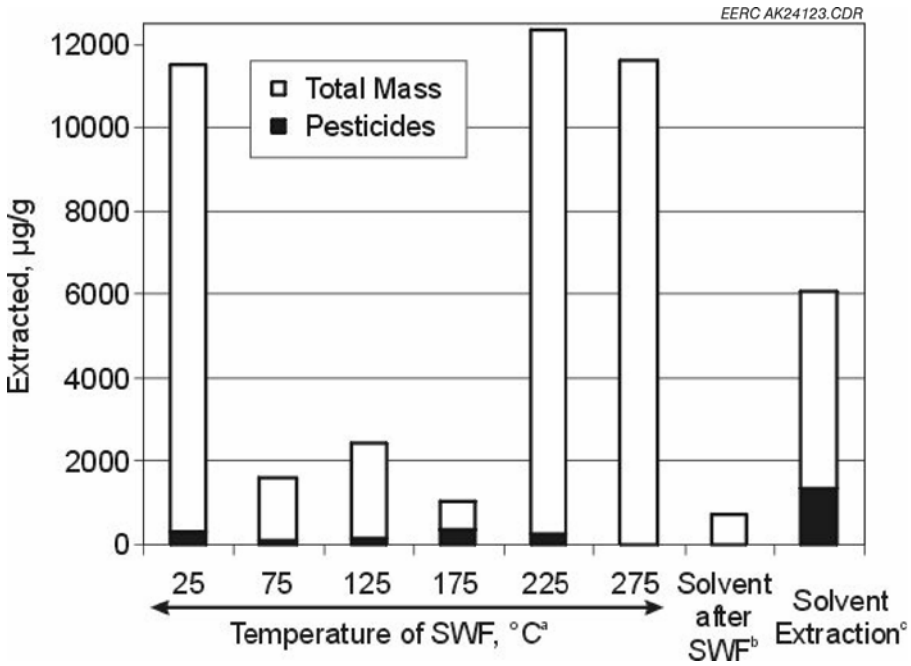


Figure I-11. Mass of material and pesticides extracted from soil using subcritical water fractionation followed by solvent extraction of residue, and using organic solvent extraction directly (a = each fraction was collected for 20 min at 1 mL/min. b = after the SWF, the residue was sonicated for 18 h with mixture methylene chloride/acetone [2/1]. c = Soil was sonicated for 18 h with mixture methylene chloride/acetone [2/1]).

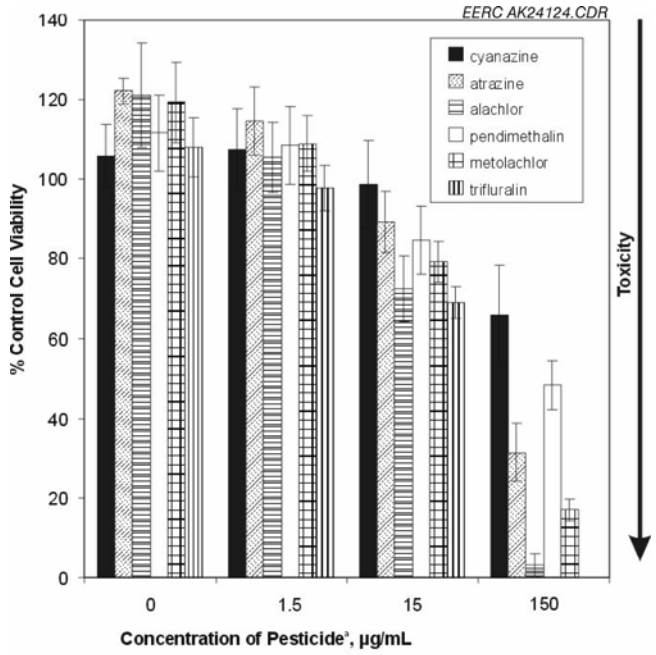


Figure I-12. Cytotoxicity (% control cell viability of mammalian COS cells) of pesticides. a = concentration of pesticide in the cell culture.

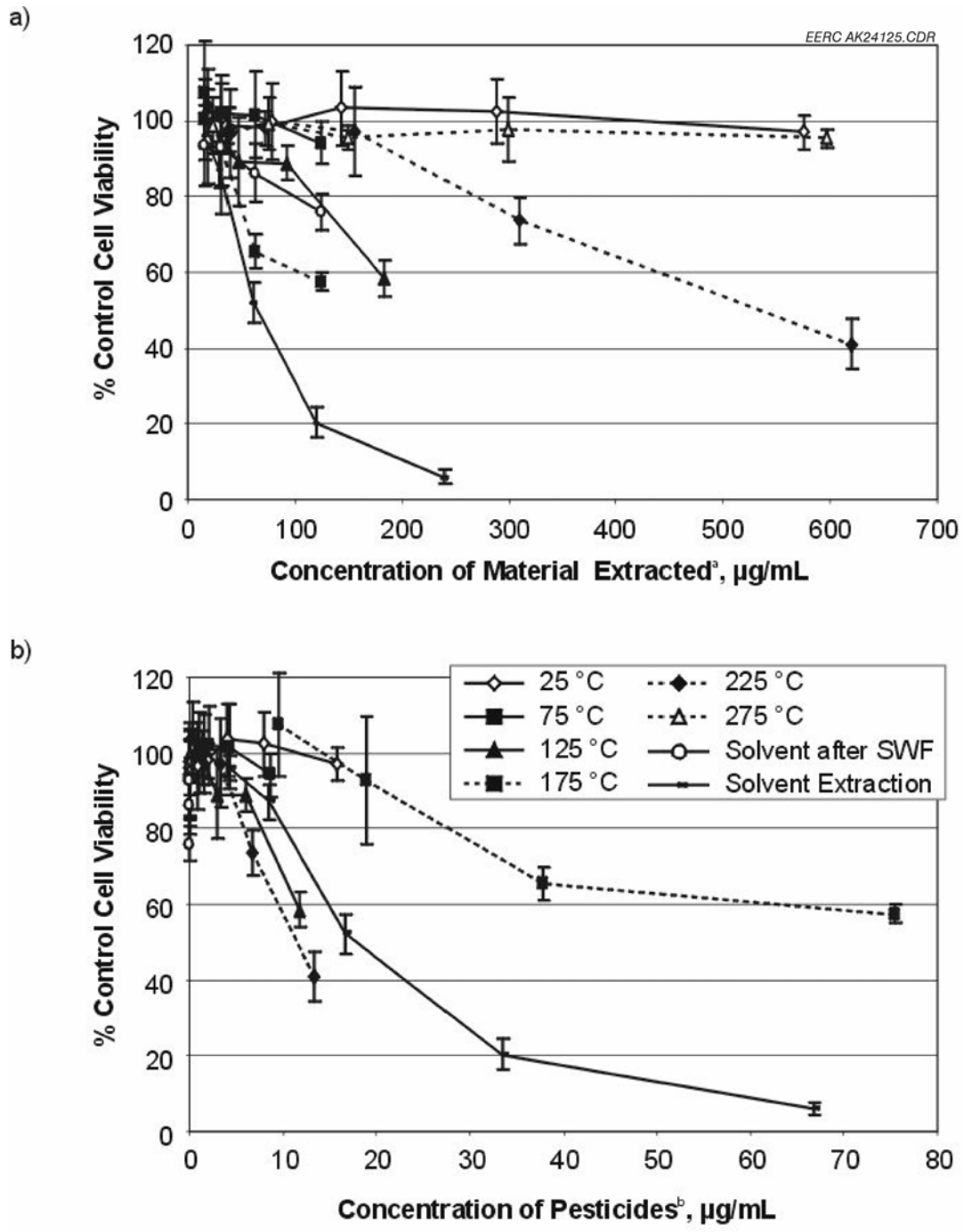


Figure I-13. Comparison of the cytotoxicity in soil extracts (2 g) obtained with SWF followed by solvent extraction of residue, and organic solvent (methylene chloride/acetone [2:1]) extraction. Standard deviations are based on quadruplicate experiments. Top: Cytotoxicity in relation to the mass of material extracted in assay. Bottom: Cytotoxicity in relation to the mass of pesticides extracted in assay. (a = the concentration material extracted is a concentration of a material found in the extract after drying which was dissolved in the cell culture. b = concentration of pesticides is total mass of pesticides found in the extract which was dissolved in the cell culture.)

The project resulted in the following conclusions:

- Subcritical water has been shown to selectively extract organic compounds ranging from polar to nonpolar.

- High toxicity was found in the polar fractions, which are not expected to be extracted by organic solvents.

- GC–MS characterization of wood smoke particulate showed phenols, benzenediols, and levoglucosan extracted preferentially in lower-temperature fractions.

- Higher content of sulfur, magnesium, iron, and zinc was found in the lowest temperature fraction (the most polar) of diesel exhaust particulate.

- Standard methods employing organic solvents do not characterize the polar fractions of aerosol particulate, which are important from a toxicological point of view.

- Tests studying leachates (water extracts at ambient temperature) might omit toxicologically important polar fractions extracted above 25°C.

This work has shown that different classes of compounds may contribute to the total toxicity of PM. Nevertheless, the current study employed surrogate samples of atmospheric particulates and general toxicity tests. Therefore, future work will involve SWF analysis of ambient atmospheric particulate and toxicity tests more closely approximating the exposure of the human respiratory system to these pollutants. Moreover, characterization of carbonaceous particulate should focus on polar species using other analytical techniques.

**References**


1. Hannigan, M.P.; Cass, G.R.; Penman, B.W.; Crespi, C.L.; Lafleur, A.L.; Busby, W.F. Jr.; Thilly, W.G. *Environ. Sci. Technol.* **1997**, *31*, 438.

2. Reichhardt, T. *Environ. Sci. Technol.* **1996**, *30*, 68A.

3. Christoforou, C.C.; Salmon, L.G.; Hannigan, M.P.; Cass, G.R. *Air & Waste Manage. Assoc.* **2000**, *50*, 43.

4. Benson, S. EERC. Personal communication, October, 2000.

5. Hawthorne, S.B.; Miller, D.J.; Lagadec A.J.M. U.S. Patent 6,001,256, 2000.

6. Hawthorne, S.B.; Miller, D.J.; Lagadec, A.J.M.; Hammond, P.J.; Clifford, A.A. U.S. Patent 6,352,644, 2002.

7. Yang, Y.; Hawthorne, S.B.; Miller, D.J. *Environ. Sci. Technol.* **1997**, *31*, 430.

8. Moolgavkar, S.H.; Luebeck E.G. *Epidemiology* **1996**, *7*, 420.

9. Squadrito, G.L.; Cueto, R.; Dellinger, B.; Pryor, W.A. *Free Rad. Biol. & Med.* **2001**, *31*, 9.

10. Bitton, G.; Koopman, B. *Rev. Environ. Contam. Toxicol.* **1992**, *125*, 1.

11. Oanh, N.T.K.; Nghiem, L.H.; Phyu, Y.L. *Environ. Sci. Technol.* **2002**, *36*, 833.

12. Buschini, A; Cassoni, F.; Anceschi, E.; Pasini, L.; Poli, P.; Rosi C. *Chemosphere* **2001**, *44*, 1723.

13. Li, N.; Venkatesan, M.I.; Miguel, A.; Kaplan, R.; Gujuluva, C.; Alam, J.; Nel, A. *J. Immunol.* **2000**, *165*, 3393.

14. Hawthorne S.B.; Miller, D.J.; Barkley, R.M.; Krieger, M.S. *Environ. Sci. Technol.* **1988**, *22*, 1191.

15. Miller, D.J.; Hawthorne S.B. *Anal. Chem.* **1998**, *70*, 1618.

16. Franson, M.A.H., Ed. *Standard methods for the examination of water and wastewater.* Am. Public Health Assoc. **1989**, Part 5210B.

17. Plumb, J.A.; Milroy, R.; Kaye, S. *Cancer Res.* **1989**, *49*, 4435.

18. Mosmann, T. *J. Immunol. Methods.* **1983**, *65*, 55.

19. Quillardet, P.; Huisman, O.; Ari, R.D.; Hofnung, M. *Proc. Nat. Acad. Sci.* **1982**, 79, 5971.

20. Maron, D.M.; Ames, B.N. *Mut. Res.* **1983**, *113*, 173.

21. Quillardet, P.; Hofnung, M. *Mut. Res.* **1985**, *147*, 65.

22. Mersch-Sundermann, V.; Kevekordes, S.; Mochaydei, *S. Mut. Res.* **1991**, *252*, 51.

23. Miller, J.H. Short Course in Bacterial Genetics, A Laboratory Manual and Handbook for Escherichia Coli and Related Bacteria. Cold Spring Harbor Laboratory Press: Woodbury, New York. 1992.

24. Mersch-Sundermann, V.; Wintermann, F.; Kern, S.; Hof, H. 1993 *Mut. Res.* **1993**, *291*, 53.

25. Picklo, M.J.; Montine, T.J. *Biochem. Biophys. Acta* **2001**, *1535*, 145.

26. Turpin, B.J.; Saxena, P.; Andrews, E. *Atm. Environ.* **2000**, *34*, 2983.

## ACTIVITY 2 – SAMPLING AND ANALYSIS OF FINE PARTICULATE MATTER ($PM_{2.5}$)

### Activity 2.1 – Characterization of the Inorganic Fraction

#### *Objectives*

The goal of the fine particulate matter ($PM_{2.5}$) program was to develop advanced sampling and analysis methods for PM that could be used for source apportionment and assist in health studies. These techniques will be used to determine sources of $PM_{2.5}$ in rural states such as North Dakota. Specific objectives for the proposed work included developing automated scanning electron microscopy (ASEM) analysis methods to elucidate key physical and chemical information, developing source apportionment methods, extensively characterizing samples collected, and developing a scientifically sound $PM_{2.5}$ database. The primary activities undertaken were to 1) collect and characterize $PM_{2.5}$ samples using instrumentation in the sampling trailer, 2) develop and improve ASEM characterization techniques, and 3) provide detailed characterization information for the samples collected.

#### *Experimental*

Six instruments were assembled and optimized for data analysis prior to field sampling and data collection of ambient $PM_{2.5}$ characterization.

*Burkard Sampler*

Ambient total suspended particulate (TSP) samples were collected on a moving carbon tape using a Burkard Manufacturing Co. Ltd. 7-day recording volumetric spore trap. The Burkard sampler is a TSP-sampling device operating on the principle of impaction, with ambient air drawn at a rate of 10 L/min through a 2-mm by 14-mm orifice. The stream impinges on a 20-mm-wide adhesive sampling tape mounted on a rotating drum. A clockwork drive rotates the drum at 2 mm/hr, allowing for continuous particulate collection for up to 7 days. The Burkard sampler has been previously used for characterization of urban TSP using scanning electron microscopy (SEM) (Battarbee et al., 1997) and has features particularly suited to the requirements of obtaining TSP samples for ASEM analysis. Although the impactor design does not collect with equal efficiency across the range of particle sizes, the variation of particle number and composition within a given size range can provide valuable information on potential sources, particularly when correlated with weather data. An adhesive-coated conductive carbon tape (Electron Microscopy Sciences, Hatfield, Pennsylvania) was found to provide a satisfactory collection medium over a temperature range of –30° to +38°C in all weather conditions. This tape is suitable for direct introduction into the SEM without further coating or other treatment, minimizing the possibility of contamination or alteration of the samples. The movement of the tape substrate results in the dispersion of the captured particles, minimizing the problems of particle adhesion and agglomeration that occur when filters are used, as well as providing collection time resolution down to hourly intervals on a single sample tape collected over a period of 6–7 days. The Burkard sampler has been found to be robust, reliable, and simple to operate, with only 1 hour of attention required for changing the sampling tape. A normal

sampling period of 6 days was found to be most convenient, which allowed greater ease in loading and securing the sampling tape, with occasional shorter 3–5-day sampling periods used as the sampling schedule dictated.

*Fine Particulate Matter Sampling*

The following equipment and EPA Compendium Methods (EPA, 1999) were used to sample ambient $PM_{10}$ and $PM_{2.5}$:

- Tapered electronic oscillating microbalance (TEOM), Rupprecht & Patashnick Model 1400a (EPA Compendium Method IO-1.3)
- Automatic cartridge collection unit (ACCU), Rupprecht & Patashnick Co., Inc.
- Sequential air sampler (SAS), Rupprecht & Patashnick Partisol-Plus Model 2025 (EPA Compendium Method IO-2.3)
- Aerodynamic particle sizer (APS), TSI, Inc. Model 3031
- Scanning mobility particle sizer (SMPS), a TSI, Inc., combination 3071A EC electrostatic precipitator and a 3022/A-S condensation particle counter (CPC)

All of the TSP, $PM_{10}$, and $PM_{2.5}$ sampling equipment was contained in a trailer (12' long, 7' wide, 6' high) to facilitate its transport between sampling sites. The trailer also contained a WX200 AccuWeather station from Radio Shack to monitor and record ambient temperature, wind speed and direction, precipitation, and barometric pressure.

TEOM–ACCU

The TEOM provides real-time data collection of ambient fine particle mass loading. While various cut-point cyclones can be mounted at the inlet of the instrument, a 2.5-µm cyclone was used for all monitoring in this activity. The instrument records and stores up to eight parameters. The parameters selected for data storage were mass rate (µg/hr), mass concentration ($\mu/m^3$), total mass (µg), ambient temperature (°C), TEOM flow (L/min), aux flow (L/min), ambient pressure (atm), and noise (µg). $PM_{2.5}$ samples were collected by pulling a slipstream of air from the TEOM inlet through the ACCU attached to the TEOM. $PM_{2.5}$ was collected on 0.4-µm-pore-size, carbon-coated, polycarbonate membranes. Precoating of the membranes enabled the direct introduction of $PM_{2.5}$ samples into a SEM for morphological and chemical analyses. The ACCU sampled outdoor ambient air under atmospheric conditions continuously for 18–31 days with individual membranes loaded in 2- to 4.5-day increments, depending on the total mass collected by the TEOM.

SAS

The Partisol-Plus Model 2025 SAS from Rupprecht & Patashnick is a multifilter (up to 16 filters) automated sampling device that collects size-selected PM on filters for later weighing

or analysis. The sequential collection feature allows for unattended operation for up to 2 weeks between site visits. The SAS has the EPA $PM_{2.5}$ reference method designation RFPS-0498-118 when fitted with the inlet to sample $PM_{2.5}$. The unit has a sample flow rate of 1 $m^3/h$ (16.7 L/min) through a single 47 mm filter. The SAS was programmed to collect $PM_{2.5}$ on a preweighed 0.45 µm Teflon filter for a 24-hour period every third day to replicate EPA-required monitoring practices.

### APS–SMPS

Real-time particle sizing measurements were made using a model 33 APS and a model 3934 SMPS, both manufactured by TSI, Inc. The APS is a laser particle counter used to measure the concentration of particles ranging in size from 0.7 to 20 µm. The SMPS system measures the number, size, and distribution of particles using electrical mobility detection. The SMPS uses a bipolar charge in the electrostatic classifier to charge particles to a known charge distribution. The particles are then classified according to their ability to traverse an electrical field and counted with a CPC. The SMPS is capable of determining the size distribution of fine particles from 0.01 to 1.0 µm.

### Analytical Scanning Electron Microscopy Methods

As part of the characterization of collected particles, ASEM was used to compositionally classify and size individual particles that make up $PM_{2.5}$. A computer program was developed to automate image collection, image analysis, and electron probe microanalysis steps involved in determining the size and chemical composition of individual $PM_{2.5}$ particles. This program classifies analyte particles chemically by comparing on a chi-squared basis their x-ray spectra to calibration x-ray spectra. The ASEM method was developed by analyzing aerosols obtained by precipitating single-species particles on filters and optimizing the electron-beam and image analysis parameters of the SEM to provide the best image resolution possible without causing significant damage to the particles. The capabilities of the ASEM method were evaluated to determine particle-size limitations, precision, and bias by analyzing multicomponent aerosol standards prepared using a procedure adapted from a method described by Haupt et al. (1996). While the ASEM method worked well for several of the aerosols used as reference materials, problems arose when a mix of particulates and multiple aerosols were tested on a single sample. Since the beam diameter was larger than the particles themselves, the largest peak on the spectrum was carbon from the sample substrate, which was either vitreous carbon or a polycarbonate filter. For the aerosol samples, this was not a problem because all of the spectra had a large carbon peak. The spectral matching was done on secondary peaks which were different enough for the matching software to differentiate them. The spectral matching software tended to match the carbon peak in subsequent samples of mixed PM and aerosols, which gave erroneous assignments as a result of the intensity of the carbon peak. Spectral matching was abandoned and each spectrum was then saved and quantified.

SEM characterization methods also were developed for the characterization and source apportionment of the ambient-air PM. For the Burkard samples, analyses were taken across the tape, providing hourly data for each 24-hour period. The 20-mm-wide carbon tape from the Burkard sampler was cut into 48-mm-long pieces, with each piece representing a 24-hour period.

Starting times were known and the carbon tapes were cut to represent midnight to midnight sampling periods. These 24-hour strips were then mounted on a standard petrographic slide and inserted directly into the SEM for analysis without further sample preparation.

A starting position on the edge of the tape was selected by the SEM technician and a backscatter electron image was acquired. A binary image was then created, with the tape or filter substrate represented by black pixels and the particles represented by white pixels. Size was determined from the pixel area represented by each particle. Chemical analysis was performed at the center of mass of each particle. The acquired x-ray spectra were saved and quantified for further characterization by statistical multivariate analysis (cluster analysis). Along with the size and chemical information from each particle, other information including particle area, perimeter, maximum diameter, minimum diameter, mean diameter, circularity, and particle location were recorded.

The number of analyzed particles per frame was unlimited, thus several hundred particles were commonly analyzed in each frame. Particles as small as 0.5 µm were chemically analyzed, and even smaller particles (0.1 µm) were sized. Analyses were performed at two magnifications to provide both $PM_{2.5}$ and $PM_{10}$ data. Two passes were made over each sample, the first at a magnification of 500× to size and analyze particles ranging from 2.5 to 10 µm in average diameter. When the 500× frames were completed, the SEM stage was returned to its original starting position and particles ranging from 0.5 to <2.5 µm in average diameter were sized and chemically analyzed at a magnification of 2500×. Because a much smaller area of the sample is analyzed at 2500× than at 500×, two passes are made at the higher magnification to analyze a sufficient number of particles. A data manipulation program was developed to download and reduce the raw SEM data, which can contain 4000 or more particle analyses for a single 24-hour period.

An analogous SEM technique was developed for analysis of the ACCU filter samples. The procedure was automated using Thermo Electron Corporation's NORAN Feature Sizing and Chemical Typing software. The software locates and sizes particles using image analysis.

A large number of particles in the size range from 0.05 to 0.1 µm were collected using the TEOM–ACCU. Particles in this range are difficult to characterize by SEM. Higher beam energy and smaller beam-spot size are required to image these particles at high magnifications (50,000×–100,000×). Under these high magnifications, few x-rays are generated, making the counting statistics for elemental identification extremely poor. Several attempts were made to address the issues of x-ray generation versus imaging conditions. No x-ray signal could be detected above the background levels for particles considerably below 0.5 µm in size using any instrument conditions. The x-ray counting statistics improved as the particles being analyzed got bigger. It was determined that the smallest particles that could be analyzed with reliable chemical analyses were 0.5 µm. Although many smaller particles were often found, chemical analysis by SEM was not possible.

Modifications were made to the automated fine-particle program to address the long analysis time and to improve the data quality for the submicron particles. Two steps were initiated to reduce the analysis time. The first was to decrease the amount of time that each

particle was subjected to chemical analysis by the electron beam. The spectral collection time was reduced from 10 to 5 seconds, which also required recollecting all the standards for the same length of time and at the same instrument parameters. Because spectral matching is used as the primary particle recognition step, the standards must be collected in the same manner as the unknowns.

The second major modification was to limit the number of particles analyzed in each frame to 100 particles. In conjunction, a second, higher magnification (2500×) routine was added to the program, which also collects up to 100 particle analyses. Each frame was analyzed at 500× for size and chemistry for up to 100 particles with an area equivalent to a particle with a diameter ranging from 2.5 to 100 µm. The magnification was increased to 2500×, and up to 100 particles in the size range of 0.1–2.5 µm are analyzed. The higher magnification improves the quality of the fine particle-size data, because the sizing program uses pixel area as the basis for sizing. Generally, the larger the number of pixels representing a single particle, the greater the accuracy of the size, shape, and area data for that particle.

The SEM data sets were evaluated using cluster analysis, which starts out with each individual analysis representing its own group. Then the software calculates the distance between groups and groups individual analyses together according to their level of similarity. With this method, it is possible to look at chemical analyses that have a high degree of similarity, which is key to understanding the source of some of the airborne particulates. The statistical analysis of particle composition was conducted using MINITAB™ Release 13.

*Multivariate Analysis*

Cluster analysis was performed on the particle chemical compositions (C, N, O, Na, Mg, Al, Si, P, S, Cl, K, Ca, Ti, and Fe) to classify them into chemical groupings. MINITAB™ Release 13 was used to perform the cluster analysis. Eight major chemical categories have been identified and used to classify $PM_{2.5}$. These are quartz, feldspar, clays (e.g., kaolinite, chlorite, muscovite, biotite, and illite), Na–K salts (NaCl and KCl), carbonates (calcite, dolomite, ankerite, siderite), iron-rich (e.g., pyrite, magnetite, ilmenite, and hematite), sulfur-rich (e.g., anhydrite and gypsum), and unclassified (chemically complex particles such as mixed clays, clay-coated mineral grains, and/or organic compounds).

*Evaluation of APS–SMPS to Measure Atmospheric $PM_{2.5}$*

The APS–SMPS was calibrated by comparing the mass data versus the TEOM mass data. The APS–SMPS instruments give accurate particle-size distributions for particles ranging from 0.03 to 15 µm. However, to determine the mass from the size distribution for any given particle-size range, it is necessary to input a particle density. The instrument software bases its calculations on spherical particles having a unit density. The effects of particle density and shape on the APS–SMPS data were evaluated using polystrene latex spheres and salt (cubic) aerosols.

*Sample Collection Media*

To evaluate membrane collection materials, ambient laboratory air was collected on a Teflon filter for SEM analysis using the TEOM–ACCU system. SEM analysis of the sample showed that the particulate was trapped in the filter matrix, making it difficult to single out individual particles. SEM analysis requires a high degree of particulate dispersion, a flat collection substrate, few or no interfering elements in the substrate, and a sample suitable for direct introduction. After various filter materials were researched, polycarbonate membrane filters were selected for testing. The filter-holder and backing-screen design of the ACCU sampler resulted in an uneven distribution of the particulate on the filter. Two different filter holders with accompanying backing screens were ordered. However, because of the ACCU system configuration, the smallest pore size that could be used was 0.8 µm. Polycarbonate was found to be the most suitable membrane material for efficacious SEM analysis.

The modifications to the polycarbonate filter improved the ease of sample preparation. Samples collected on gold- and carbon-coated polycarbonate filters using the TEOM–ACCU system underwent SEM analysis. The filters were precoated with a conductive material for direct introduction into the SEM without further sample preparation. Gold-coated filters were best for high resolution of particles smaller than 0.1 µm; however, the gold interfered with the identification of sulfur during chemical analysis. Carbon-coating the filters resulted in poorer resolution of the ultrafine particles, but did not interfere with the chemical analysis, except for carbon-based particles, which are difficult to analyze by SEM.

*Sampling Site Descriptions*

Significant point sources of $PM_{2.5}$ emissions and PM sampling sites are indicated in Figure II-1. Potential sources of $PM_{2.5}$ at all four rural sampling sites include diesel- and gasoline-fueled motor vehicles, fugitive dust from gravel roads and agricultural vegetation, and fires.

North Dakota Urban Site (Site 4)

In December 1999 and January 2000, sampling was performed at the northwest corner of an urban area, Grand Forks, North Dakota, with a population of approximately 50,000 (Site 4). Interstate highway I-29 is located approximately 2 km to the west of Site 4. A potato processing plant, a concrete fabrication plant, a railroad yard, and other light industry are located in the vicinity of Site 4. Lack of normal snow cover along with heavy truck traffic on nearby unpaved roads resulted in significant wind-blown soil and road dust at the site. Total $PM_{2.5}$ mass concentrations were obtained at 15-minute intervals with the TEOM; these data were subsequently lost when the data storage buffer was inadvertently overwritten. $PM_{2.5}$ mass loadings also were obtained every third day using the SAS to provide an EPA-approved reference. The Burkard sampler was used to collect TSP continuously for subsequent SEM analysis. Daily ambient air particulate samples were collected from November 30, 1999, to February 23, 2000, with the Burkard sampler.

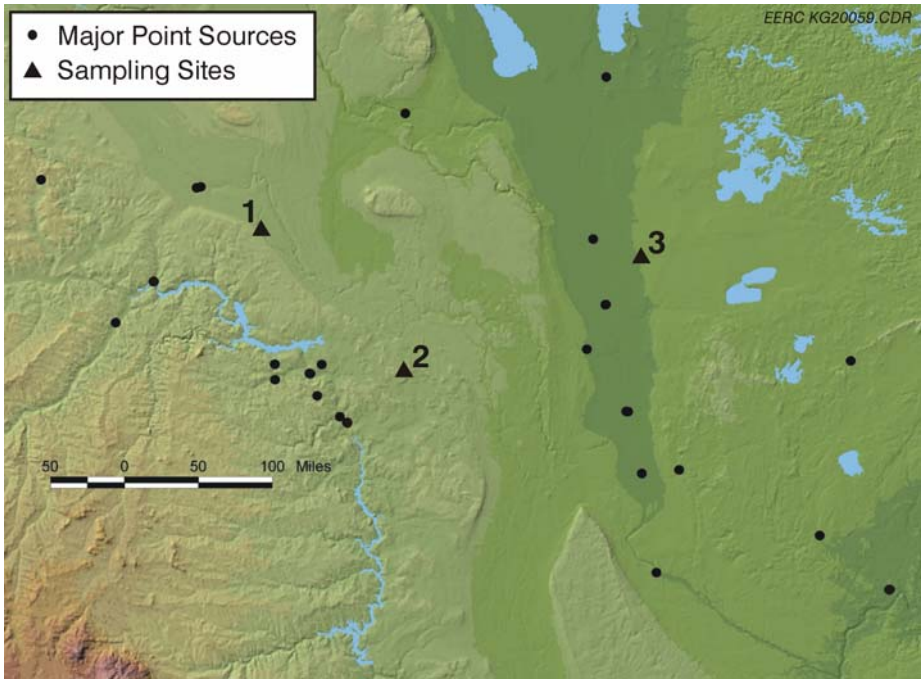


Figure II-1. $PM_{2.5}$ sampling locations and major point sources.

Minnesota Farm Site (Site 3)

Sampling was conducted at a rural farm site near Newfolden, Minnesota, approximately 80 km northeast of Grand Forks, North Dakota, for a 36-day period from mid-May through mid-June, 2000. The site is remote from any large population centers, industrial activity, and major fossil-power generation particulate sources. It is situated 170 km south-southeast of Winnipeg, Manitoba, the nearest major urban area. The sampling period coincided with agricultural spring tillage and planting operations in the region. Nearly continuous online measurements and sample collection were performed during this time. Instrumental measurements of ambient particle-size distributions were made at 15-minute intervals with the APS and the SMPS. Total $PM_{2.5}$ mass concentrations were obtained at 15-minute intervals with the TEOM. $PM_{2.5}$ mass loadings were also obtained using the SAS to provide an EPA-approved reference. Local weather conditions were logged at 15-minute intervals. Samples of $PM_{2.5}$ particulate were collected over 2–3 day periods on carbon-coated polycarbonate filters using the ACCU, and the Burkard sampler was used to collect TSP continuously for subsequent SEM analysis. Daily ambient air particulate samples were collected from May 18 through June 21, 2000, with both the Burkard sampler and the TEOM–ACCU.

North Dakota Farm Site (Site 1)

The westernmost site is similarly in an oil-producing and agricultural area remote from large population centers and industrial activity; however, several large (500-MW) coal-fired power plants and a large coal gasification facility are 110–150 km to the south-southwest of the site. Prevailing winds result in the site being approximately 100 km downwind of two large coal-

fired power plants to the northwest. Sampling was conducted for 2.5 weeks in late summer during the grain harvest. In contrast to the previous site, which was primarily agricultural, this site provided detailed information on particulate material from energy-related sources as well as agriculture-related sources. Instrumental measurements of ambient particle-size distributions were made at 15-minute intervals with the APS and the SMPS. Total $PM_{2.5}$ mass concentrations were obtained at 15-minute intervals with the TEOM. $PM_{2.5}$ mass loadings were also obtained using the SAS to provide an EPA-approved reference. Local weather conditions were logged at 15-minute intervals. Samples of $PM_{2.5}$ particulate were collected over 2–3 day periods on carbon-coated polycarbonate filters using the ACCU, and the Burkard sampler was used to collect TSP continuously for subsequent SEM analysis. Daily ambient air particulate samples for SEM analysis were collected August 8–25, 2000, with both the Burkard sampler and the TEOM–ACCU.

North Dakota Ranch Site (Site 2)

Ranching dominates the area of the central southernmost site. A well-traveled paved and an infrequently traveled gravel road exist within 100 m of sampling Site 2. An oil refinery and several coal-fired power plants are located 95 km west of this site. Instrumental measurements of ambient particle-size distributions were made at 15-minute intervals with the APS (power brown-outs damaged the SMPS, which was therefore ineffective for most of the sampling period). Total $PM_{2.5}$ mass concentrations were obtained at 15-minute intervals with the TEOM. $PM_{2.5}$ mass loadings were also obtained using the SAS. Local weather conditions were logged at 15-minute intervals. Samples of $PM_{2.5}$ particulate were collected over 3-day periods on carbon-coated polycarbonate filters the ACCU, and the Burkard sampler was used to collect TSP continuously for subsequent SEM analysis. Daily ambient air particulate samples for SEM analysis were collected August 27–September 14, 2001, during hay cutting, baling, and hauling.

*Dispersion Modeling*

The National Oceanic and Atmospheric Administration's Hybrid Single-Particle Lagrangian Integrated Trajectory model (HYSPLIT) was used to model PM dispersion from the point sources located in the west central and northwest portions of the region shown in Figure II-1, corresponding to Site 1 and 2 sampling periods. HYSPLIT uses Lagrangian puff-and-particle dispersion techniques to model in the horizontal and vertical dimensions, respectively. Concentrations are calculated by summing the mass of all the particles in a grid cell. The model assumes that a cluster of particles released from the same point will expand in space and time to simulate atmospheric dispersion. HYSPLIT utilizes archived atmospheric conditions from an eta meteorological model ("eta" derived from the Greek letter-denominated vertical pressure gradient coordinate system used in the model).

***Results and Discussion***

*SEM Analytical Methods*

Data analysis of ACCU and Burkard samples was performed, and correlations of particle size, composition, and weather conditions were made using cluster analysis. The major particle types were identified as:

- Silica, clays (crustal material—dust).
- Calcite, dolomite (crustal material—industrial material such concrete and cement).
- Sulfur-rich (sulfates, organic material).
- Nitrogen-rich (nitrates, organic material).
- Carbon-rich (carbonates, organic material, soot).

Figure II-2 is a plot of the total particles in the >2.5-µm (more particles) and the <2.5-µm particles ($PM_{10}$ and $PM_{2.5}$, respectively). The plot shows that in this sample, the $PM_{2.5}$ particles followed the same trends as the $PM_{10}$ particles. It is likely that the materials are closely related and that the $PM_{2.5}$ particles are smaller versions of the $PM_{10}$ particles. This plot also shows a dramatic decrease in particle collection during rain and increased wind. Sustained winds show sustained particle loading in the Burkard sampler.

Figure II-3a shows a breakdown of the $PM_{10}$ particles into their type categories, which are dominated by quartz and clays. Figure II-3b shows a breakdown of the $PM_{2.5}$ particles into their

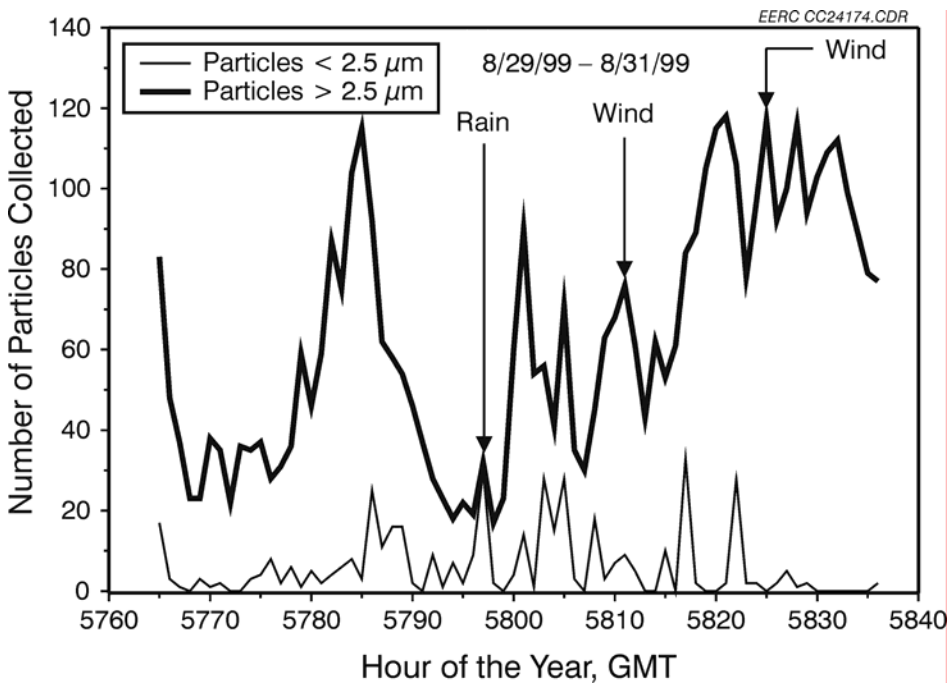


Figure II-2. Comparison of $PM_{2.5}$ to $PM_{10}$ fraction collected at the Energy & Environmental Research Center (EERC), August 29–31, 1999.

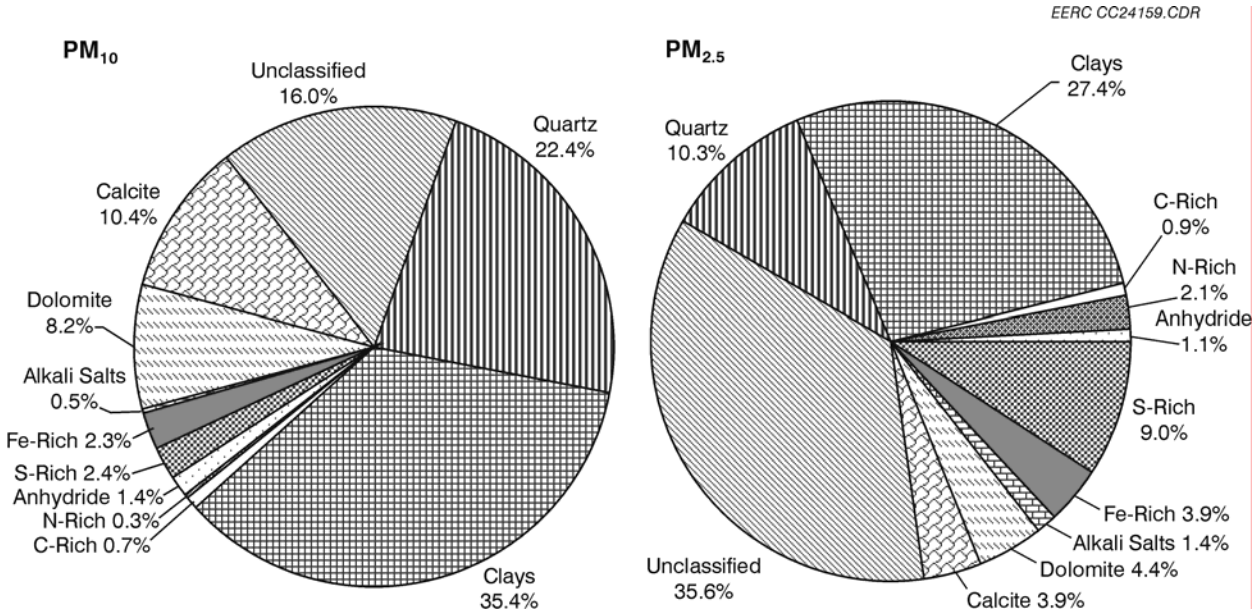


Figure II-3. SEM characterization of the $PM_{10}$ and $PM_{2.5}$ fractions.

type categories. Although there were fewer particles in the $PM_{2.5}$ portion of the sample, the organic component increased.

*Evaluation of APS–SMPS to Measure Atmospheric $PM_{2.5}$*

The $PM_{2.5}$ concentrations measured during March 1999 using the APS–SMPS system were compared with the 30-minute mass concentrations measured using the TEOM. The APS–SMPS mass concentrations were calculated assuming spherical particles with a density of 2.5 g/cm$^3$. The concentrations measured using the APS–SMPS system were generally lower than those reported by the TEOM, except on March 19. The results show that, for the most part, the APS–SMPS $PM_{2.5}$ mass concentrations were within 20% of those measured using the TEOM. Sampling times for the APS were usually 15 minutes, 30 minutes, or 1 hour. Since the longest scan time for the SMPS is 300 seconds, typically six or twelve 300-second tests were run back-to-back and added together to obtain a representative particle count and particle-size distribution.

*Grand Forks (Site 4)*

The monitoring activities at the Grand Forks site were, in part, shakedown tests. $PM_{2.5}$ particulate loadings were monitored using the SAS and TEOM instruments at Site 4 (Figure II-1). The TEOM data, however, were inadvertently lost. SAS data are presented in Table II-1. The results show the same trends between the mass loading and one-particle counting techniques.

Figure II-4 compares the inorganic phase compositions of PM greater than and less than or equal to 2.5 µm ($>PM_{2.5}$ and $\leq PM_{2.5}$, respectively) collected from Site 4. Compositions of the two size fractions are similar. The majority of particles in both size ranges are unclassified

**Table II-1. Daily $PM_{2.5}$ Mass Loadings at Site 4, Grand Forks**

| Date | Mass Concentration, $\mu g/m^3$ | Total Mass, mg |
|---|---|---|
| 12/08/99 | 11.6 | 0.278 |
| 12/10/99 | 14.6 | 0.350 |
| 12/12/99 | 6.2 | 0.148 |
| 12/14/99 | 7.6 | 0.183 |
| 12/16/99 | 5.0 | 0.121 |
| 12/18/99 | 11.7 | 0.280 |
| 12/20/99 | 4.8 | 0.116 |
| 12/22/99 | 15.8 | 0.380 |
| 01/04/00 | 6.6 | 0.158 |
| 01/07/00 | 7.8 | 0.188 |
| 01/10/00 | 7.5 | 0.179 |
| 01/13/00 | 66.8 | 1.602 |
| 01/16/00 | 5.2 | 0.125 |
| 01/19/00 | 7.8 | 0.187 |
| 01/22/00 | 13.4 | 0.322 |
| 01/25/00 | 3.7 | 0.089 |
| Field Blank | | |
| 12/15/99 | | 0.010 |

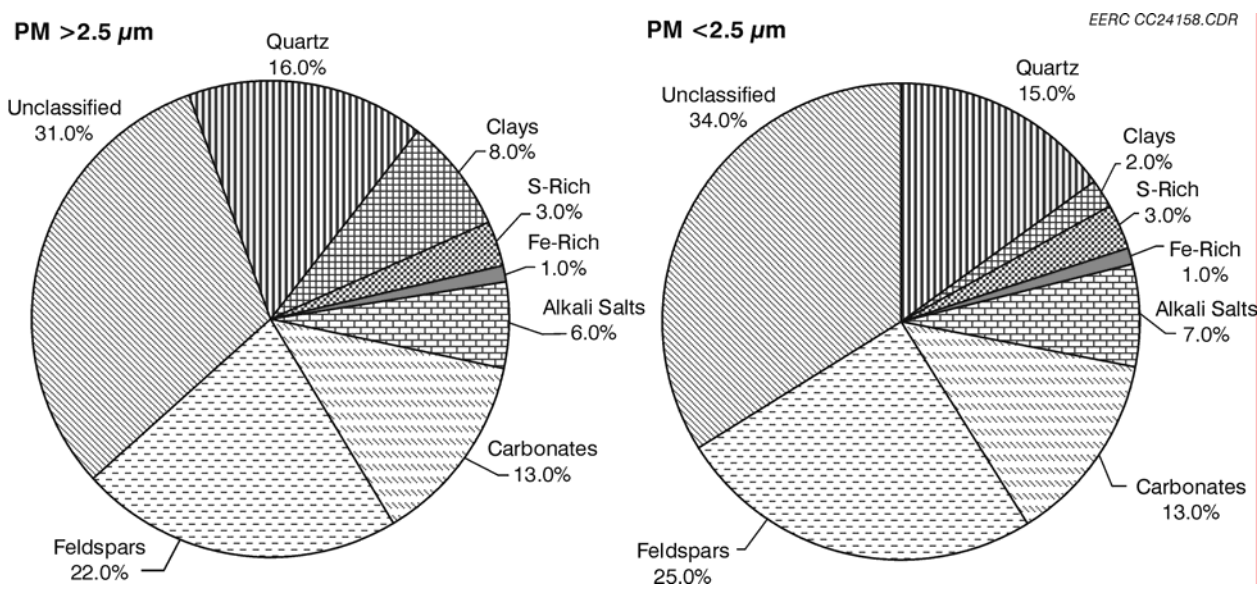


Figure II-4. SEM characterization of the $PM_{10}$ and $PM_{2.5}$ fractions at Site 4 (Grand Forks urban site).

because they are mostly organic particles, such as spores, pollen, and topsoil. The clay, quartz, carbonate, and feldspar particles probably represent dust derived from vehicular traffic on a nearby gravel road. The sulfur-rich particles are probably gypsum released from a concrete fabrication facility in the area.

*Minnesota Farm Site (Site 3)*

Comparison of SAS, TEOM, and APS Measurements

A comparison of $PM_{2.5}$ particulate loadings obtained from the SAS, TEOM, and APS instruments at Site 3 (Figure II-1) is shown in Figure II-5. The 15-minute TEOM and APS measurements have been averaged over 24-hour periods to correspond to the SAS measurements. APS data were not available for much of the period shown because of instrument problems. The measurements from the three instruments show the same trends in $PM_{2.5}$ concentration, although the TEOM measurements are consistently higher than those from the SAS. The APS measurements also are consistently lower than the SAS values. However, the APS measurements are related to the physical size of the particles and require an assumption of particle density (a value of 1.0 was assumed to create Figure II-5) to calculate a mass concentration. Further, the 2.5-µm cut point used to define the APS $PM_{2.5}$ material is a physical, rather than an aerodynamic, diameter. Both an assumption of a greater particle density and the inclusion of larger particle diameters could increase the calculated APS mass loadings to values comparable with the SAS measurements.

The identification of the specific mineral species present during periods of high and low particle loading will allow assessment of probable sources. As an example, the APS data in Figure II-6 show a small spike at approximately 3305 hours and a larger spike at 3307 hours. The smaller spike has an increase in both $PM_{10}$ and $PM_{2.5}$ particulate, which is known to be the result of agricultural cultivation near the sampling trailer at that time. The second, larger $PM_{10}$ peak

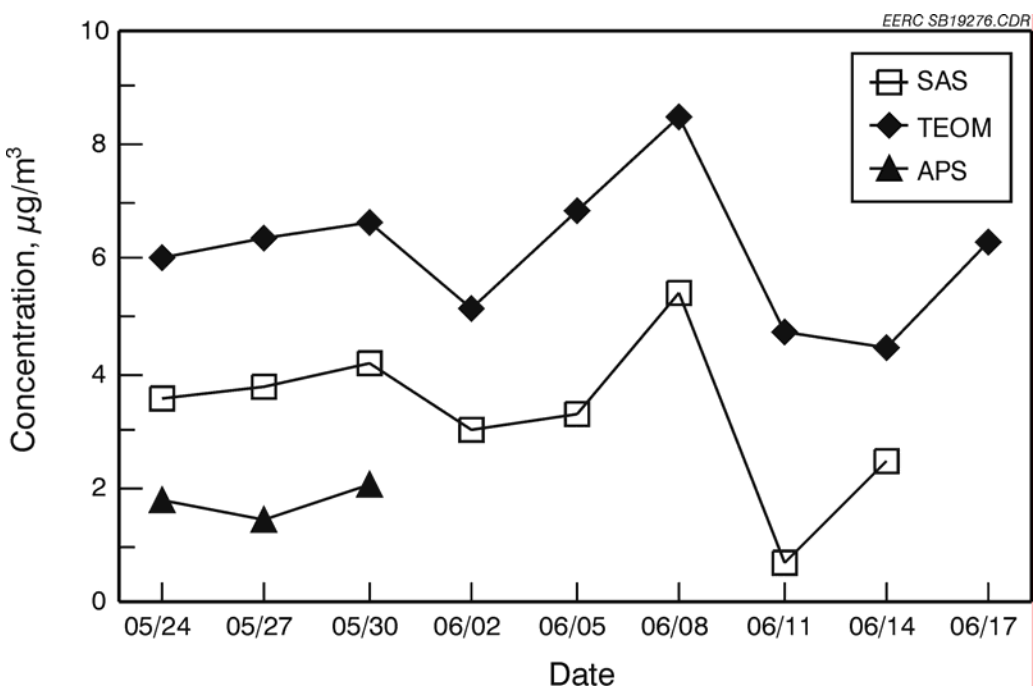


Figure II-5. SAS, TEOM, and APS $PM_{2.5}$ loadings at Site 3 (Minnesota farm), May 24 to June 17, 2000.

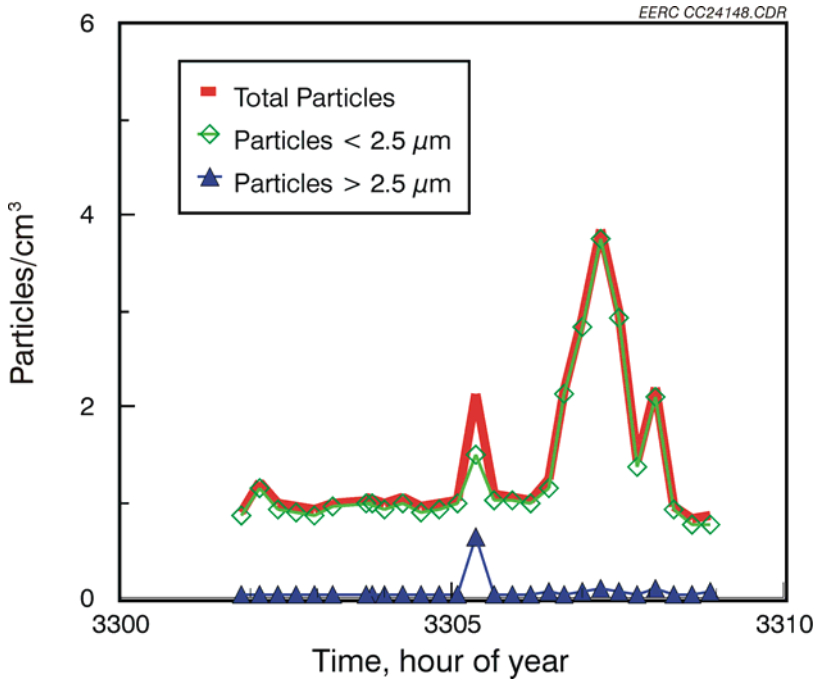


Figure II-6. APS particle size distribution at Site 3 (Minnesota farm), May 17, 2000.

also is believed to be related to agricultural cultivation, but at a greater distance. Examination of the SEM particle analysis data for the same period would be expected to show a characteristic signature of field dust as the source.

Comparison of ACCU and Burkard Data

A total of 16,605 and 13,324 individual particles from the Burkard and ACCU samples, respectively, collected at Site 3 were analyzed using ASEM. The Burkard samples provide time-resolved data in 1-hour increments, while the ACCU filter samples represent 72-hour intervals. Figure II-7 shows the particle compositions obtained from the Burkard sampler during a 5-hour period when the wind was consistently light from the northeast. For this period, the particles collected in the Burkard sampler are dominantly crustal material and generally larger than 2.5 µm in diameter. In contrast, 87% of the particles collected by the ACCU filter were classified as biologic in origin.

Figure II-8a shows the mineral distribution of particles >2.5 µm analyzed from May 24 to May 30, 2000. Figure II-8b shows the mineral distribution for those particles ≤2.5 µm, which generally follows the pattern of the larger particles. The amount of unclassified particles in both size ranges is rather large, 51% of the particles >2.5 µm and 58% of the particles ≤2.5 µm. These data points in particular were evaluated using cluster analysis, which showed that the majority of the unclassified analyses were mostly mixed clays that have variable amounts of Ca, K, Fe; Na and Si around 30 wt%; and Al around 10 wt%. This group was the largest, with 746 out of 1517. The next largest group was clearly the mineral quartz ($SiO_2$). The cluster group had 196 analyses in it and the data from the spectral matching portion of the analysis had 197 analyses in the

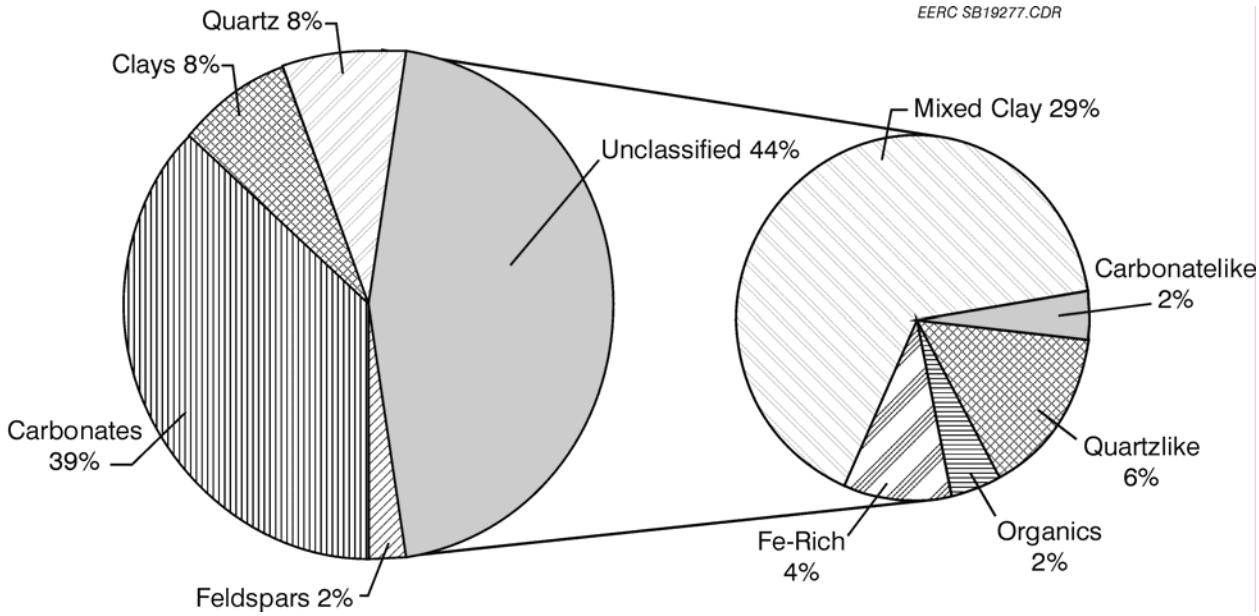


Figure II-7. SEM characterization of Burkard sample data collected at Site 3 (Minnesota farm) under a light northeasterly wind, May–June 2000, where the second pie chart shows the results of the cluster analysis on the unclassified fraction.

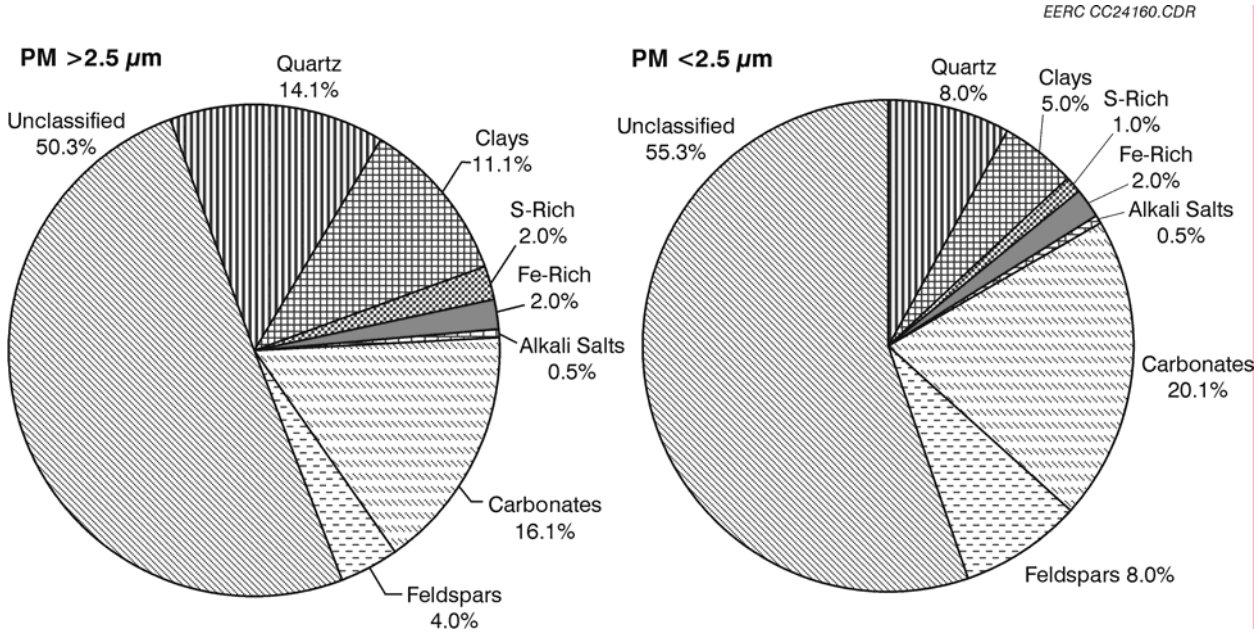


Figure II-8. Classification of particles a) >2.5 µm and b) <2.5 µm collected at Site 3 (Minnesota farm), May 24–30, 2000.

quartz group. Other groups such as the carbonates, calcite, and dolomite need further refinement. The total carbonates from the spectral matching routine showed 245 particles, while the cluster method showed a total of 324 particles.

Table II-2 shows the eight significant groupings of the data from the farm site. These eight groups were determined using 40 cut points, i.e., stopping the grouping with 40 clusters. At 20 clusters, there were seven significant groups, but the largest contained both quartzlike and the mixed-clay phases. By looking at the cluster data, it was possible to determine when the two large subgroups were grouped together. Stopping the grouping at that point (40 cluster groups) allowed more meaningful definitions of the various groups to be determined.

**Table II-2. Mean Composition of the Eight Significant Groups as Defined by Cluster Analysis of the Farm Site Data**

| Variable | Cluster 1 | Cluster 2 | Cluster 3 | Cluster 4 | Cluster 5 | Cluster 6 | Cluster 7 | Cluster 8 |
|---|---|---|---|---|---|---|---|---|
| N | 0.5 | 0.4 | 0.2 | 8.9 | 0.0 | 0.8 | 0.2 | 1.6 |
| Na | 1.5 | 0.2 | 0.3 | 1.4 | 0.8 | 0.2 | 1.0 | 0.7 |
| Mg | 3.2 | 12.0 | 0.5 | 1.6 | 1.0 | 1.4 | 3.4 | 3.7 |
| Al | 10.2 | 1.3 | 2.5 | 1.7 | 1.0 | 0.3 | 6.1 | 0.3 |
| Si | 29.8 | 3.9 | 55.5 | 3.8 | 4.8 | 1.3 | 16.5 | 1.5 |
| P | 0.4 | 0.2 | 0.4 | 3.1 | 0.1 | 0.2 | 0.4 | 22.9 |
| S | 0.8 | 0.3 | 0.2 | 6.2 | 0.2 | 21.9 | 0.3 | 3.7 |
| Cl | 0.2 | 0.1 | 0.1 | 0.9 | 0.1 | 0.4 | 0.2 | 0.6 |
| K | 3.8 | 0.3 | 0.6 | 3.6 | 0.2 | 0.5 | 0.7 | 26.7 |
| Ca | 7.1 | 37.8 | 0.8 | 2.4 | 0.9 | 29.2 | 3.8 | 3.5 |
| Ti | 0.4 | 0.2 | 0.2 | 0.8 | 0.4 | 0.1 | 0.5 | 0.1 |
| Fe | 6.8 | 1.3 | 1.6 | 2.6 | 79.2 | 0.4 | 45.6 | 0.2 |
| O | 35.3 | 42.1 | 36.9 | 63.0 | 11.8 | 43.1 | 21.3 | 35.4 |

Cluster 4 is an example of an organically associated group characterized by high N and O, and small amounts of all other elements. Cluster 3 is primarily the mineral quartz, Cluster 2 is primarily calcite and dolomite, Cluster 6 is primarily anhydrite, and Cluster 5 is primarily hematite ($Fe_2O_3$). Groups such as Cluster 8, which shows high K and P, are not likely mineral phases and are probably related in some way to the agricultural fertilizers used in the area.

Table II-3 shows the compositional centroids of the dominant clusters from three 72-hour periods from the Minnesota rural site.

Figure II-9 shows the phases identified from the ACCU filter samples and their approximate distribution among the inorganic particles. Similar to the Burkard sample, carbonate minerals are predominant in the ACCU filter sample.

Further reductions were applied to these data by checking all of the analyses for stoichiometric relationships between various elements to identify possible sulfate, nitrate, and phosphate phases. These results show that several of these phases may exist, with the sulfate

**Table II-3. Average Composition of Significant Clusters, wt%**

| Element | S-555 | S-557 | S-558 |
|---|---|---|---|
| N | 4.6 | 3.7 | 3.8 |
| Na | 1.8 | 1.4 | 1.4 |
| Mg | 2.6 | 2.7 | 2.5 |
| Al | 3.5 | 4.8 | 3.7 |
| Si | 9.5 | 12.8 | 10.2 |
| P | 1.1 | 0.7 | 0.8 |
| S | 7.8 | 7.6 | 14.0 |
| Cl | 1.4 | 3.5 | 2.5 |
| K | 2.8 | 2.5 | 2.7 |
| Ca | 6.6 | 8.0 | 7.8 |
| Ti | 1.5 | 1.0 | 0.9 |
| Fe | 4.4 | 5.0 | 4.2 |
| O | 52.6 | 46.0 | 45.4 |

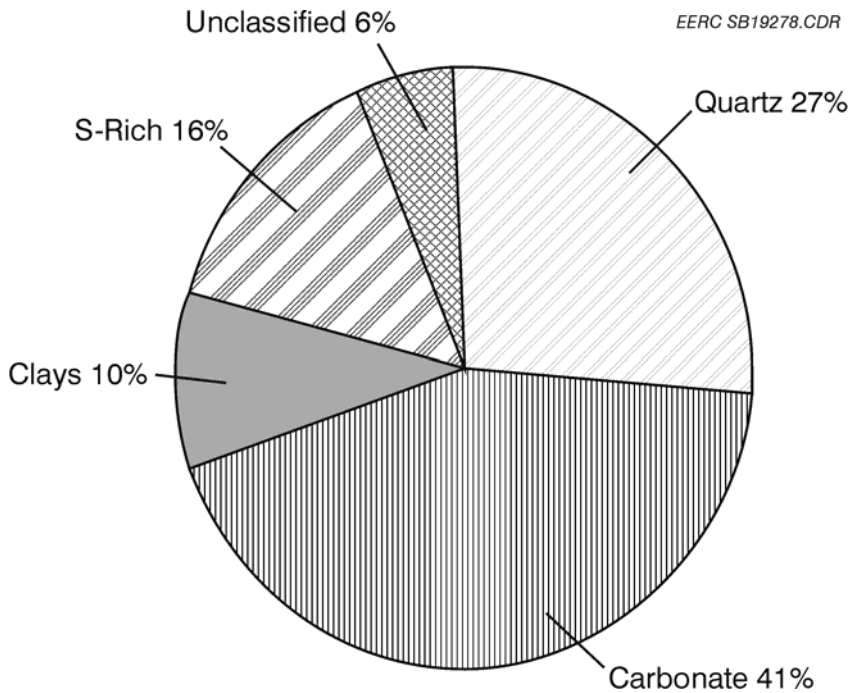


Figure II-9. Mineral phases from ACCU filter samples collected at Site 3 (Minnesota farm), May–June 2000.

predominating. The ACCU filter sample contains more sulfur-rich phases, mostly gypsum–anhydrite ($CaSO_4$) and thenardite ($Na_2SO_4$). Sulfur- and N-rich particle compositions were compared to sulfate and nitrate compound compositions that are known to exist in the environment. Stoichiometric relationships were used to classify these sulfate and nitrate particles as shown in Figures II-10 and II-11.

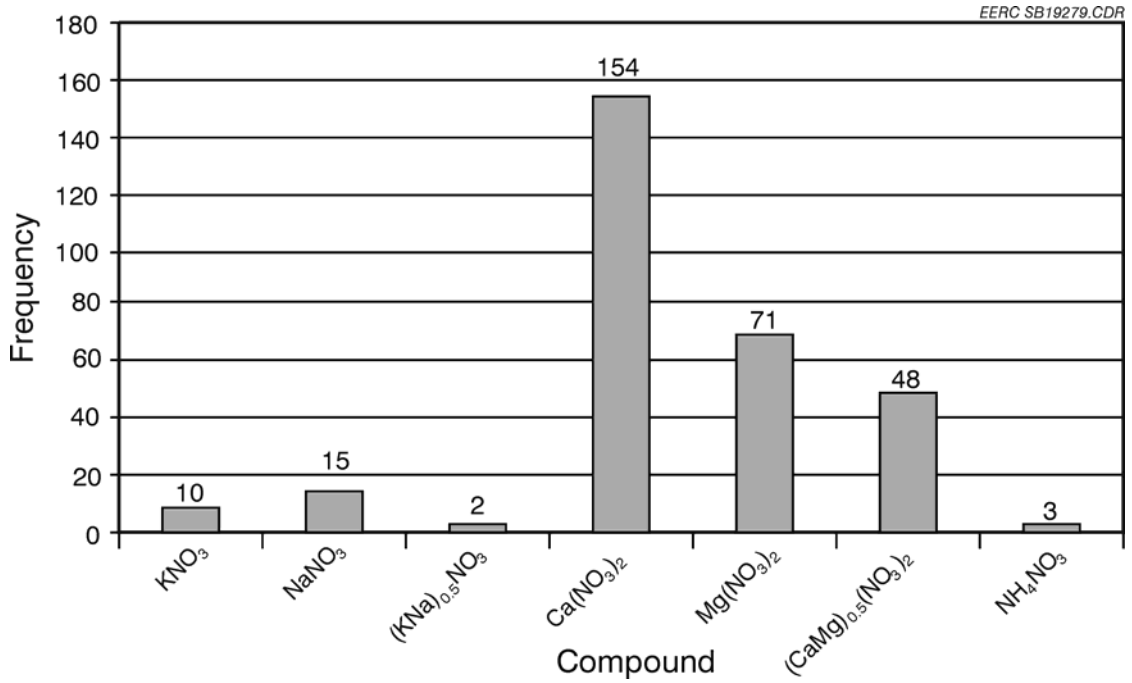


Figure II-10. Nitrate frequency distribution from SEM characterization of ACCU filter samples collected at Site 3 (Minnesota farm), May–June 2000.

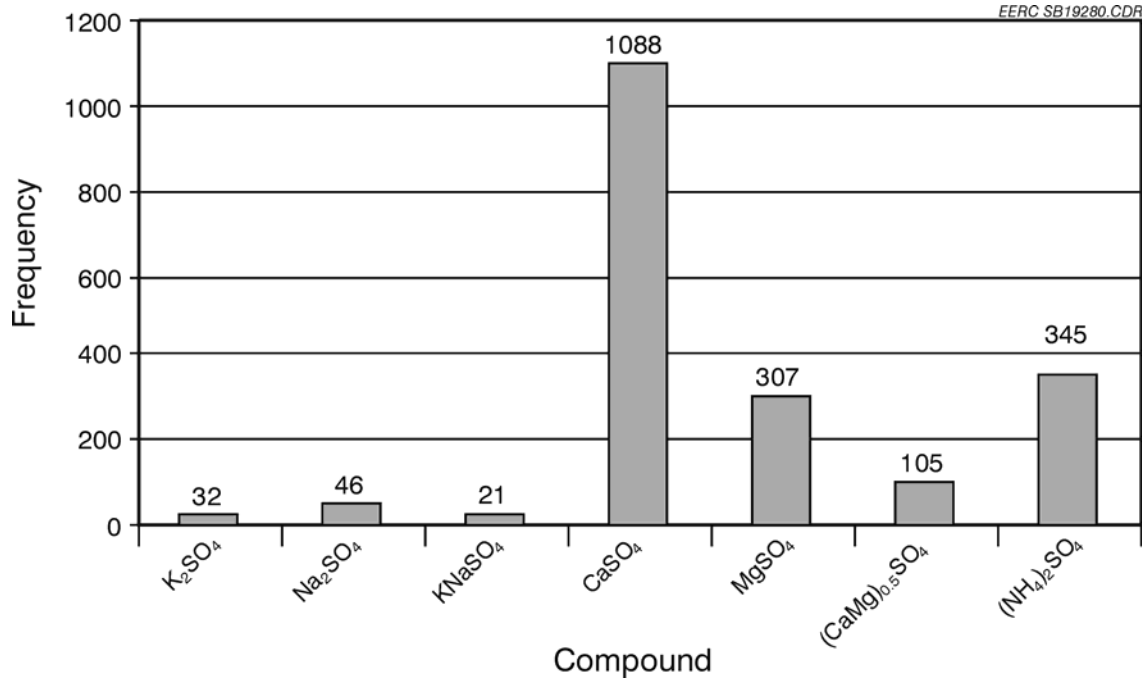


Figure II-11. Sulfate frequency distribution from SEM characterization of ACCU filter samples collected at Site 3 (Minnesota farm), May–June 2000.

Weather and PM Loading

The weather during the sampling period was often rainy with frequent power surges that interrupted data collection. The mean high temperature was 72°F (22°C) and the range was from 54°F (12°C) to 91°F (33°C). Temperature lows for the sampling period ranged from 34°F (1.2°C) to 60°F (16°C) with a mean of 46°F (7.8°C). Several surges temporarily interrupted power to the instruments. Maximum wind speed recorded when the weather station was operational was 30 mph (48 kph), although most days had a maximum wind speed closer to the mean of 14 mph (22 kph). The total recorded rainfall was 100 in. (250 cm), which reflects the influence of wind on the gauge tip cups. The actual rainfall for the sampling period was approximately 7.1 in. (18 cm). A sample of rainwater was collected and underwent anion analysis. The results are presented in Table II-4.

**Table II-4. Anion Analysis of Rainwater Collected at Sites 1 and 3, Summer 2000**

| Analyte | Site 1 | Site 3 |
|---|---|---|
| Chlorine, Cl | 1.5 | 1.3 |
| Bromine, Br | 1.2 | Not detected |
| Nitrate, $NO_3$ | 5.7 | 1.3 |
| Phosphate, $PO_4$ | 2.2 | Not detected |
| Sulfate, $SO_4$ | 5.93 | 2.8 |

Relationships between weather events and particle loading also have been examined. As an example, Figure II-12 shows radar plots of two different time periods with sustained winds greater than 6 mph (10 kph). The radii represent different wind directions, while the concentric circles represent the particle concentration. No large differences were observed in particle concentration, and wind directions extending from NW to NE were observed. Particle concentration ranged from 0.5 to 2.0 particles per cubic centimeter.

*North Dakota Farm Site (Site 1)*

A comparison $PM_{2.5}$ particulate loadings obtained from the SAS, TEOM, and APS instruments at Site 1 (Figure II-1) is shown in Figure II-13. The 15-minute TEOM and APS measurements have been averaged over 24-hour periods to correspond to the SAS measurements. The results show the same trends between the mass loading and single-particle counting techniques. The TEOM again shows consistent but higher loadings than the SAS. The mass measurements are for ambient particles obtained in North Dakota and Minnesota using the TEOM. The PM mass measurements were found to be higher in North Dakota as compared to Minnesota as illustrated in Figure II-14.

Comparison of ACCU and Burkard Data

Daily ambient air particulate samples for SEM analysis were collected with both the Burkard spore sampler and the ACCU. Large numbers of particles were analyzed to determine the size, shape, and composition. Statistical methods, including cluster analysis, were used to

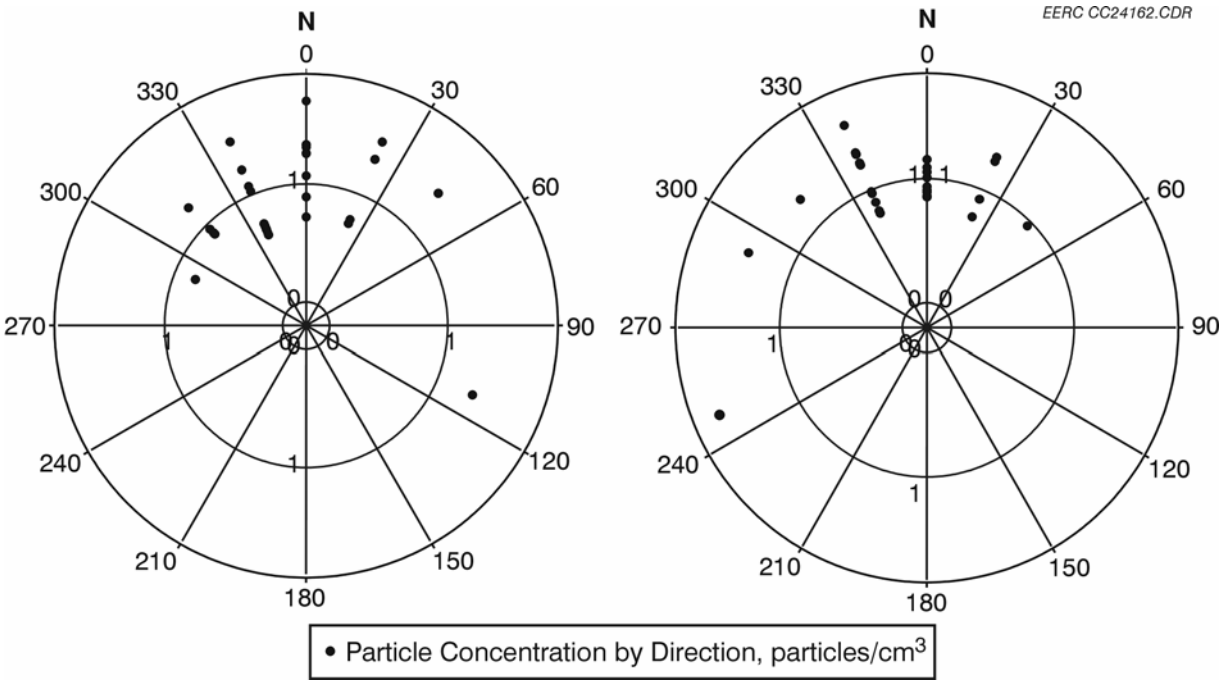


Figure II-12. Particle concentration and wind direction for two time periods (with sustained winds ≥6 mph [10 kph]) at Site 3 (Minnesota farm).

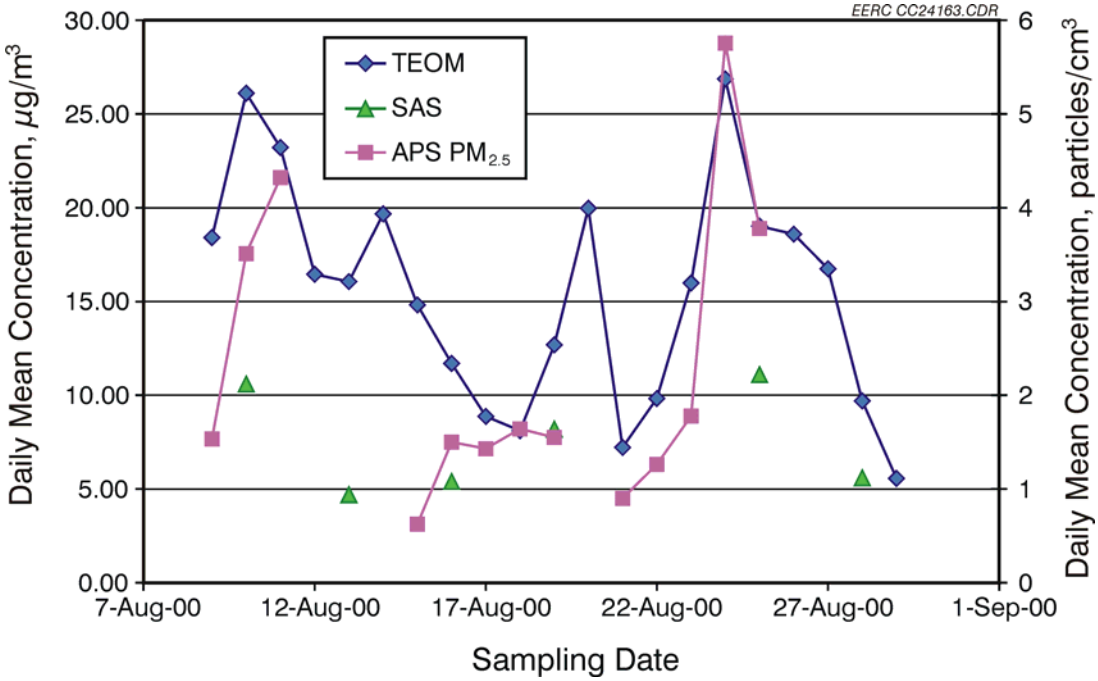


Figure II-13. SAS, TEOM, and APS $PM_{2.5}$ loadings at Site 1 (North Dakota farm), August 9–29, 2000.

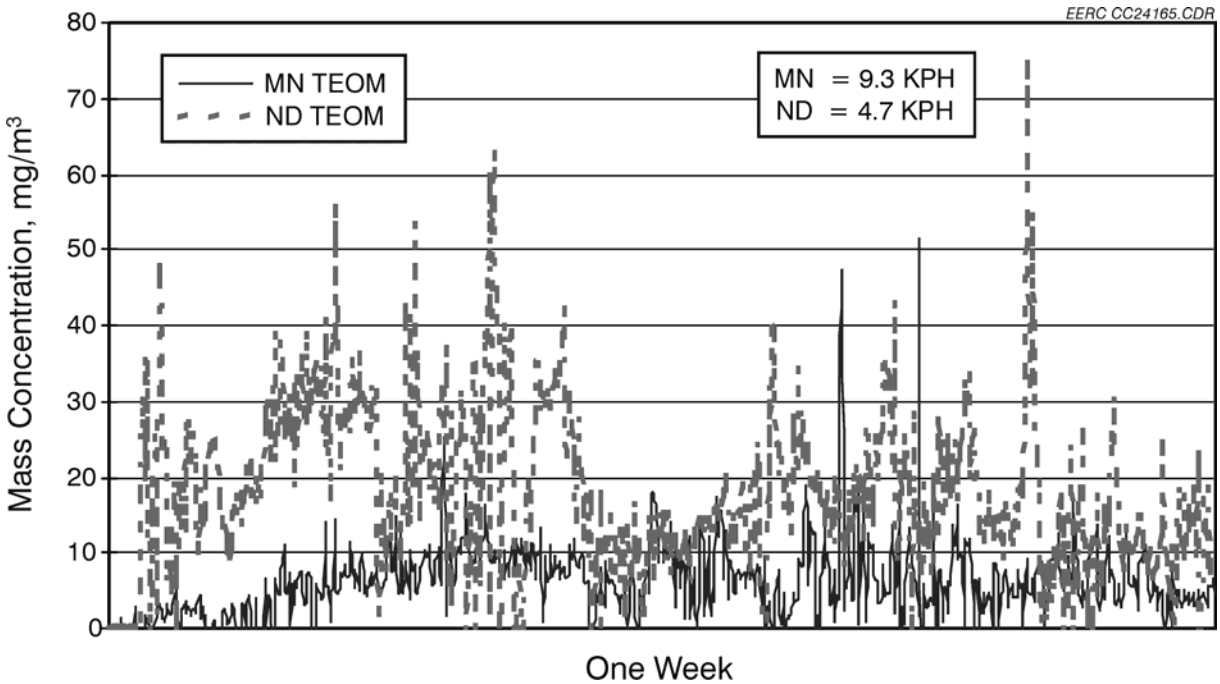


Figure II-14. Comparison of mass concentration of ambient air $PM_{2.5}$ at Sites 1 and 3 during 1 week of sampling, August and May 2000, respectively.

develop classification schemes for particle types. Analysis of ACCU samples indicated approximately 15% of the more than 10,000 particles sampled at this site may be attributed to combustion particles.

The results of the mineral classification of samples collected at Site 1 using the Burkard spore sampler are illustrated in Figure II-15 for the >2.5-µm size fraction and for the <2.5-µm size fraction. The differences in the types of materials are larger quantities of feldspar materials in the larger sizes and the larger quantity of unclassified materials in the submicron-size fraction.

Weather Conditions

Most days during the sampling period were clear and sunny a mean high temperature of 77°F (25°C) and a range of 58°–91°F (15°–33°C). Lows for the sampling period ranged from 47°F (8.6°C) to 64°F (18°C) with a mean of 54°F (12°C). Two storms caused power outages during the sampling period, interrupting the collection of weather and particulate data. Maximum wind speed recorded when the weather station was operational was 11 mph (18 kph), although most days had a maximum wind speed closer to the mean of 7.8 mph (12.5 kph). The estimated rainfall for the sampling period was 5 in. (13 cm). A sample of rainwater was collected and analyzed. The results are reported in Table II-4.

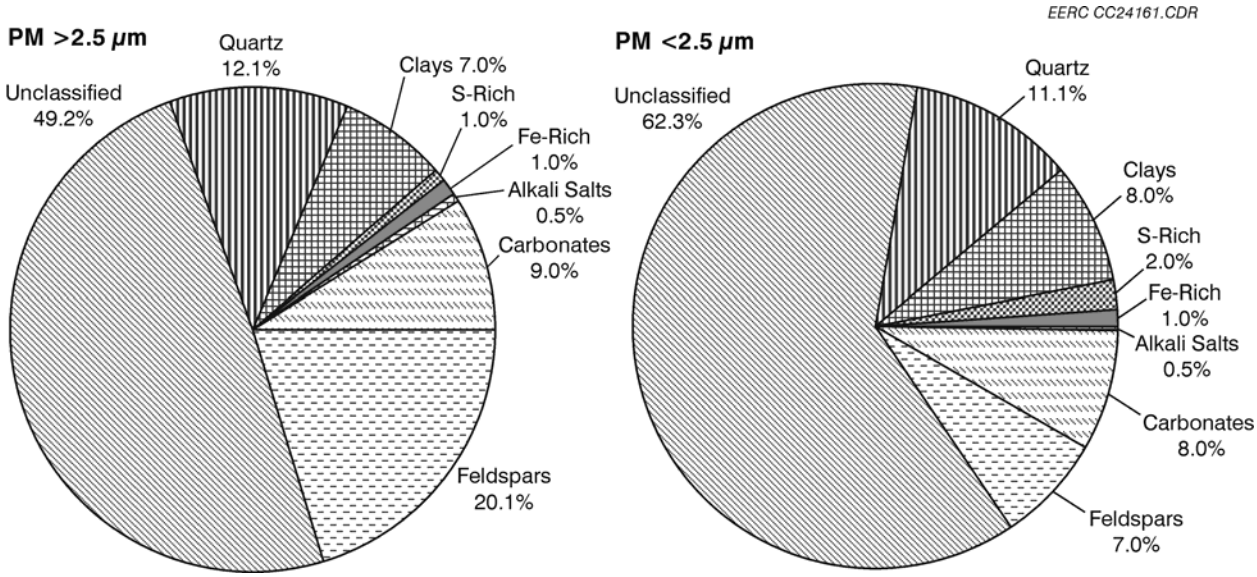


Figure II-15. Classification of particles a) >2.5 µm and b) <2.5 µm collected at Site 1 (North Dakota farm), August 2000.

*North Dakota Ranch Site (Site 2)*

A comparison $PM_{2.5}$ particulate loadings obtained from the SAS, TEOM, and APS instruments at Site 2 (Figure II-1) is shown in Figure II-16. The 15-minute TEOM and APS measurements have been averaged over 24-hour periods to correspond to the SAS measurements. However, the APS data are too limited to make a good comparison between the mass loading and single-particle counting techniques. The TEOM again shows generally consistent but higher loadings than the SAS. The PM mass measurements at Site 2 were much lower than at Site 1, as illustrated in Figure II-16. The TEOM daily mean concentration for Site 2 is 9.6 vs. 15 $\mu g/m^3$ at Site 1.

As illustrated in Figure II-17, 79% of the $PM_{2.5}$ consists of unclassified and organic components. The particles in these classification categories are mostly spores, pollen, soil, and fugitive dust. The remaining 13%–21% of $PM_{2.5}$ collected at the sites is inorganic-rich. The clays, quartz, carbonates, and feldspars are primarily associated with fugitive dust from nearby gravel roads and fields. The alkali-salt content of all three samples is consistent, suggesting a regional, and perhaps natural, source for this particle type. $PM_{2.5}$ samples from Sites 1 and 3 are compositionally similar. $PM_{2.5}$ from Site 2, however, contains a greater proportion of sulfur-rich particles, presumably composed of secondary sulfate compounds. High-temperature combustion-derived particles (fly ash) were not significant PM components at this site, with only three instances from about 1,200 particles that were analyzed.

Weather Conditions

Weather conditions at Site 2 were generally clear and sunny with warm days in the mid-70°F and clear, progressively cooler nights reaching near-freezing temperatures by the end of the

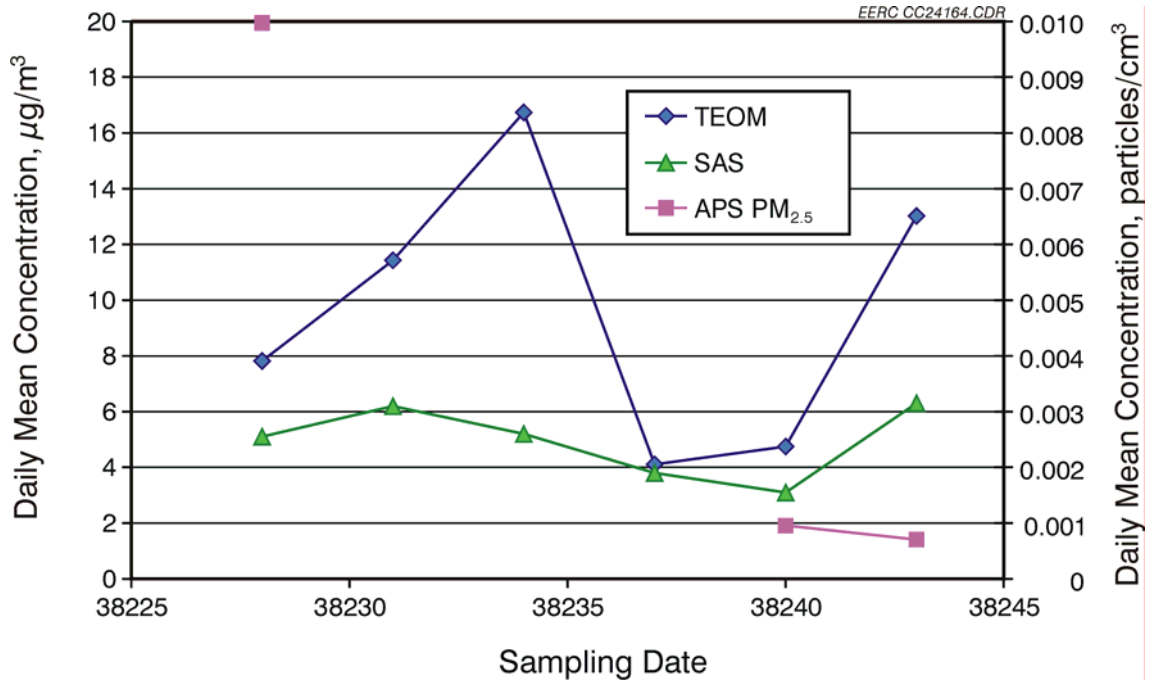


Figure II-16. SAS, TEOM, and APS $PM_{2.5}$ loadings at Site 2 (North Dakota ranch), August 29 to September 13, 2001.

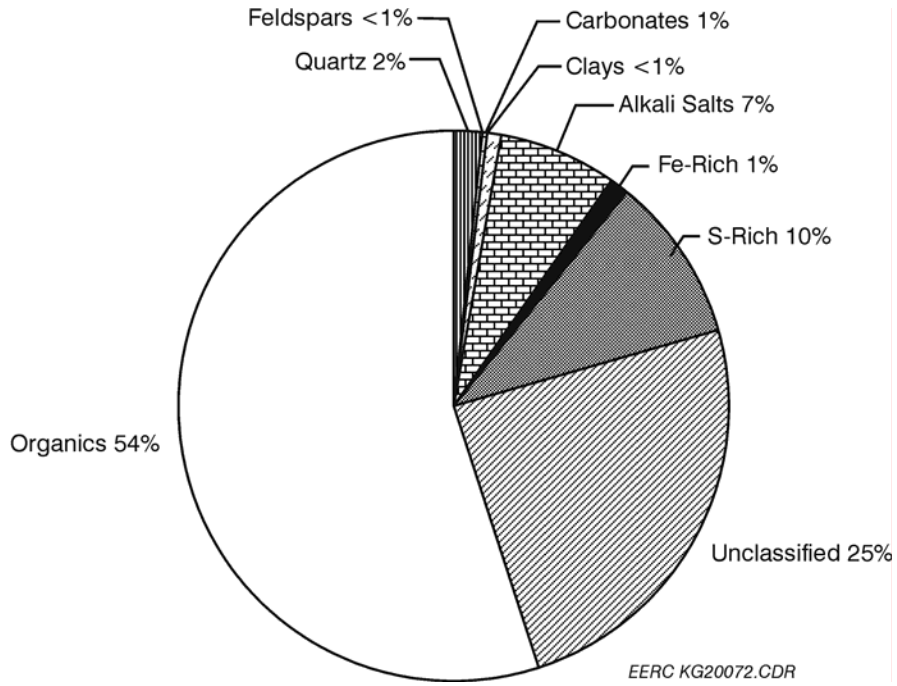


Figure II-17. Chemical classification of $PM_{2.5}$ from ACCU samples collected at Site 2 (North Dakota ranch).

sampling period. The mean high temperature was 76°F (24°C) and the range was 50°–99°F (10°C–37°C). Lows for the sampling period ranged from 38°F (3.6°C) to 58°F (14°C) with a mean low of 49°F (9.3°C). Several power brownouts temporarily interrupted power to the instruments. Storm activity, however, was light, with a total recorded rainfall of 4 in. (11 cm). The daily maximum wind speed recorded when the weather station was operational fluctuated from 8.8 mph (14 kmh) to 24 mph (39 kph). The mean was 16 mph (26 kph). While the wind direction varied, it was rarely from the west, with the exception of September 9, when the readings were west or west-southwest interspersed with readings around the compass throughout the day. Given the overall wind direction during this sampling, it is doubtful that winds were favorable for direct deposition of combustion materials from the power-generation facilities located west of the sampling site.

*Dispersion Modeling*

The monitoring results from the North Dakota farm and ranch Sites 1 and 2 were drastically different—in particle loading, in composition, and in appearance. Site 1 sampling results indicate high amounts of fly ash that predominantly were attributable to a combustion process. Emission from the coal-fired power plant northwest of the sampling site is the likely source of these materials. Dispersion modeling results similar to those shown in Figure II-18 indicated time periods during monitoring activities at Sites 1 and 2 when emissions could be contributing to the surface ambient air sample composition. With respect to Site 1, these periods have a dispersive movement from the northwest toward the southeast where the sampling site was located. Time periods in coordinated Universal Time (Z time zone, five hours ahead of

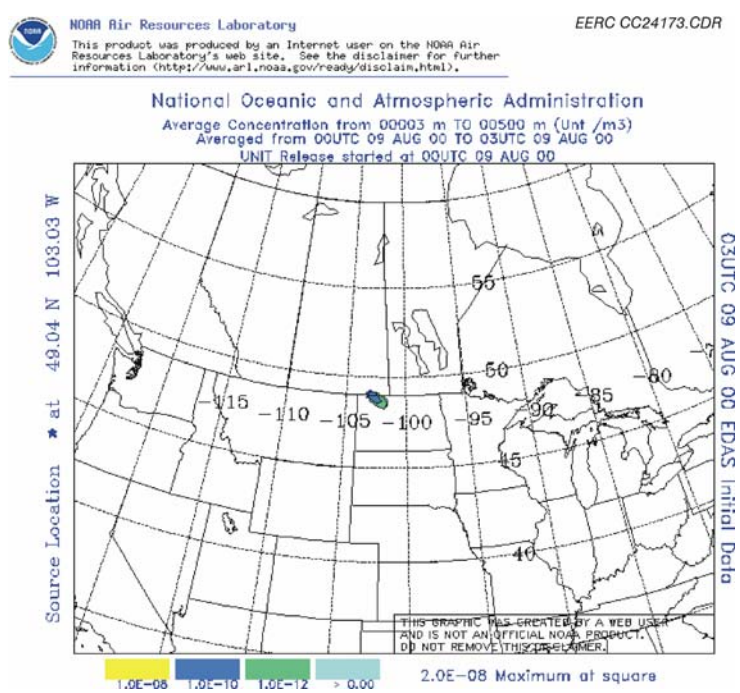


Figure II-18. Dispersion modeling results for August 8, 7–10 PM, at Site 1.

Central Daylight Time—S time zone—where the monitoring activities took place) of this occurrence were:

- From 0700Z on 8/17/00 to 0300Z on 8/18/00 (21 hours).
- From 0000Z to 0700Z on 8/21/00 (7 hours).
- From 1900Z on 8/22/00 to 0700Z on 8/23/00 (12 hours).
- From 1600Z on 8/24/00 to 0700Z on 8/25/00 (15 hours).

The power generation region near Site 2 could also have influenced the PM composition at Site 1 during periods from south to northerly dispersion. Time periods when this region may have contributed are as follows:

- From 0900Z on 8/18/00 to 0500Z on 8/19/00 (20 hours).
- From 0700Z on 8/19/00 until 0700Z on 8/21/00 (48 hours).
- From 0300Z to 2100Z on 8/22/00 (18 hours).
- From 1700Z on 8/23/00 to 1000Z on 8/24/00 (17 hours).
- From 0900Z on 8/26/00 to 0700Z on 8/29/00 (70 hours).

Dispersion model results at Ranch Site 2 indicated the probable influence of coal-fired power generation activity in the area west of the sampling site. Time periods of west to east dispersion would result in an effect on sampling results from sources. These time periods were determined as follows:

- From 2300Z on 8/29/01 to 1300Z on 8/31/00 (38 hours).
- From 1400Z on 9/1/01 to 2100Z on 9/2/02 (31 hours).
- From 0700Z on 9/6/00 to 0700Z on 9/7/00 (24 hours).
- From 0700Z on 9/9/00 to 0700Z on 9/11/00 (48 hours).

High amounts of sulfur indicated from the surface sampling results could be attributed to secondary particle formation from coal-fired power generation and oil refining, and also from natural decomposition processes of the many wetlands in the area. Particle analysis was not able to distinguish the source.

### Ternary Diagram Analysis

Since the North Dakota Site 1 Burkard and ACCU samples were collected under a variety of wind directions, analyses collected during times of northwesterly, southerly, and easterly winds were compared for chemical composition and appearance to determine whether wind direction had a measurable effect on PM composition. Ternary diagrams, essentially three-dimensional histograms, compare the concentration of three elements in a sample relative to each other, with the center of the diagram representing equal portions of each element in the material analyzed. As with any frequency diagram, the vertical axis represents the number of particles in each bin, i.e. containing each ratio of the elements represented at the vertices. Elemental groupings were selected to represent combinations of mineral elements typical of fly ash and/or fugitive dust particles. Figure II-19 are the Al:Si:(Ca + Na + K + Mg) ratios for both the Burkard and ACCU samples collected August 15–17, 2000. The diagrams show similar frequency

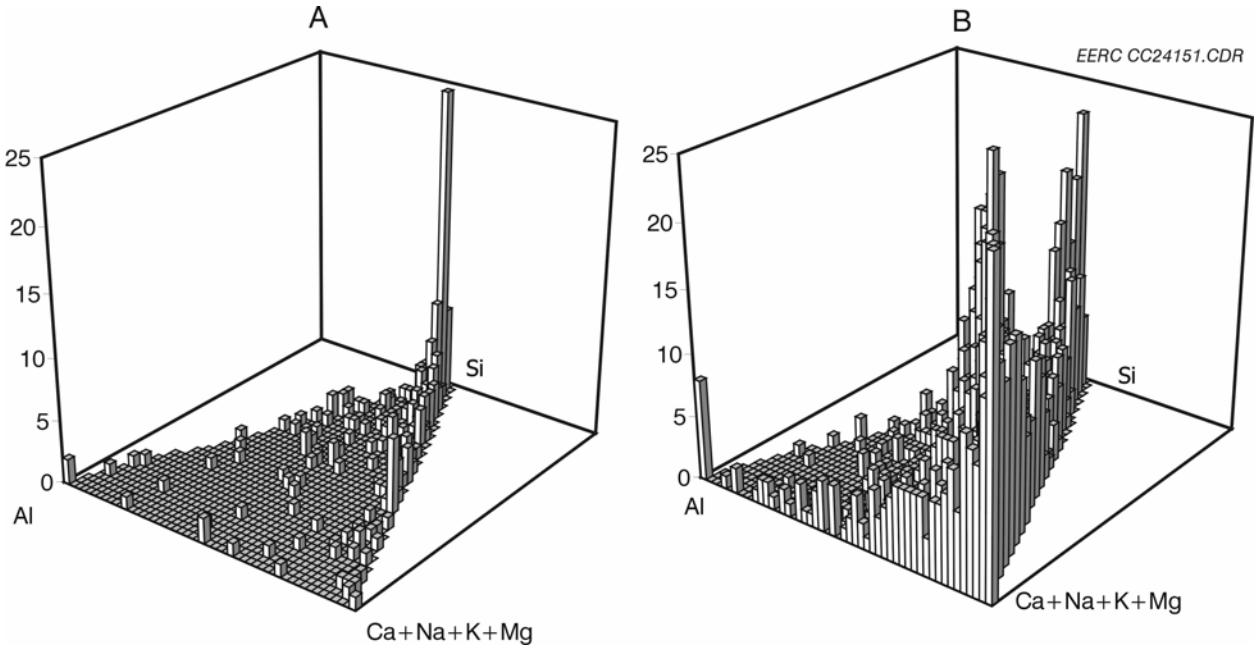


Figure II-19. The ratio of aluminum and silicon to alkali metals in the a) Burkard and b) ACCU samples collected from noon to noon, August 15–17, 2000, at Site 1 when the wind was from the north-northwest.

patterns, few particles containing Al, many particles high in Si, and many particles high in alkali metals, suggesting that the content of the material is not size-fractioned with respect to the ratios of these six elements. In some instances, the Burkard sample appears to contain greater quantities of parameters such as Si, Ca, Al, and Na (Aug 9–11, 2000, noon to noon). In other cases, the ACCU samples contain larger ratios of alkali elements and S (Aug 15–17, 2002, noon to noon).

*Northwesterly Wind Conditions*

Presented in Figure II-20a, the ternary diagram of the Si–Al–Fe ratios from the Burkard sample collected noon to noon August 15–17, 2000, shows quartz and clay groupings of particles. It also shows a strong contingent of SiFe particles along the Fe–Si axis. While present in both sample types, it has greater frequency of occurrence in the ACCU sample collected during the same time period (Figure II-20b).

Fe–Al-silicates and Fe–Si compounds are potential signatures of fly ash. Pure Fe could be rust; pure Si could be sand. However, compounds rich in both Fe and Si indicate the presence of fly ash particles in the ambient sample. The ACCU sample in particular had a high frequency of particles of this type. The Burkard sample ternary indicated some Fe–Si particles, but more Fe–Al-silicates, Al–Si, and Si were present. The Fe–Al-silicates indicate fly ash particles. In contrast, Al–Si can arise from either fly ash and/or clay particles from fugitive dust.

More analyses consistent with fly ash particles were observed in the ACCU than in the Burkard sample. This can be explained by air current–particle settling. As in an aquatic stream,

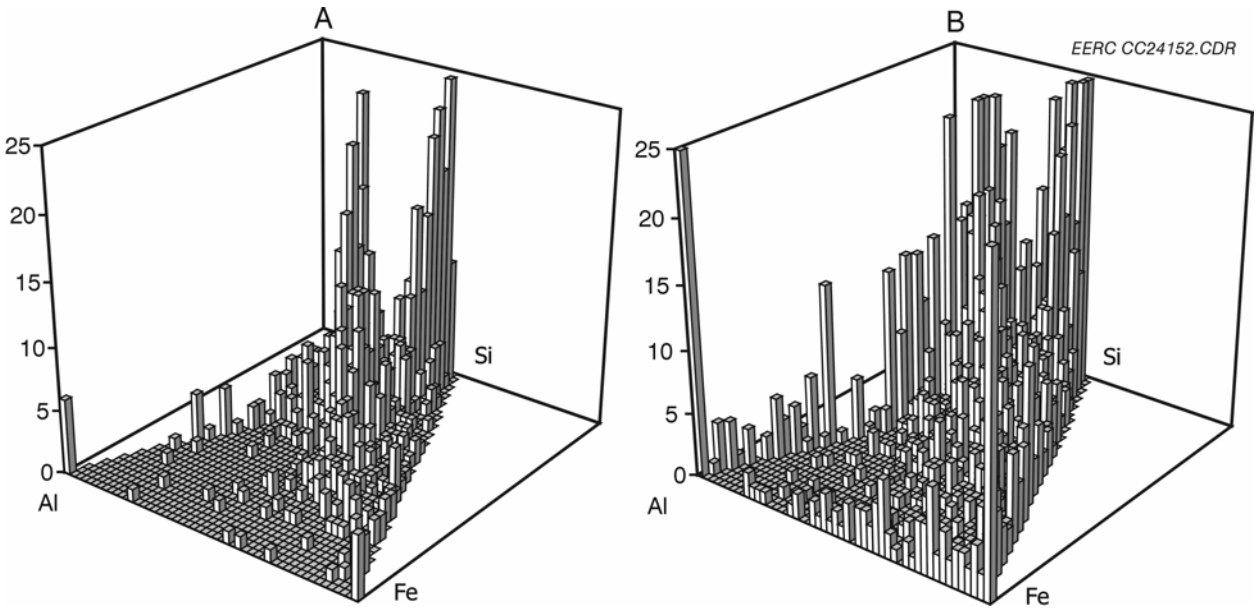


Figure II-20. The ratio of silicon, aluminum, and iron in a) Burkard and b) ACCU samples collected from noon to noon, August 15–17, 2000, at Site 1, when the wind was from the north-northwest.

the coarse particle fraction in the atmosphere will settle faster than the fine fraction. Since the ACCU collects only the $PM_{2.5}$ fraction, we can infer that the sampling site is a long distance from the possible high-temperature combustion sources, and more of the coarse particle fraction has settled out of the ambient air before reaching the sampling site.

Confirmation of the presence of fly ash particles is the spherical morphology indicative of the particle passing through a high-temperature combustion process. This is seen in Figure II-21, where the spherical fly ash particles are easily visible among angular dust and organic materials in the SEM micrograph of the Burkard sample collected during this time period. The $PM_{2.5}$ mass concentration during this sampling time was 10.9 $\mu g/m^3$ and the total accumulated mass was 63.9 µg.

Na and Ca sulfates can be combustion by-products or fertilizers. As illustrated in the ternary diagram in Figure II-22a, the Burkard sample appeared to have small amounts of $CaSO_4$, but the primary material present had higher Na–Ca content and low S content. These would likely represent clay particles. In contrast, the ternary diagram of the ACCU sample in Figure II-22b indicates a relatively larger number of particles of $CaSO_4$ and $Na_2SO_4$. Because the particles are finer, these are consistent with combustion-generated PM.

*Southerly Wind Conditions*

Presented in Figure II-23, the ternary diagram of the Si–Al–Fe ratios from the Burkard and ACCU samples collected noon to noon August 9–11, 2000, shows quartz and clay groupings of particles. Compared to the samples collected during a northwesterly wind, the Burkard sample

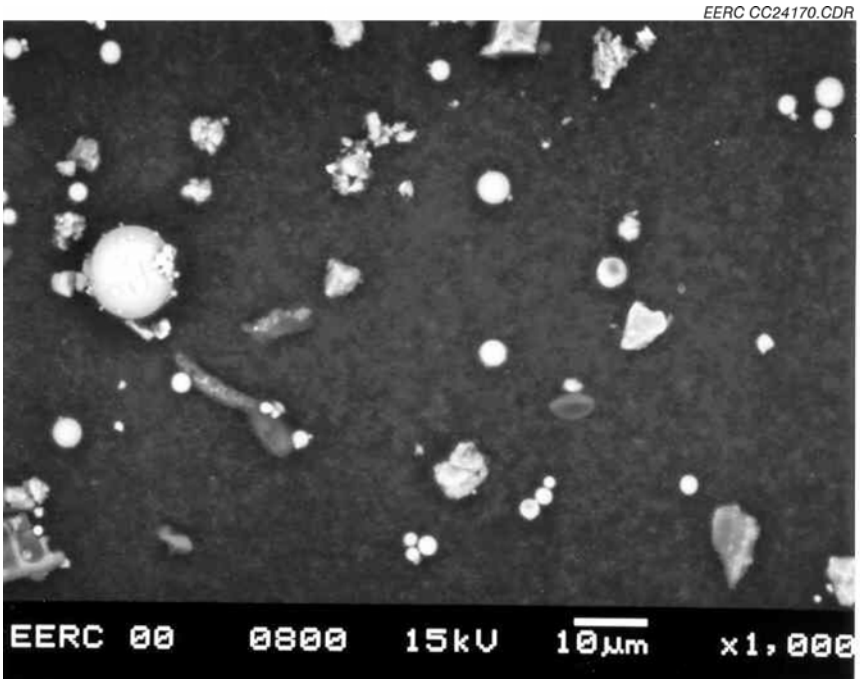


Figure II-21. SEM micrograph of Burkard sample collected between noon and noon, August 15–17, from Site 1, when the wind was from the north-northwest.

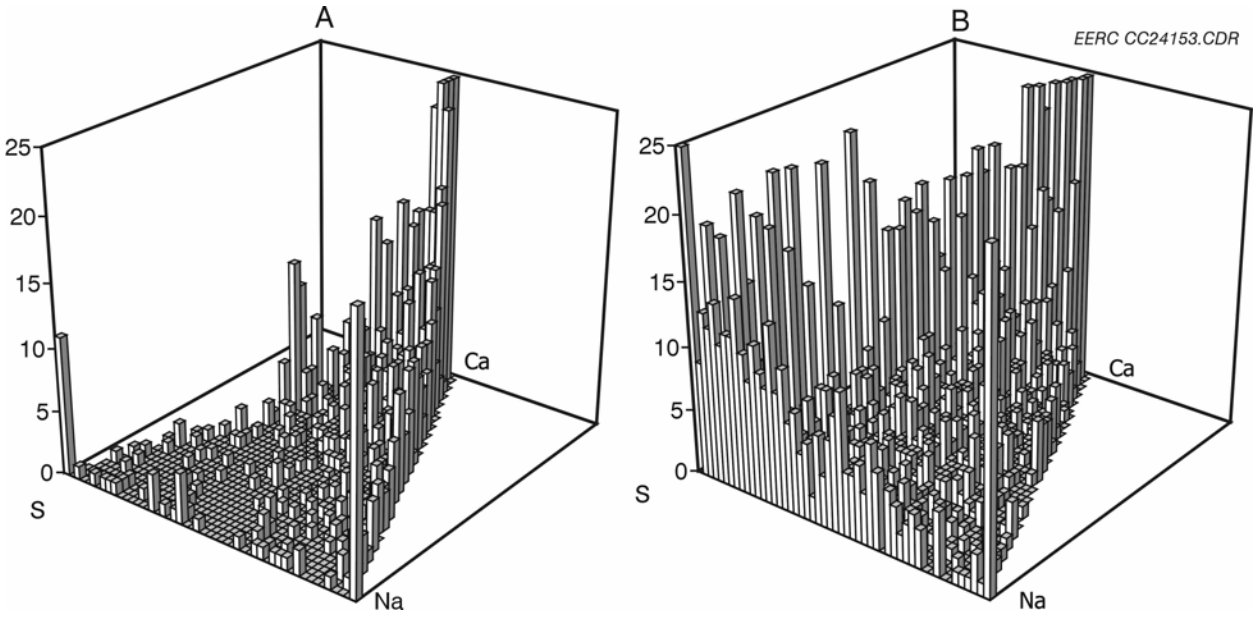


Figure II-22. The ratio of calcium, sulfur, and sodium in a) Burkard and b) ACCU samples collected from noon to noon, August 15–17, 2000, at Site 1, when the wind was from the north-northwest.

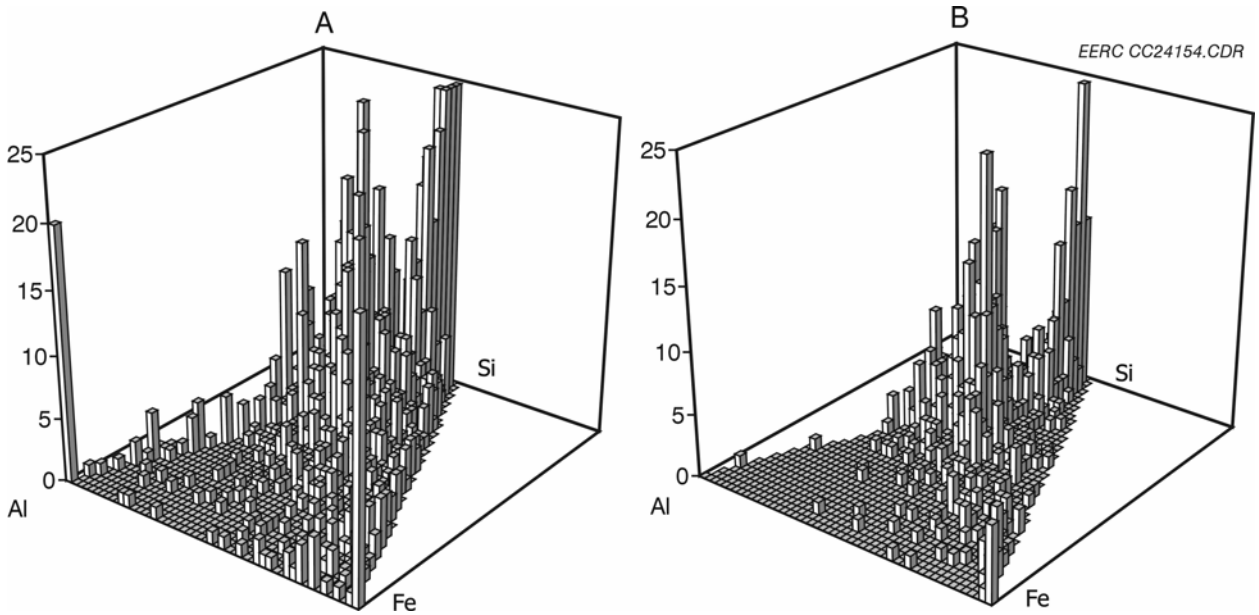


Figure II-23. The ratio of silicon, aluminum, and iron in a) Burkard and b) ACCU samples collected from noon to noon, August 9–11, 2000, at Site 1, when the wind was from the south.

collected when the wind was from the south contained primarily Al–Si particles (aluminosilicates), which are common compositions in both fly ash and crustal material. Likewise, the ACCU sample contained a larger portion of Al–Si particles. However, particles rich in Fe–Al–Si were present, suggesting that a certain level of fly ash was present in the sample. In this case, the Burkard sampler had greater frequency of occurrence than the ACCU samples.

SEM micrographs of the samples (Figure II-24) collected during the southerly wind period show large and small agglomerated spherical particles present with angular forms. The Burkard sample image includes organic matter visible at the bottom of the micrograph. The $PM_{2.5}$ mass concentration during this sampling time was 23 $\mu g/m^3$ and the total accumulated mass was 148 µg.

The Ca–S–Na ratios for these Burkard and ACCU samples are depicted in Figure II-25 These diagrams indicate that the Burkard sample collected under a south wind contained more $CaSO_4$ and Ca–Na-rich particles suggestive of clay particles. A comparison of the ternary diagram from the northwest wind and the south wind Burkard samples (Figures II-22a and II-25a) indicate that more Ca–Na–S particles were collected from the south than from the northwest. While TSP was not measured quantitatively, the TEOM total mass measurement for the $PM_{2.5}$ fraction during each period suggests that the total particle loading for the southerly wind period was greater (150 vs. 62 µg total mass at the loading rate of 13 LPM). A comparison of the ternary diagram from the northwest wind and the south wind ACCU samples (Figures II-22b and II-25b) indicates a lower particle loading in the ambient air from the south with respect to particles containing Ca, Na, and S. The ACCU sample collected under a south

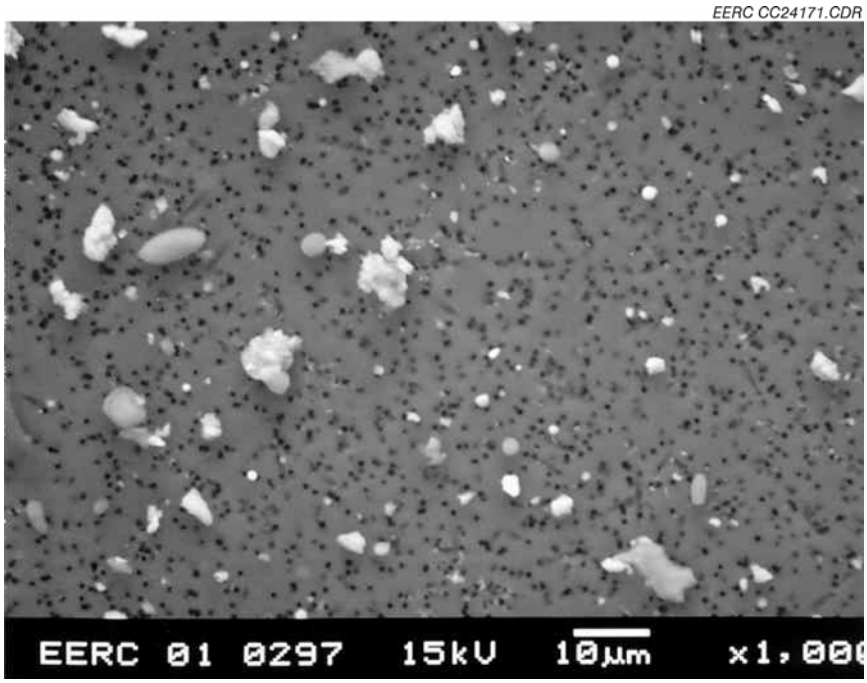


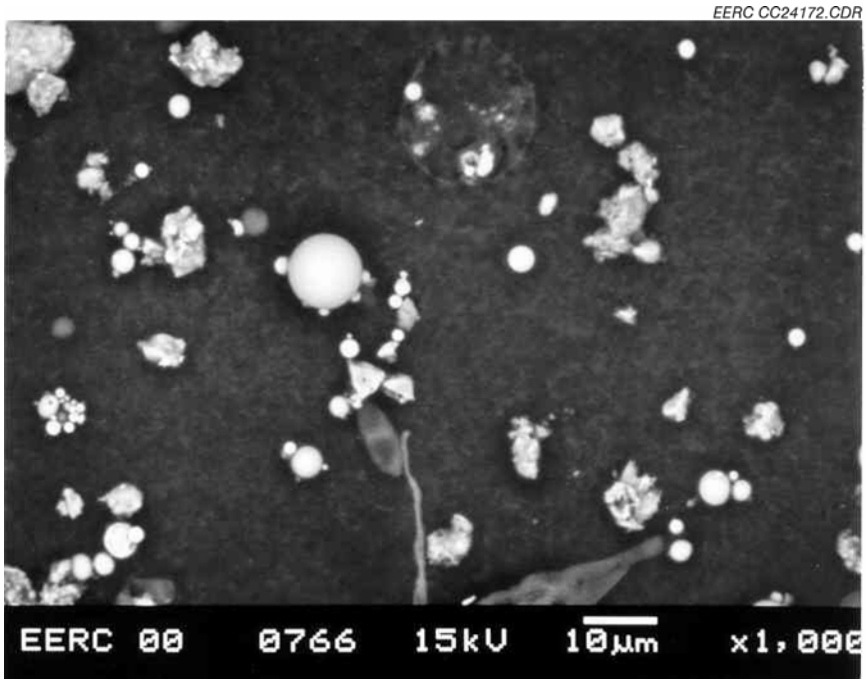


Figure II-24. SEM micrograph of Burkard, top, and ACCU, bottom, sample, collected from noon to noon, August 9–11, 2000, at Site 1, when the wind was from the south.

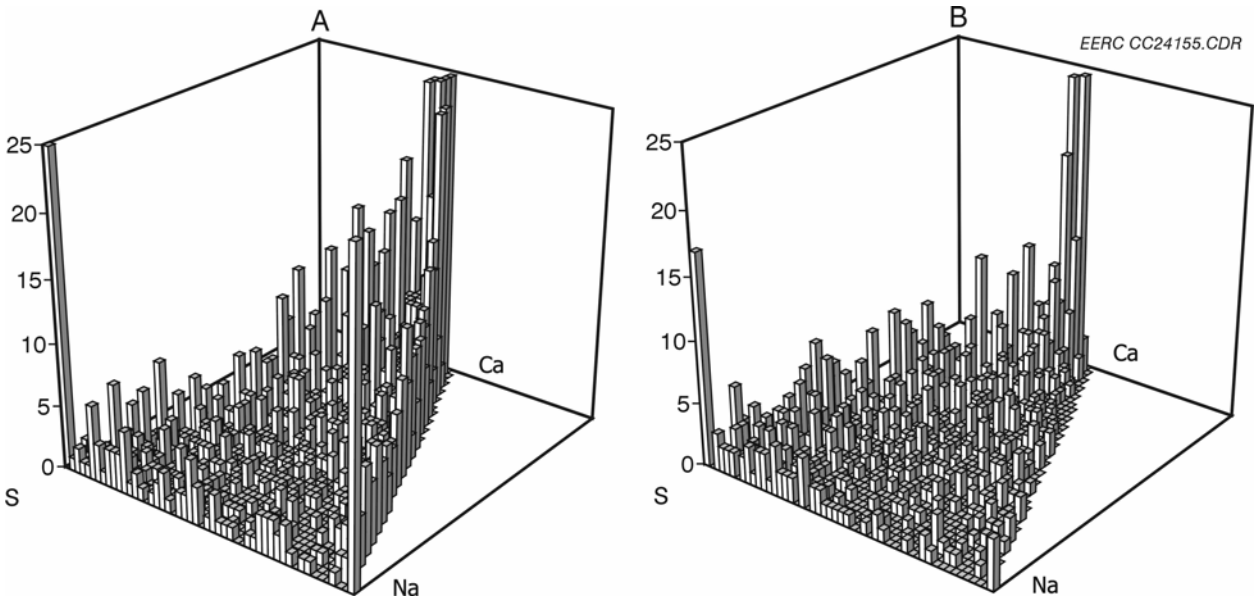


Figure II-25. The ratio of calcium, sulfur, and sodium in a) Burkard and b) ACCU samples collected from noon to noon, August 9–11, 2000, at Site 1, when the wind was from the south.

wind also contained lower concentrations of $CaSO_4$ than the sample collected under a northwest wind and fewer $CaSO_4$ and Ca–Na-rich particles than the larger size fraction.

*Easterly Wind Conditions*

The ternary diagram for the Burkard sample collected on August 21, 2000, from 3:00 to 23:00 is presented in Figure II-26. This represents 42% of the period evaluated for the two previous wind directions, so one might expect the frequencies to be lower. However, as the figure indicates, the TSP loading during this time period was comparatively very low with respect to particles containing Al, Fe, and Si. The pattern is consistent with some Fe aluminosilicate fly ash along with crustal materials. Likewise, the ternary diagram illustrating the Ca–S–Na ratio (Figure II-27) show low particle frequency and the highest incidence of calcium-rich materials and Na–Ca-rich particles with very low S content, suggestive of clays. Little $NaSO_4$ or $CaSO_4$ was present. Figure II-28 shows a micrograph of the Burkard sample collected during this time period, containing fewer particles and which are non-spherical, indicative of crustal materials, i.e. no fly ash was present. There is no corresponding ACCU sample because the sampling timeframe from the east was limited, and each ACCU sample overlapped with wind conditions from either the NW or S. The $PM_{2.5}$ mass concentration during this sampling time was 6.1 $\mu g/m^3$ and the total accumulated mass was 9.0 µg.

*Results from the Magnetic Sampler*

Particles of nearly pure metallic Fe, which are often agglomerated with Al–Si particles, are a definitive signature of fly ash produced from high-temperature combustion. Such material is attracted to a magnet and therefore can be collected easily with a magnet. A magnetic sampler

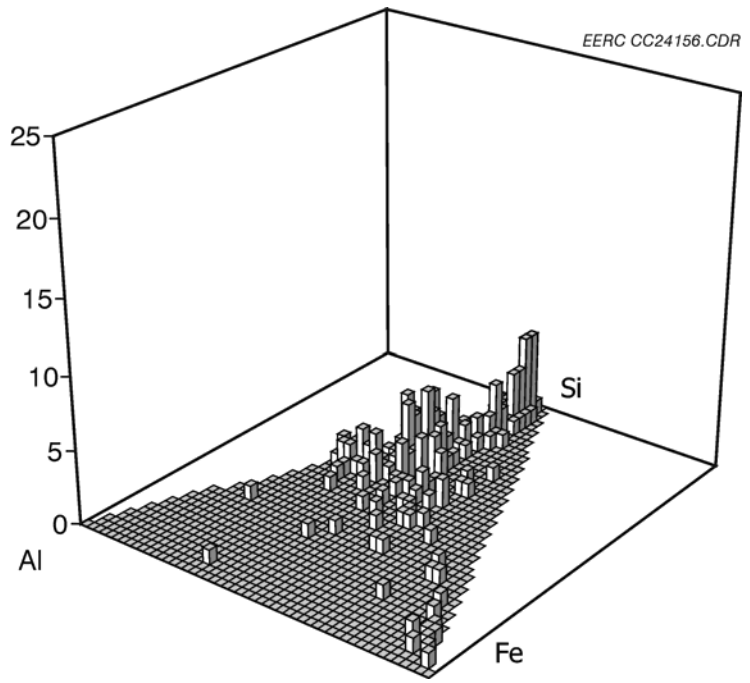


Figure II-26. The ratio of silicon, aluminum, and iron in Burkard samples collected from 3:00 to 23:00 on August 21, 2000, when the wind was from the east.

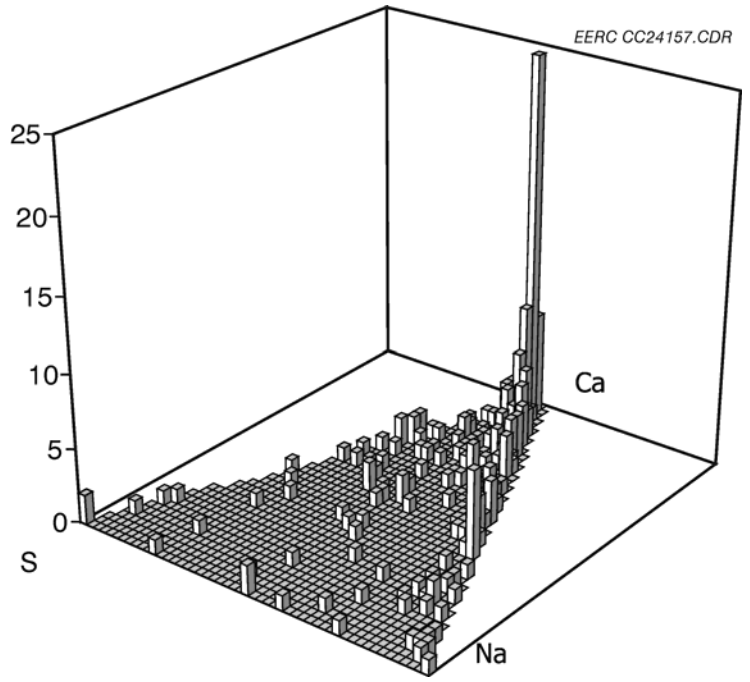


Figure II-27. The ratio of calcium, sulfur, and sodium in Burkard samples collected from 3:00 to 23:00 on August 21, 2000, when the wind was from the east.

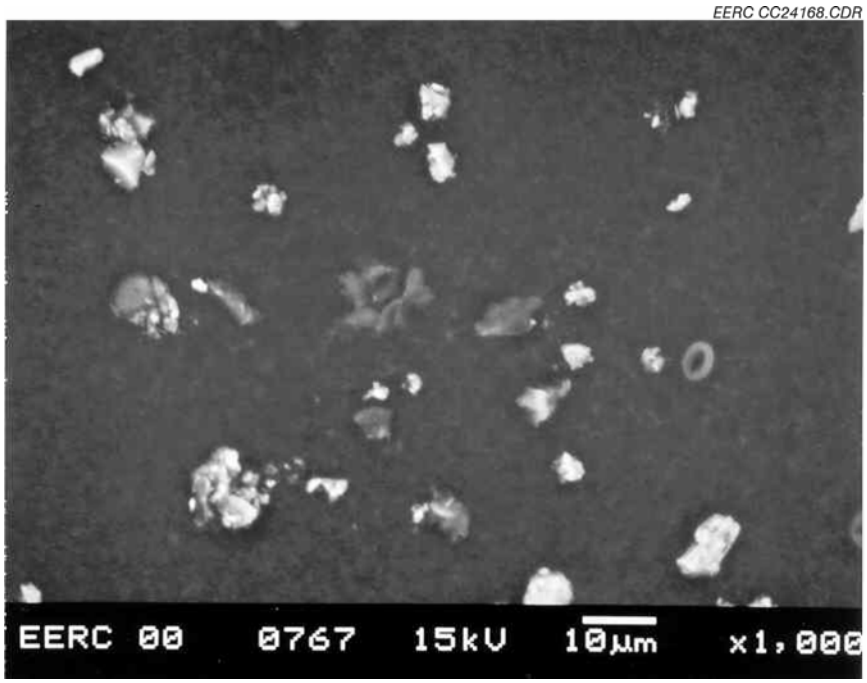


Figure II-28. SEM micrograph of Burkard sample collected from 3:00 to 23:00 on August 21, 2000, when the wind was from the east.

was assembled as a screening tool for fly ash particles at Site 1. The sampler consisted of a 1-L high density polyethylene sample bottle, a large magnet, and a plastic filter case in which the sample polycarbonate-coated filter membranes used to collect samples in the ACCU were affixed with double-stick tape. The magnet was packed into the sample bottle surrounded by polyurethane foam to hold it stable. A hole cut in the lid of the sample bottle was sized to secure the removable filter case so that the cover of the case could be removed for collection and replaced for transport to the laboratory. The sampler was mounted upside down under the Burkard sampler platform.

Figure II-29 shows an example of the morphology of particles collected with the magnetic sampler. Of the particles collected, all were spherical, except for two angular particles of pure Fe-oxide (rust). Table II-5 contains the SEM analysis of the representative particle shown in Figure II-29. The large particle containing mostly Fe with some O is typical of the material collected by the magnetic sampler. Of the smaller particles, the center one is a Fe-rich fly ash particle, but the one on the right is an Al–Si fly ash particle attached to the large Fe-rich particle.

*Comparison of Particulate Matter Compositions from Sampling Sites 1–4*

Figure II-4 compares the inorganic phase compositions of PM greater than and less than or equal to 2.5 microns ($>PM_{2.5}$ and $\leq PM_{2.5}$, respectively) collected from Site 4. Compositions of the two size fractions are similar. The majority of particles in both size ranges are unclassified and are mostly organic particles, such as spores, pollen, and topsoil. The clay, quartz, carbonate, and feldspar particles probably represent dust derived from vehicular traffic on a nearby gravel

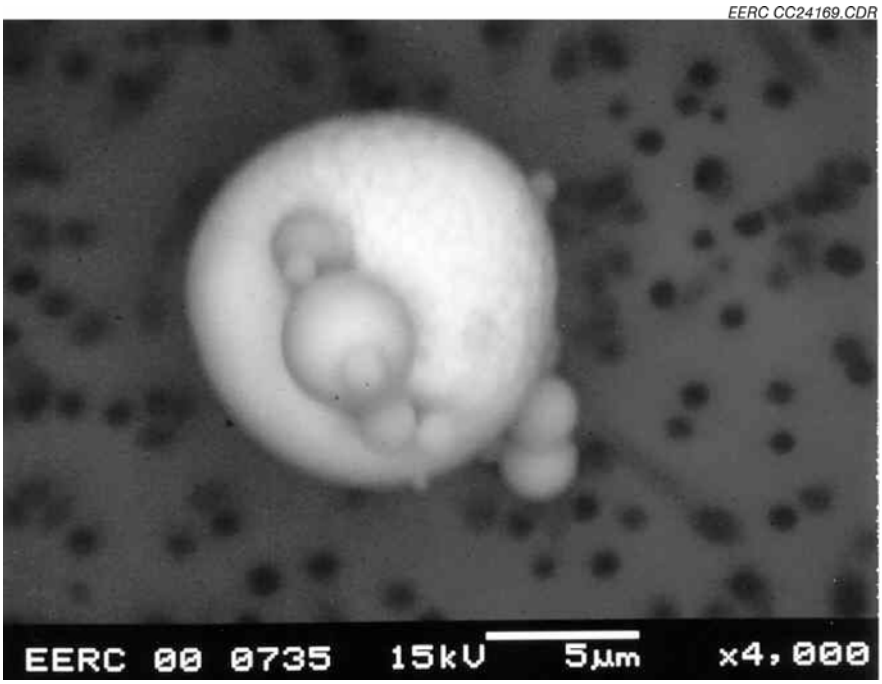


Figure II-29. SEM micrograph of the magnetic sampler substrate collected from Site 1 on August 8–10, 2000, when the wind was generally from the south.

**Table II-5. SEM Analysis of Particles Presented in Figure II-29 Collected from the Magnetic Sampler at Site 1**

| Element, wt% | Large | Center | Right |
|---|---|---|---|
| Na, wt% | 0.47 | | 3.68 |
| Mg, wt% | Trace | | 2.8 |
| Al, wt% | 2.02 | | 8.97 |
| Si, wt% | 2.95 | | 21.9 |
| S, wt% | Trace | | |
| K, wt% | Trace | 3.71 | 0.87 |
| Ca, wt% | 2.31 | 11.23 | 5.82 |
| Fe, wt% | 74.52 | 61.87 | 20.69 |
| O, wt% | 17.13 | 16.72 | 34.97 |

road. The sulfur-rich particles are probably gypsum released from a concrete fabrication facility in the area.

As with the urban site (Site 4), many of the particles from Site 3 are unclassified. The majority of these organic particles are derived from spring planting activities, which occurred near the Burkard sampling device. Figure II-8 indicates that the inorganic particles are classified as clays, feldspars, carbonates, and quartz. At this site, there were slight differences between the $>PM_{2.5}$ and $\leq PM_{2.5}$ fractions; $\leq PM_{2.5}$ contained more unclassified and carbonate particles.

Sampling at Site 1 was conducted during the late summer grain harvest. This explains the high (63%) concentration of unclassified particles in Figure II-15. During harvest, large amounts of fine dust and wheat chaff are airborne. The same separation between the two size fractions was also evident at this site.

The cluster analyses were performed to group large numbers of analyses into particle type, or categories, for source apportionment. The results of the cluster analyses indicate that cluster types are unique for each sample type as shown in Figures II-30 and II-31 for the Minnesota and North Dakota sites, respectively. The results for each of the data sets analyzed to date are summarized below.

North Dakota Site 4 Data

- The most significant cluster was the result of mixed clays.
- Other significant groups include quartz, biological material (spores, pollen, and other plant material), and calcite.

Minnesota Site 3 Data

- The most significant cluster was the result of mixed clays.
- Week 1 data also included dolomite, quartz, a calcium silicate phase, and calcite.
- Week 2 data also included a Na–P phase thought to be a result of agricultural fertilizers, calcite, and iron oxides.
- Secondary phase formation.
- A phase containing primarily sodium and phosphorus was found associated with an alumina-silicate phase thought to be primarily clays, and is thought to result from phosphorus applied to soils as fertilizer.

North Dakota Site 1 Data

- The most significant cluster was the result of mixed clays.
- Other significant groups included a calcium silicate phase, biological materials, an iron silicate phase, and iron oxides such as hematite.
- The calcium silicate phase and biological material were significantly higher at the North Dakota farm site than at the Minnesota farm site.

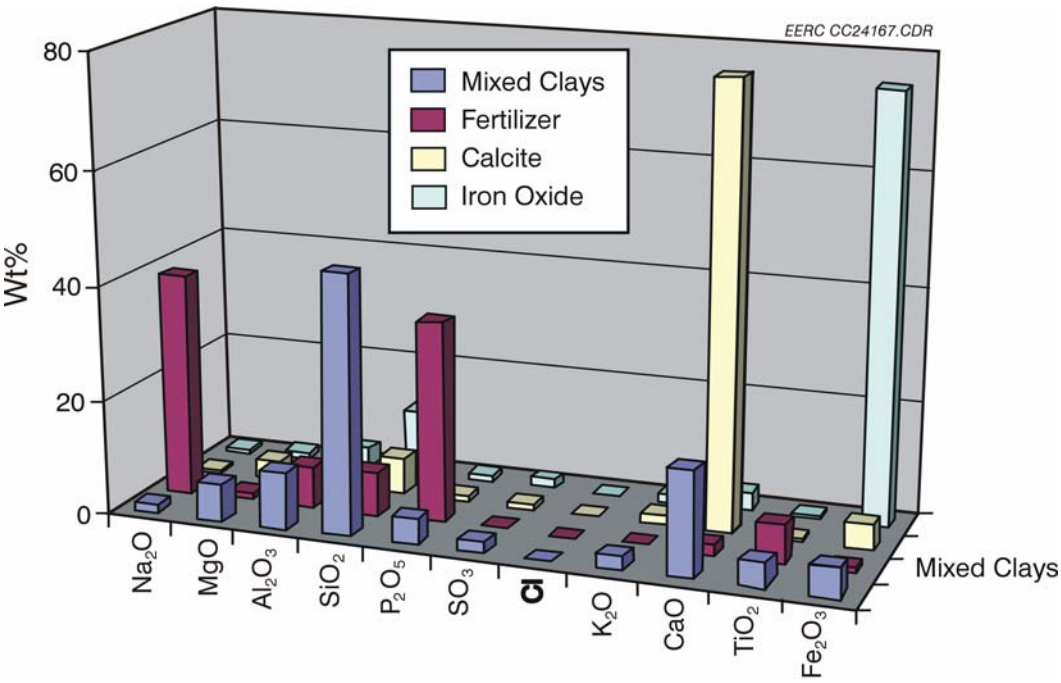


Figure II-30. Particle type categories determined for Site 3 (Minnesota farm, Week 2) using cluster analysis.

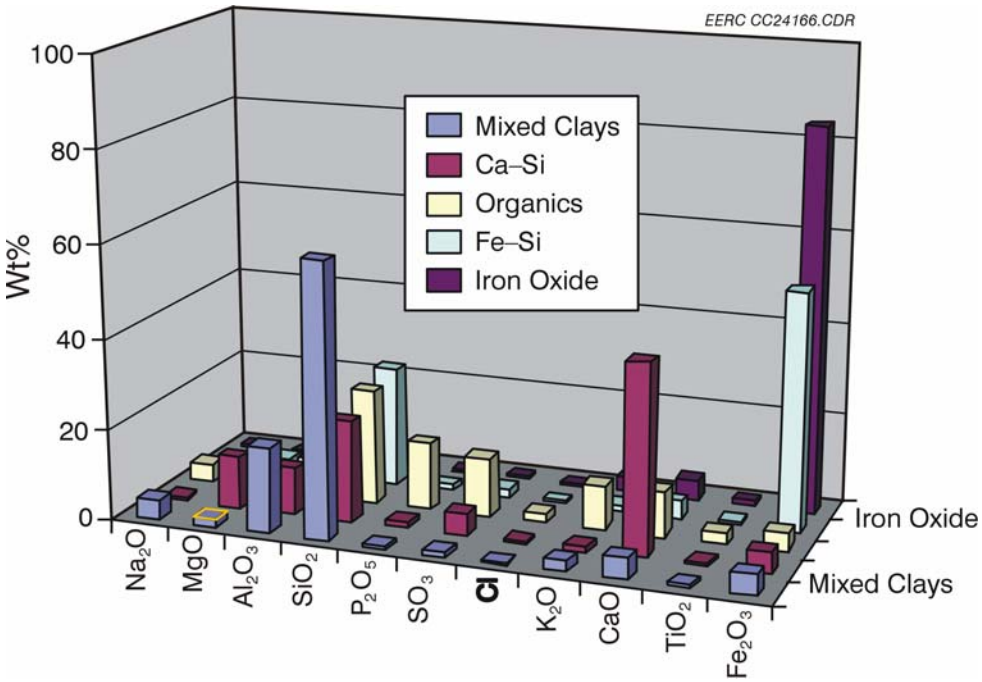


Figure II-31. Particle type categories determined for Site 1 (North Dakota farm, Week 1) using cluster analysis.

Unclassified Particles

The unclassified particles collected by the Burkard spore sampler identified by the previous cluster analysis were examined further and split into appropriate groups. Cluster analysis of the unclassified particle compositions are shown in Table II-6. Most of the unclassified particle compositions are characterized by Si contents of about 20–30 wt%, Ca from 10 to 15 wt%, Fe .5 wt%, and O from 35 to 40 wt%. The ratio of Si to Al is higher than that of montmorillonite, a type of clay, (1.5 < Si/Al < 2.5) and it consistently ranges from 3.2 to 3.5. These compositional characteristics are most consistent with mixed-clay particles. Indeed, presented in Figure II-15b is an SEM photomicrograph showing small-particle agglomerates consisting of tightly packed clay particles or silt-sized quartz grains held together with clay particles. These particle types account for the greatest portion of unclassified particles from all four sites, with the exception of the large number of biologically derived particles from Site 3. The mixed clays are likely from road dust. Biologic particles are distinguished by N contents >2 wt% and low x-ray counts. Shape also is important in identifying biological particles which generally have high aspect ratios rather than the low ratios that correspond to blocky or rounded particle surfaces. These particles are likely from harvest activities and spring planting that was under way during sample collection. Sites 1 and 3 contained several Na- and P-rich particles, which are probably derived from agricultural fertilizers. The less frequent groups included coated Si particles and fertilizer particles.

**Table II-6. Cluster Analysis Results of Unknowns from Selected Burkard Sample Data Sets, elemental wt%**

| Site No. | 4 | 4 | 4 | 3 | 3 | 3 | 1 | 1 | 1 |
|---|---|---|---|---|---|---|---|---|---|
| N | 0.8 | 0.4 | 1.0 | 1.3 | 4.1 | 1.3 | 0.4 | 8.2 | 1.8 |
| Na | 1.0 | 38.5 | 0.3 | 1.2 | 1.3 | 38.7 | 1.5 | 1.4 | 0.2 |
| Mg | 3.0 | 0.9 | 1.6 | 3.6 | 2.6 | 0.4 | 2.9 | 2.4 | 0.5 |
| Al | 5.7 | 4.4 | 5.3 | 7.0 | 5.8 | 4.2 | 9.4 | 0.7 | 2.2 |
| Si | 22.6 | 5.1 | 67.4 | 23.5 | 19.3 | 5.4 | 30.2 | 2.3 | 73.2 |
| P | 1.9 | 23.3 | 0.2 | 1.6 | 3.6 | 20.6 | 0.6 | 8.9 | 0.3 |
| S | 1.3 | 0.2 | 0.2 | 0.8 | 2.9 | 0.2 | 0.7 | 5.9 | 0.4 |
| Cl | 0.6 | 1.0 | 0.3 | 0.3 | 1.0 | 0.3 | 0.2 | 1.0 | 0.3 |
| K | 1.5 | 0.7 | 3.0 | 2.9 | 5.0 | 0.1 | 3.2 | 10.9 | 1.4 |
| Ca | 16.5 | 1.0 | 3.2 | 11.2 | 6.7 | 2.0 | 9.3 | 4.1 | 1.9 |
| Ti | 3.6 | 18.5 | 0.6 | 1.7 | 1.4 | 5.4 | 0.6 | 0.7 | 0.6 |
| Fe | 5.3 | 0.4 | 5.6 | 5.7 | 4.8 | 0.6 | 6.2 | 0.9 | 1.9 |
| O | 35.7 | 1.1 | 11.6 | 39.0 | 41.3 | 0.7 | 34.6 | 52.6 | 15.2 |
| Source | Mixed clay | Fertilizer | Coated Si | Mixed clay | Biological | Fertilizer | Mixed clay | Biological | Coated Si |
| Freq. | 4130 | 54 | 34 | 6597 | 3408 | 28 | 3110 | 492 | 19 |

Dispersion modeling results, similar to those shown in Figure II-18 indicate that the prevailing westerly and northwesterly winds during the sampling campaigns may have contributed primary and secondary combustion $PM_{2.5}$ to the samples collected at Sites 1 and 2. $PM_{2.5}$ collected on the membrane filters generally ranged from <0.4 to 1 µm in diameter. As indicated in Figures II-17, II-32, and II-33, 79%–87% of the $PM_{2.5}$ consists of unclassified and organic components. The particles in these classifications are mostly spores, pollen, soil, and

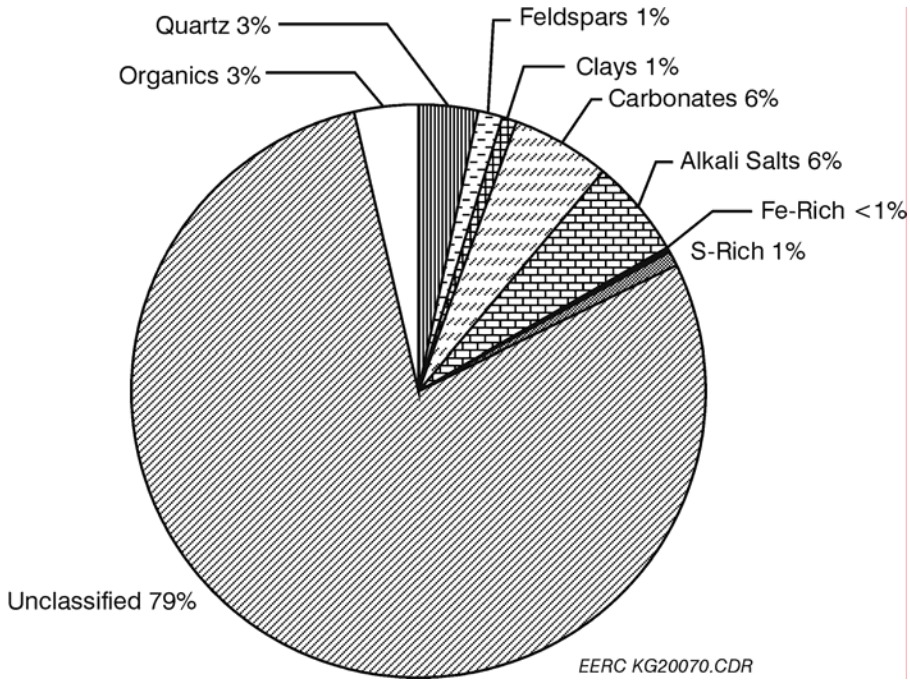


Figure II-32. Chemical classification of the ACCU $PM_{2.5}$ fraction from Site 3.

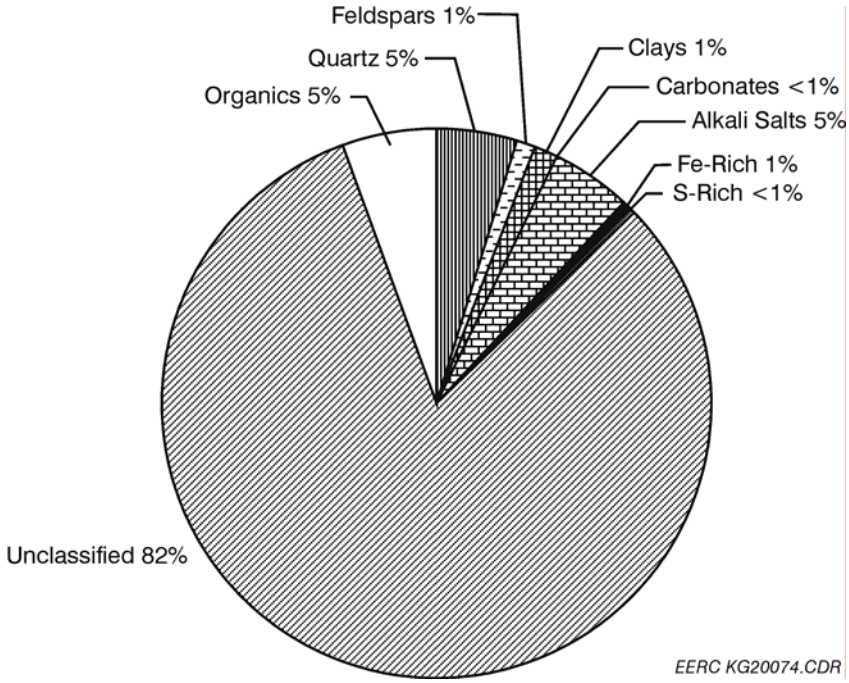


Figure II-33. Chemical classification of the ACCU $PM_{2.5}$ fraction from Site 1.

fugitive dust. The remaining 13%–21% of $PM_{2.5}$ collected is inorganic-rich. The clays, quartz, carbonates, and feldspars are primarily associated with fugitive dust from nearby gravel roads and fields. The alkali salt content of all three samples is consistent, suggesting a regional, and perhaps natural, source for this particle type. $PM_{2.5}$ samples from Sites 1 and 3 are compositionally similar. $PM_{2.5}$ from Site 2, however, contains a greater proportion of sulfur-rich particles, probably composed of secondary sulfate compounds.

### *Conclusions*

Comparison of SAS, TEOM, and APS showed the same trends in particle concentration. The differences measured by these instruments likely are the result of the way each instrument measures $PM_{2.5}$. If particle densities could be measured, the mass loading would be more comparable. This anomaly reinforces the need for more than one sampler to obtain a complete picture of $PM_{2.5}$.

The characteristics of particles collected with the ACCU and Burkard samplers showed significant differences. The Burkard sampler collects particles >0.5 µm; these particles consist of crustal materials such as clays and road dust. The ACCU sampler collects particulate <2.5 µm, including low-density organic particles and sulfates and nitrates. Both sampling techniques combined with computer-controlled SEM analysis provided better representation of the PM, and facilitated the tracking of PM sources.

### *References*

*Air Quality in Minnesota: Problems and Approaches*, Minnesota Pollution Control Agency, January, 2001.

*Annual Report of North Dakota Air Quality Monitoring Data*, North Dakota Department of Health, Division of Air Quality, Sept., 2001.

Battarbee, J.L.; Rose, N.L.; Xuezhu L. *Atmos. Environ*. **1997**, *31*, 171–181.

Davis, S.B.; Fernandez, A.; Wendt, J.O.L.; Cenni, R.; Young, R.S.; Witten, M. Potential Respiratory Distress Due to the Composition of Particulate Emissions from Biomass Co-Combustion with Coal. Nature 2000 Dec.

EPA. National Ambient Air Quality Standards for Particulate Matter-Final Rule. **199**, Fed. Regist. 62(138):38651–38760.

Haupt, O.; Schaefer, C.; Strauß, S.; Dannecker, W. Production of Calibration Standards for X-Ray Fluorescence Analysis of Aerosol Particles Precipitated on Different Filter Materials. *Fresenius J. Anal. Chem.* **1996**, *355*, 375–378.

*North Dakota Children's Health Study*, Final Report prepared for North Dakota Department of Health and Industrial Commission of North Dakota by Environmental Health and Engineering, Inc. and Johns Hopkins Bloomberg School of Public Health, Nov. 15, 2001.

U.S. Environmental Protection Agency. C*ompendium of Methods for the Determination of Inorganic Compounds in Ambient Air*; EPA/625/R-96/010a, June 1999.

Veranth, J.M.; Smith, K.R.; Aust, A.E.; Dansie, S.L.; Griffin, J.B.; Hu, A.A.; Huggin, M.L.; Lighty, J.S. *Aerosol Sci. Technol.* **2000a**, *32*, 127–141.

Veranth, J.M.; Smith, K.R.; Hu, A.A.; Lighty, J.S.; Aust, A.E. *Chem. Res. Toxicol.* **2000b**, *13*, 382–389.

Veranth, J.M.; Smith, K.R.; Huggin, M.L.; Hu, A.A.; Lighty, J.S.; Aust, *A.E. Chem. Res. Toxicol.* **2000c**, *13*, 161–164.

***Bibliography***

Benson, S.A.; Laumb, J.D.; Jensen, R.R.; Eylands, K.E.; McCollor, D.P. Comparing Particulate Matter Characteristics Collected Using Various Sampling Instruments. *Prep. Am. Chem.—Soc., Div. Fuel Chem*. **2001**, *46* (1), 599–601.

Benson, S.A.; McCollor, D.P.; Eylands, K.E.; Laumb, J.D.; Jensen, R.R. Characterization of Particulate Matter Collected with a Burkard Sampler. *Prep. Am. Chem.—Soc., Div Fuel Chem.* **2001**, *46* (1) 396–301.

Benson, S.A.; McCollor, D.P.; Eylands, K.E.; Laumb, J.D.; Jensen, R.R. Characterization of Particulate Matter with Computer-Controlled Scanning Electron Microscopy. In *Environmental Challenges and Greenhouse Gas Control for Fossil Fuel Utilization in the 21st Century*; Plenum Press: New York, 2002; pp 29–42.

Crocker, C.R.; Eylands, K.E.; McCollor, D.P.; Helmowski, B.S.; Benson, S.A.; Galbreath, K.C. Characterization of PM $_{2.5}$ from Rural Midwestern U.S. Sites. *Prepr. Pap.—Am. Chem. Soc., Div. Fuel Chem.* **2002**, *47* (2), 632–637.

Crocker, C.R.; Eylands, K.E.; McCollor, D.P.; Helmowski, B.S.; Benson, S.A.; Galbreath, K.C. Characterization of $PM_{2.5}$ from rural midwestern U.S. sites, 224th American Chemical Society Meeting, Division of Fuel Chemistry, *Symposium on Monitoring and Control of Air Toxics and Fine Particulate Matter ($PM_{2.5}$)*, Boston, Massachusetts, August 18–22, 2002.

Helmowski, B.S. $PM_{2.5}$ Ambient Sampling Analyzed in Conjunction with Dispersion Modeling at Three Upper Midwest Locations," Seminar presented at: University of North Dakota John D. Odegard School of Aerospace Sciences, November 7, 2002.

Helmowski, B.S.; Benson, S.A.; Laumb, J.D.; Crocker, C.R.; Eylands, K.E.; McCollor, D.P.; Galbreath, K.C.; Jensen, R.R. Characterization and source apportionment of particulate matter from rural sites, *International Conference On Air Quality III: Mercury, Trace Elements, and Particulate Matter*, Arlington, V.A., September 9–12, 2002.

Laumb, J.D.; Eylands, K.E.; McCollor, D.P.; Crocker, C.R.; Jensen, R.R.; Benson, S.A. Upper Midwest Particulate Matter Sampling and Analysis. Presented at the Air Quality II: Mercury, Trace Elements, and Particulate Matter Conference, McLean, VA, Sept 18–21, 2000.

## Activity 2.2 – DNA Breakage Catalyzed by Coal-Derived Air Particulates

### *Introduction*

Several mechanisms of the toxicity of respirable particles have been proposed. The three leading hypotheses for cellular damage resulting from these particles are water-soluble transition metals (e.g. Fe, Cu, Ni, Zn) present in the particles, general acidity, and a general negative effect due to the ultrafine size of some particles (Dreher et al., 1997). The impacts of the water-soluble transition metals are postulated to be a consequence of their ability to catalyze the formation of reactive oxygen species such as the hydroxyl radical (OH·). These reactive oxygen species can induce damage to cellular components such as deoxyribonucleic acid (DNA), resulting in cleavage or base-pair changes and leading to inflammation, cancer, and other pathologies (Kamp et al., 1995). Respirable particles of asbestos and fly ash have been shown to have mobilizable iron, which can participate in the formation of reactive oxygen species (Lund and Aust, 1990a, Lund and Aust, 1990b, Smith et al., 1998, Weitzman and Graceffa, 1984). In addition, extracts from diesel engine particles and National Institute of Standards and Technology (NIST) ambient PM have been found to catalyze the formation of reactive oxygen species (Ball et al., 2000). In addition to catalyzing reactive oxygen species, asbestos has been shown to induce reactive oxygen species-mediated DNA breakage in both in vitro and in vivo (Lund and Aust, 1992, Kamp et al., 1995).

Based on this literature, it is clear that at least one mechanism of toxicity by respirable particles is through the formation of reactive oxygen species. Moreover, there is some evidence that these reactive oxygen species can damage DNA (damaged DNA is a potential mechanism for cancer). We evaluated the potential for coal-derived fly ash to catalyze reactive oxygen species DNA strand breakage. The assay used is essentially that of Lund and Aust (1992); it incubates the sample with bacteriophage DNA in the presence and absence of chelators and other chemicals. This DNA is a closed-circular superhelical DNA molecule; when it is cleaved, the superhelix unwinds, resulting in a relaxed molecule. The samples are separated on an agarose gel by electrophoresis. Although the molecular weight of the superhelical and relaxed forms are equal, the superhelical form migrates more quickly in the gel because of its apparent smaller size.

### *Methods*

Samples of ash were obtained from the combustion of Beulah lignite in the conversion and environmental process simulator at the Energy & Environmental Research Center (EERC). Two samples were analyzed for their ability to catalyze DNA breakage, a larger size fraction identified as from Cyclone #1, and a smaller size from Filter 115. The assay methods followed Lund and Aust (1992). Closed-circular superhelical φX174 RFI DNA was obtained from New England Biolabs (Beverly, Massachusetts). The DNA was removed from the shipping buffer by ethanol precipitation as described by Maniatis et al. (1984) and redissolved in 50 mM NaCl,

pH 7.5. Sodium citrate, D-mannitol, deferoxamine mesylate, and Chelex 100 were obtained from Sigma-Aldrich (St. Louis, Missouri). J.T. Baker L-ascorbic acid was obtained from Mallinckrodt Baker, Inc. (Phillipsburg, New Jersey). Sodium chloride was from Fisher Scientific (Fairlawn, New Jersey). Electrophoresis-grade agarose was from Bethesda Research Labs (Gaithersburg, Maryland). Contaminating metals were removed from 50 mM NaCl by chromatography using Chelex 100. The remaining solutions were prepared using Chelex-treated NaCl. Solutions of ascorbate and deferoxamine mesylate were prepared immediately before use. All solutions were prepared under incandescent yellow light and stored in the dark.

Ash samples (100 μg) were placed in sterile, metal-free polypropylene microcentrifuge tubes and incubated with φX174 RFI DNA (0.5 μg) in a total volume of 100 μL 50 mM NaCl, pH 7.5 with 1 mM chelator (citrate) and/or 1 mM ascorbate, for 30 minutes at 30°C. After the incubation period, an EDTA-free tracking dye was added, and the samples were centrifuged for 4 min. at 14,000 rpm. Samples were then loaded onto a 0.6% agarose gel and subjected to electrophoresis at 40 mA for 2 hours to separate closed-circular, superhelical (Form I) from DNA with single-stranded breaks (Form II). The gel was stained with ethidium bromide, transilluminated with ultraviolet light and the image captured using a UVP, Inc. (Upland, California) Minidarkroom equipped with a 16-bit charge-coupled device camera. The image was analyzed using UVP Labworks 4.0 software and the densities of each form of DNA were estimated. The density of Form I was divided by the total lane density to give the fraction of Form I remaining. All samples were then compared by expressing each as a percentage of the control DNA (i.e., DNA treated under identical conditions minus ash) and subtracted from 100% to give the percentage of DNA with single-stranded breaks. Inhibition of DNA breakage was determined with the iron chelator deferoxamine mesylate (1 mM), or by a competing $OH^{\cdot}$ scavenger (100 mM mannitol).

***Results***

The results of the assays of ash-catalyzed DNA strand breakage are shown in Tables II-7 and II-8 for the larger particle size Cyclone #1 and the smaller Filter 115 ashes, respectively. In order to interpret these data, the role of the treatments must be understood. Ascorbic acid can reduce the oxidation state of metals. Citric acid is a chelator that can increase the solubility of transition metals, resulting in increased activity. Deferoxamine mesylate is a specific chelator of iron and can decrease its availability. Mannitol, a sugar alcohol, is added as a scavenger of hydroxyl radicals.

Cyclone #1 ash catalyzed much higher strand breakage with ascorbic acid, suggesting that the reduction of metals was important. The addition of citric acid did not increase strand breakage, suggesting that metals were sufficiently soluble with chelation. The presence of deferoxamine mesylate decreased strand breakage, suggesting that iron was important in catalyzing strand breakage. The addition of mannitol did not decrease strand breakage, suggesting that hydroxyl radicals were not the breakage mechanism.

Filter 115 ash showed a different pattern than was observed for the larger particle-size ash. As with the Cyclone ash, the presence of ascorbic acid increased strand breakage. However, the addition of citric acid showed a much larger effect in increasing strand breakage. This suggests

**Table II-7. Percent DNA Breakage Induced by Cyclone #1 Ash**

| Treatment | % Breakage Relative to Control | % Breakage Relative to Blank |
|---|---|---|
| None | 16.8 | 16.8 |
| Ascorb[1] | 69.4 | 71.5 |
| Defer | — | 1.4 |
| Ascorb + Cit | 25.9 | 43.5 |
| Ascorb + Cit + Defer | — | 8.2 |
| Mann | — | 71.3 |
| Ascorb + Mann | — | 92.0 |
| Ascorb + Mann + Defer | — | 4.2 |
| Ascorb + Cit + Mann + Defer | 2.3 | 0.9 |

[1] Ascorb = ascorbic acid, Defer = deferoxamine mesylate, Cit = citric acid, Mann = mannitol.

**Table II-8. Percent DNA Breakage Induced by Filter #115 Ash**

| Treatment | % Breakage Relative to Control | % Breakage Relative to Blank |
|---|---|---|
| None | 0.0 | 0.0 |
| Ascorb[1] | 65.4 | 73.8 |
| Defer | — | 0.0 |
| Ascorb + Cit | 82.2 | 90.2 |
| Ascorb + Cit + Defer | — | 39.4 |
| Mann | — | 0.0 |
| Ascorb + Mann | — | 28.2 |
| Ascorb + Mann + Defer | — | 15.8 |
| Ascorb + Cit + Mann + Defer | 10.3 | 15.8 |

[1] Ascorb = ascorbic acid, Defer = deferoxamine mesylate, Cit = citric acid, Mann = mannitol.

that chelation was important in solubilizing metals. The addition of deferoxamine mesylate decreased strand breakage, as was observed with the Cyclone ash; however, the decrease in breakage was less than for the Cyclone ash. The addition of mannitol completely halted strand breakage in the Filter ash, but not in the Cyclone ash. This suggests that hydroxyl radical formation was the chief mechanism of strand breakage in this sample.

Both ashes showed significant activity in catalyzing DNA strand breakage. But the mechanism of strand breakage differed between the two samples. These differences could be due to the types of metals, the soluble concentrations of the metals, or both. More work is necessary to evaluate the effects of other conditions on catalysis of strand breakage. Additionally, it would be valuable to compare the composition and solubility of the two samples.

### *References*

Ball, J.C.; Straccia, A.M.; Young W.C.; Aust, A.E. The Formation of Reactive Oxygen Species Catalyzed by Neutral, Aqueous Extracts of NIST Ambient Particulate Matter and Diesel Engine Particles. *J. Air Waste Manage. Assoc.* **2000** *50*, 1897–1903.

Dreher, K.L.; Jaskot, R.H.; Lehamnn, J.R.; Richards, J.H.; McGee, J.K.; Ghio, A.J.; Costa, D.L. Soluble transition metals mediate residual oil fly ash induced lung injury. *J. Toxicol. Environ. Health* **1997** *50*, 285–305.

Kamp, D.W.; Israbian, V.A.; Preusen, S.E.; Zhang, C.X.; Weitzman, S.A. Asbestos causes DNA strand breaks in cultured pulmonary epithelial cellls: role of iron-catalyzed free radicals. *Am. J. Physiol.* **1995** *268*, L471–L480.

Lund, L.G.; Aust, A.E. Iron mobilization from asbestos by chelators and ascorbic acid. *Arch. Biochem. Biophys.* **1990a** *278*, 60–64.

Lund, L.G.; Aust, A.E. Mobilization of iron from crocodilite asbestos certain chelators results in enhanced crocodilite-dependent oxygen consumption. *Arch. Biochem. Biophys.* **1990b** *287*, 91–96.

Lund, L.G.; Aust, A.E. Iron mobilization from crocodilite asbestos greatly enhances crocodilite-dependent formation of DNA single-strand breaks in φX174 RFI DNA. *Carcinogenesis* **1992** *13*, 637–642.

Maniatis, T.; Fritsch, E.F.; Sambrook, J. Molecular cloning: a laboratory manual. Cold Spring Harbor Laboratory, Cold Spring Harbor, NY, 1984.

Smith, K.R.; Veranth, J.M.; Lighty, J.S.; Aust, A.E. Mobilization of iron from coal fly ash was dependent upon the particle size and the source of coal. *Chem. Res. Toxicol.* **1998** *11*, 1494–1500.

Weitzman, S.A.; Graceffa. P. Asbestos catalyzes hydroxyl and superoxide radical generation from hydrogen peroxide. *Arch. Biochem. Biophys.* **1984** *228*, 373–376.

## ACTIVITY 3 – INDOOR AIR QUALITY

### Activity 3.1 – Characterization of Indoor Air Quality

#### *Introduction*

Epidemiologic studies have shown a significant association between PM and mortality (1, 2). Growing concerns about the health risks of fine particles have led to the promulgation of a revised National Ambient Air Quality $PM_{2.5}$ by EPA. Because people spend 85% of their time indoors (3), it is widely recognized that a significant portion of total personal exposure to ambient PM occurs in indoor environments.

Ambient PM is a complex mixture of particle sizes and types from many sources. Studies (4, 5) show that the indoor particles not only came from outside, but indoor activities, such as cooking, space heating, office machines, ventilation, etc., also can generate submicrometer

particles. As a result of these indoor sources, indoor particle concentrations are often higher than ambient concentrations (6).

Despite the public health implications of indoor particle exposures, few studies have characterized sources of indoor $PM_{2.5}$. It is important, therefore, to quantify the major sources of indoor exposure, as well as the particle size and chemical composition distributions. Also, there are virtually no data on the effectiveness of air cleaning in reducing indoor exposures to $PM_{2.5}$ (7). It is important to evaluate control technology for indoor exposure.

*Objective*

The objective of this activity is to characterize indoor air particle concentration, size distribution, and composition.

***Experimental***

A SMPS and an APS were used to measure particle concentrations and size distributions at various locations in the EERC buildings: office area, hallway, lobby, demonstration facility, laboratory, and welding area. The sampling activities were conducted for 1-hour at each location during daytime.

A TEOM combined with ACCU system was set up and used to sample $PM_{1.0}$ at three different locations: the shipping/receiving room, an analytical laboratory, and a welding area. The sampling time was varied from 250 to 400 hr, depending on the sampling location. The collected samples were analyzed for chemical composition by SEM, which was also used to investigate particle morphology.

***Results and Discussion***

*APS and SMPS Measurement*

Figures III-1–III-6 show the indoor particle size distributions (from 0.02 to 20 μm) at different locations in the EERC building: lobby, office, demonstration facility, laboratory, hallway, and welding room. A summary of the measurement is listed in Table III-1. As expected, most of the PM in indoor environment is in the submicron range (more than 95% of particles based on number concentration).

The lobby area had the lowest particle number concentration because of new ventilation system and a lack of human activity. Most of the office area is maintained at a reasonably low particle concentration level, ranging from $4.0 \times 10^3$ to $7.0 \times 10^3$ particles/cm$^3$. Higher particle concentration (7942 particles/cm$^3$) at the EERC demonstration facility resulted in a high particle number concentration of $1.1 \times 10^4$ in the hallway connecting it to the office area because of entrainment caused by frequent door opening. A particle concentration of $5.1 \times 10^4$ (the highest value is $9.3 \times 10^6$ particles/cm$^3$) was measured in the welding area during welding. Particle size distributions were measured at the ventilation inlet and outlet simultaneously, and the results

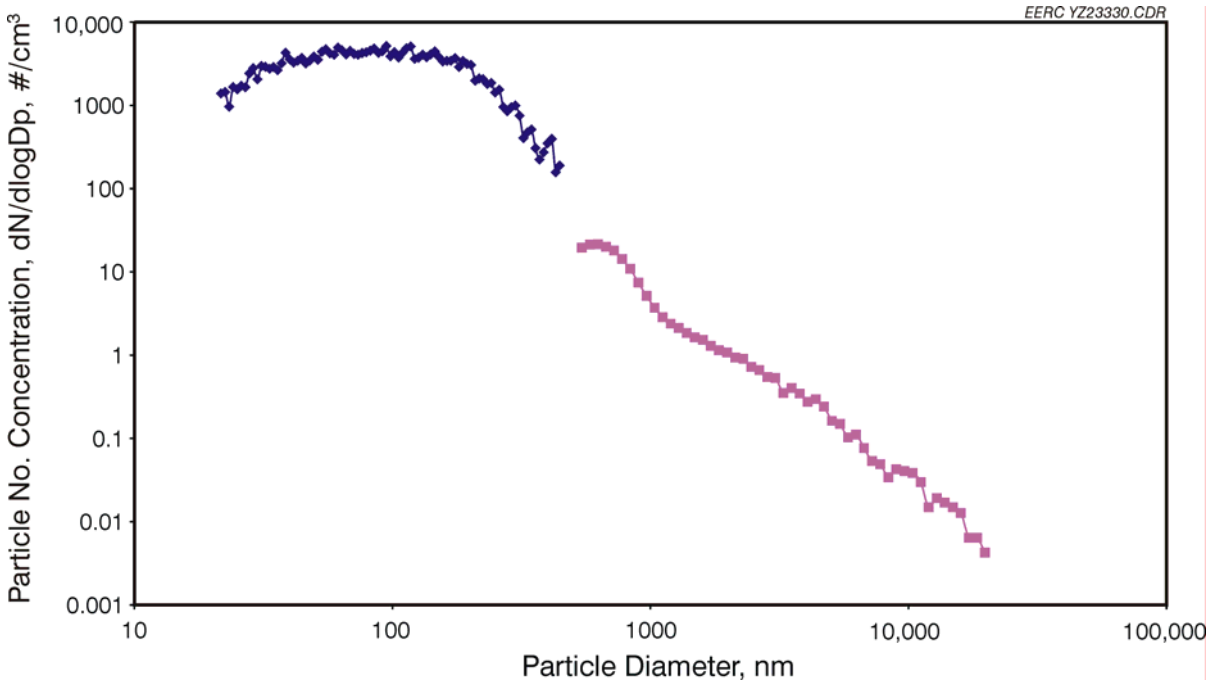


Figure III-1. Particle size distribution in the lobby — APS and SMPS results.

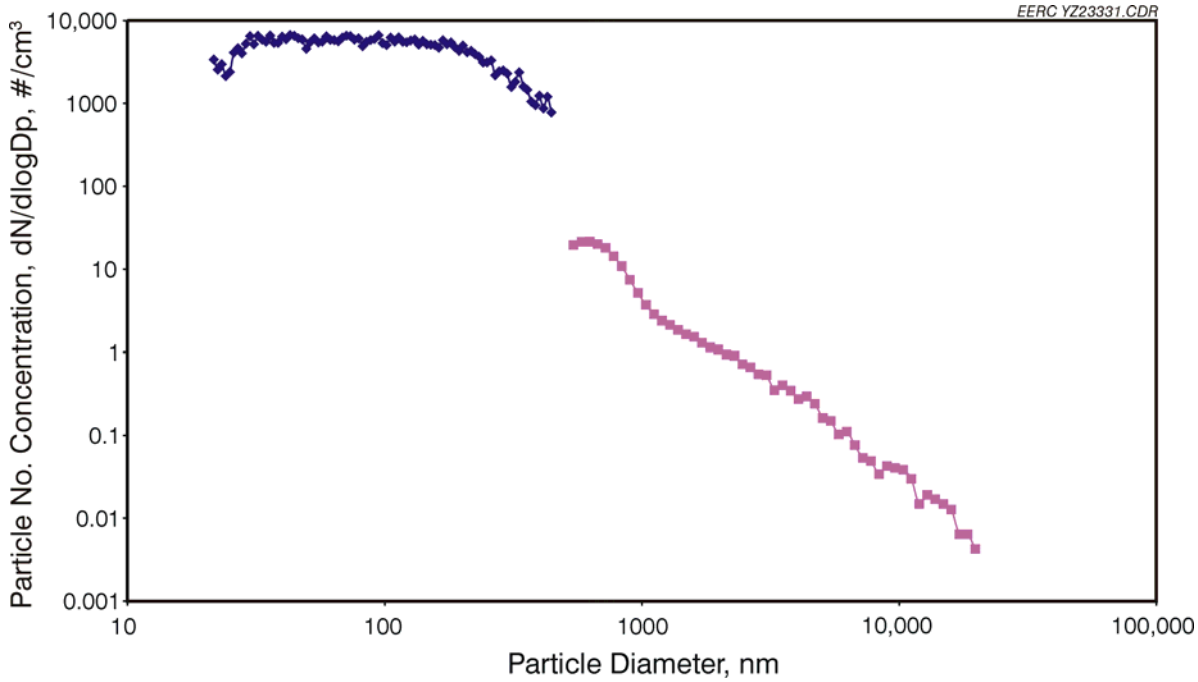


Figure III-2. Particle size distribution in the office area — APS and SMPS results.

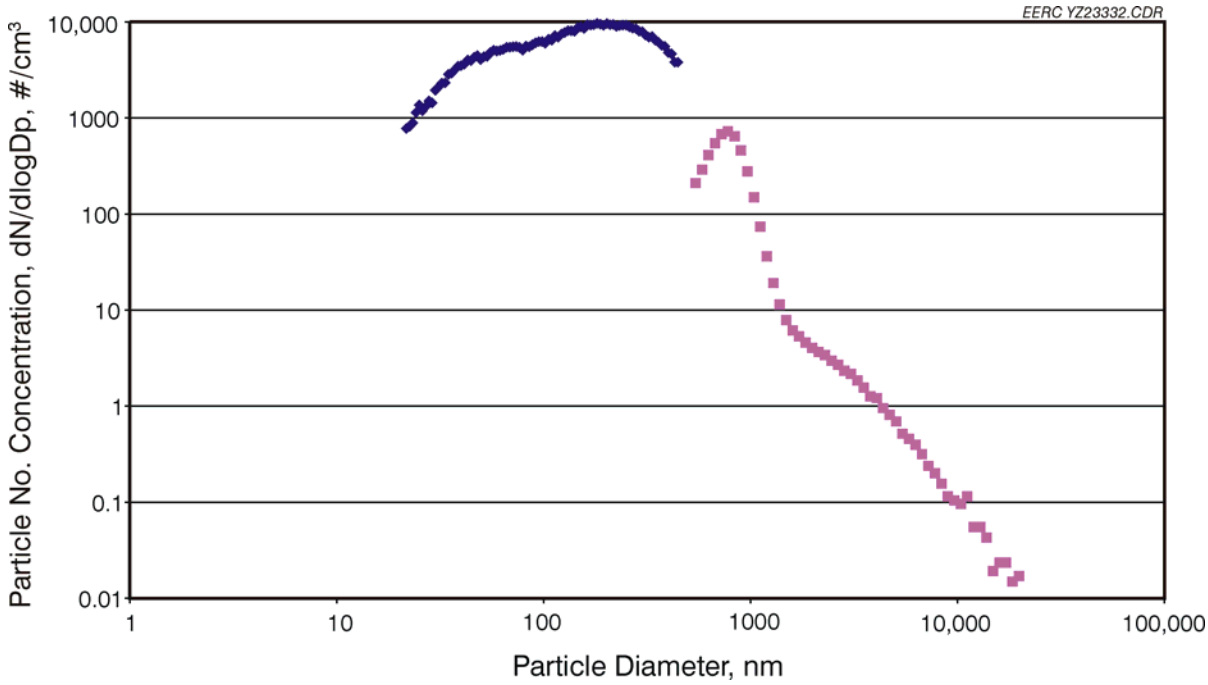


Figure III-3. Particle size distribution in the demonstration facility — APS and SMPS results.

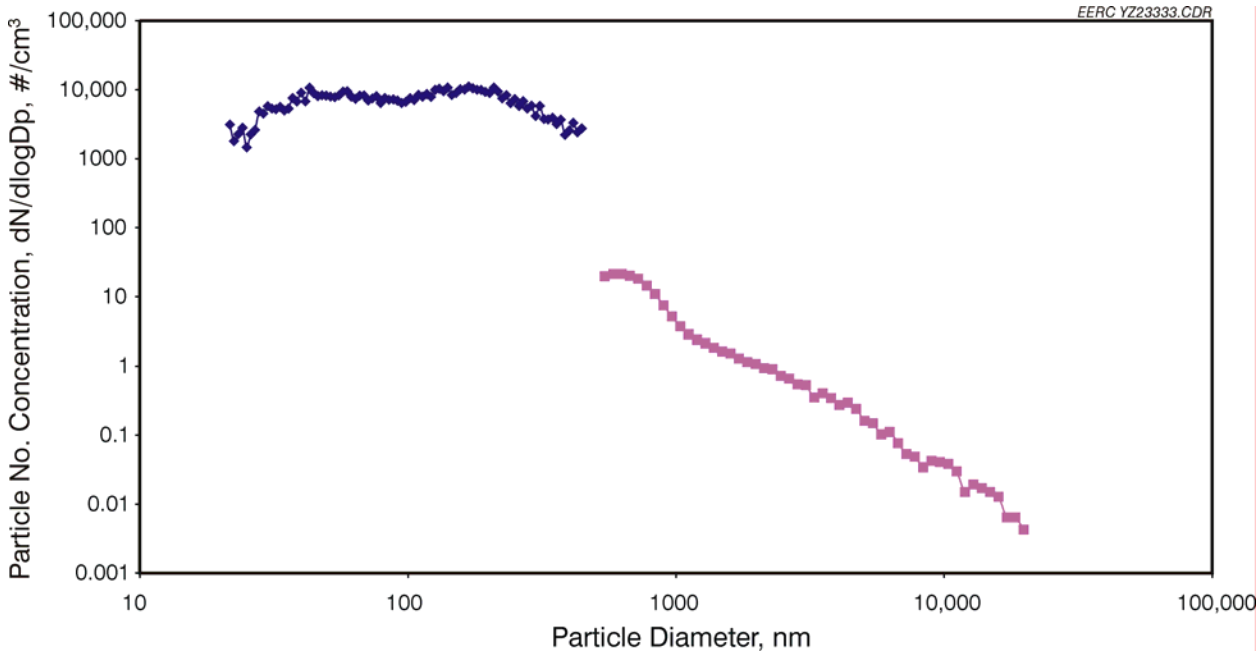


Figure III-4. Particle size distribution in the laboratory — APS and SMPS results.

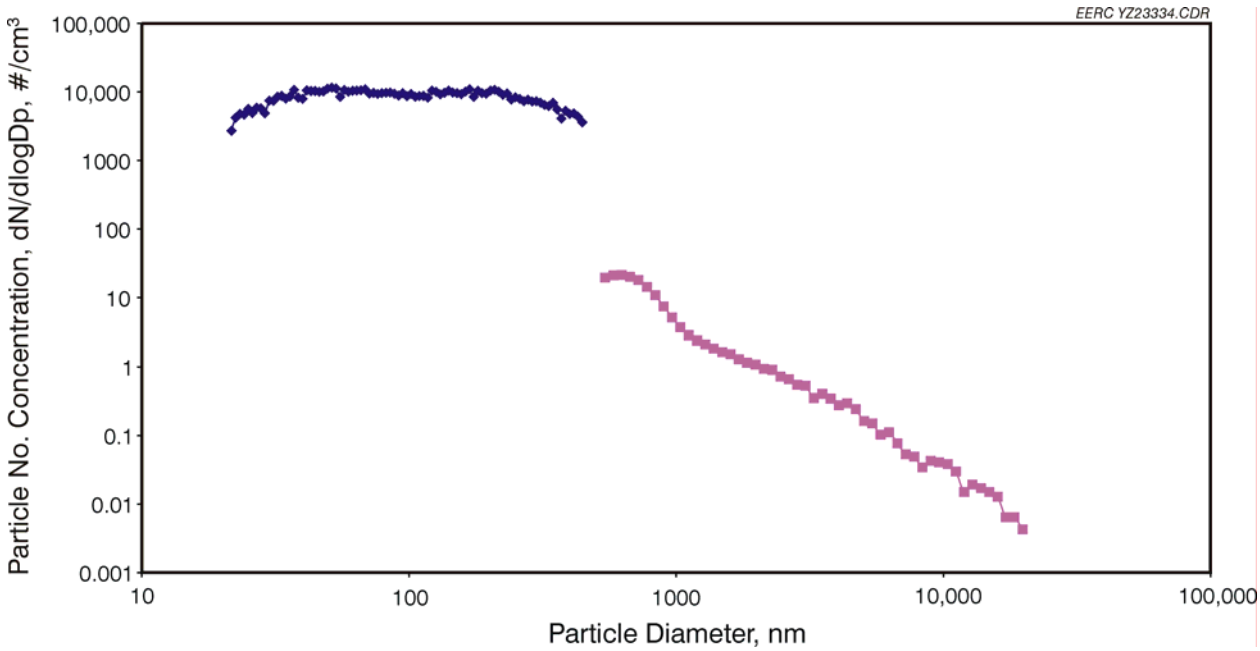


Figure III-5. Particle size distribution in the hallway — APS and SMPS results.

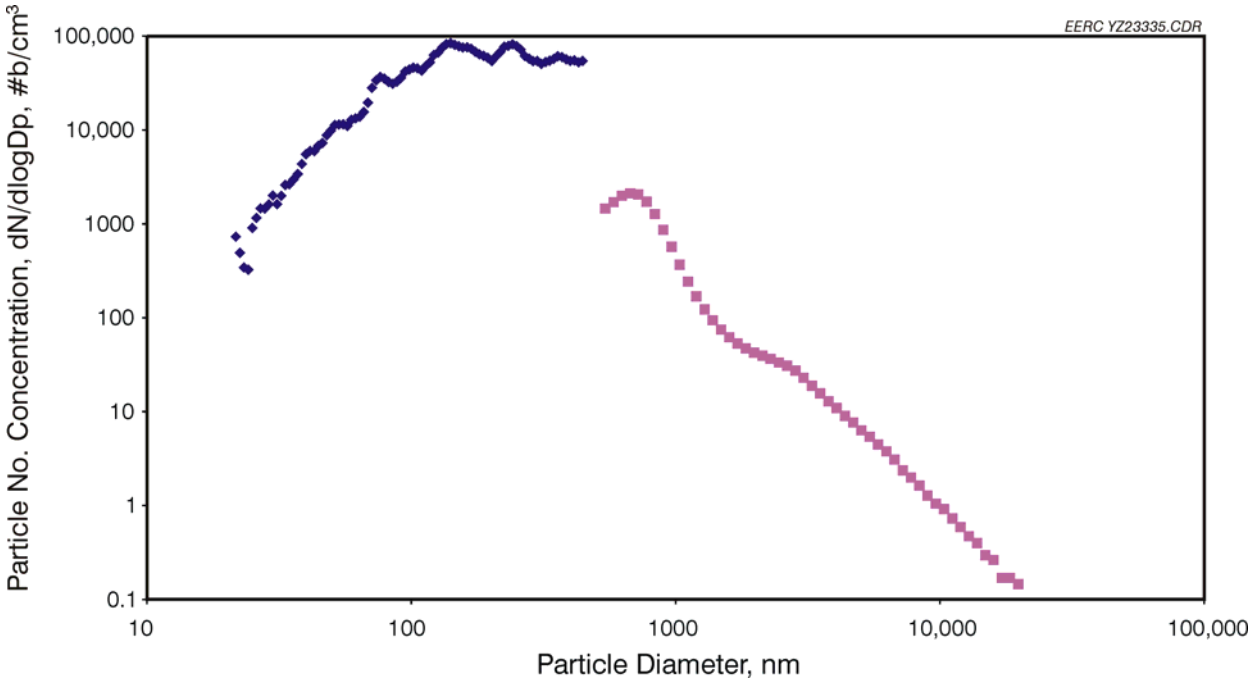


Figure III-6. Particle size distribution in the welding area — APS and SMPS results.

**Table III-1. Particle Size Distributions by SMPS and APS at Various Locations**

| Location | Total Number conc., #/cm$^3$ | Geometric Mean Diameter, µm |
|---|---|---|
| Lobby | 3814 | 0.083 |
| Office Room | 4062–7093 | 0.096–0.085 |
| Demonstration Facility | 7942 | 0.137 |
| Laboratory | 9006 | 0.10 |
| Hallway (next to the demonstration facility) | $1.1 \times 10^4$ | 0.094 |
| Welding Area | $5.1 \times 10^4$ | 0.173 |

showed that the particle size distributions at the inlet and outlet were almost identical, indicating an insufficient capture of $PM_{2.5}$ by the current filtration system.

*TEOM Measurement*

A TEOM–ACCU system was used to sample $PM_{1.0}$ at three different locations: an analytical laboratory, the shipping/receiving room, and the welding area. The sampling time was varied from 250 to 400 hr, depending on the sampling location, to ensure enough particulate for chemical analysis. The mass concentrations of $PM_{1.0}$ were plotted as a function sampling time for the three locations and are shown in Figures III-7–III-9. As shown in Figure III-7, the mass concentration of $PM_{1.0}$ in the Analytical Research Laboratory mainly fluctuated in the range of 2–12 µg/m$^3$ with an average value of 5.85 µg/m$^3$ and a standard deviation of 2.07. The highest concentration was 19.6 µg/m$^3$. The $PM_{1.0}$ mass concentration in the shipping/receiving room is

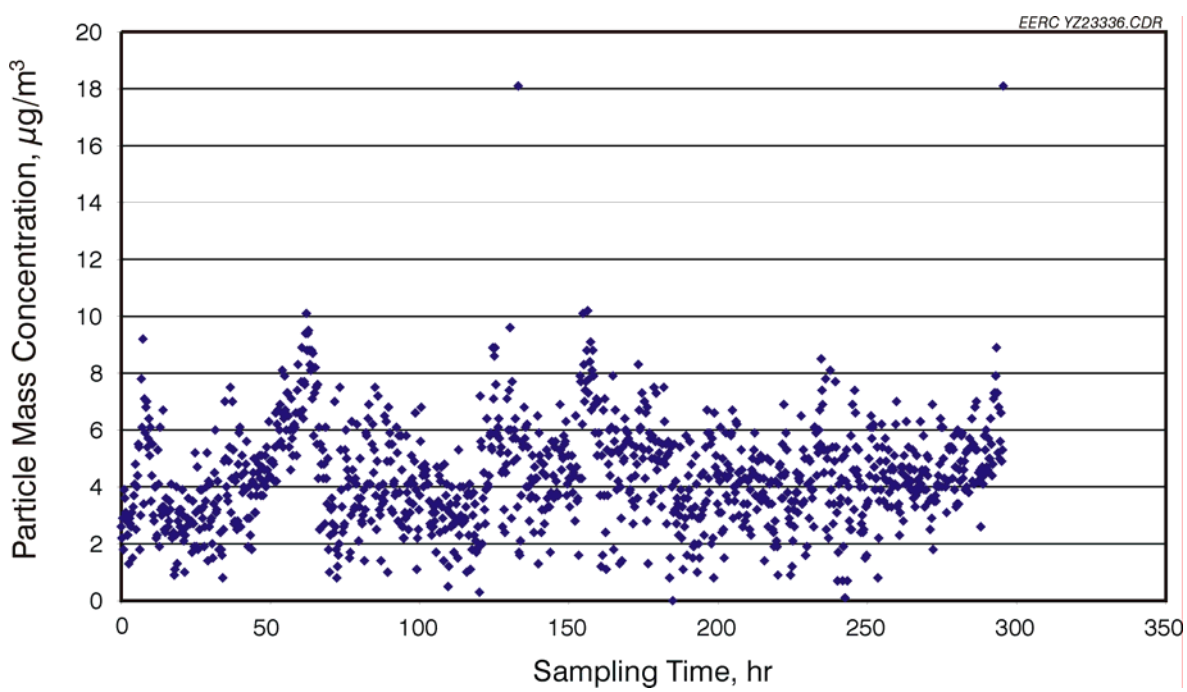


Figure III-7. $PM_{1.0}$ mass concentration in the shipping/receiving room.

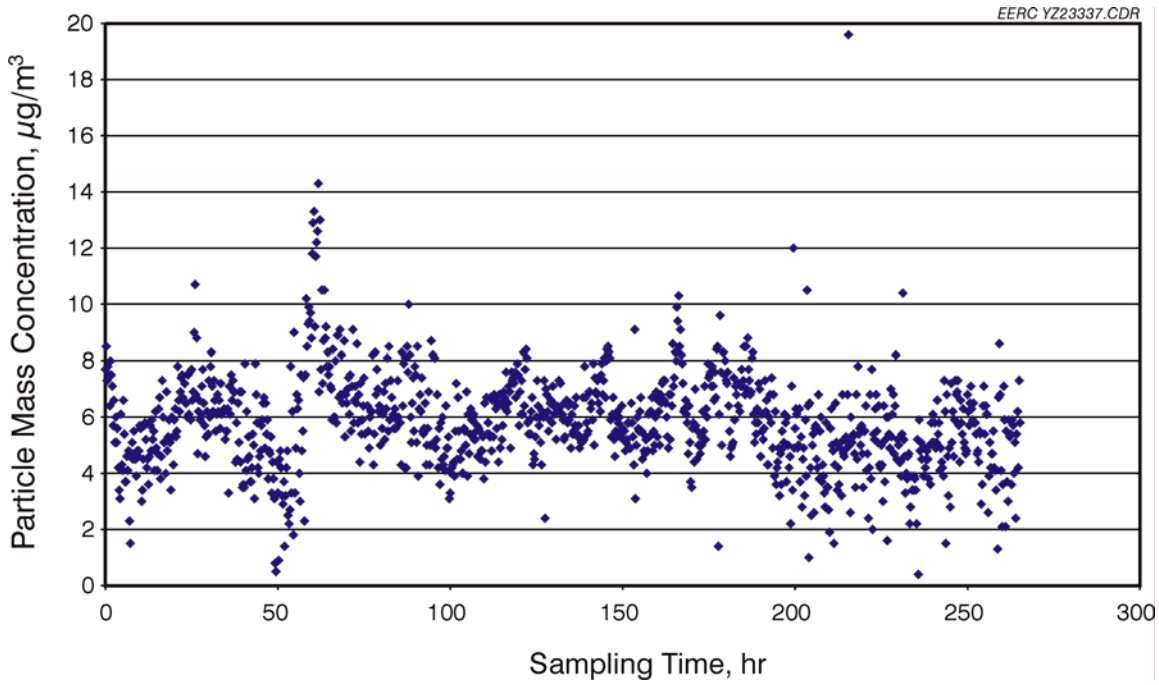


Figure III-8. $PM_{1.0}$ mass concentration in the analytical research laboratory.

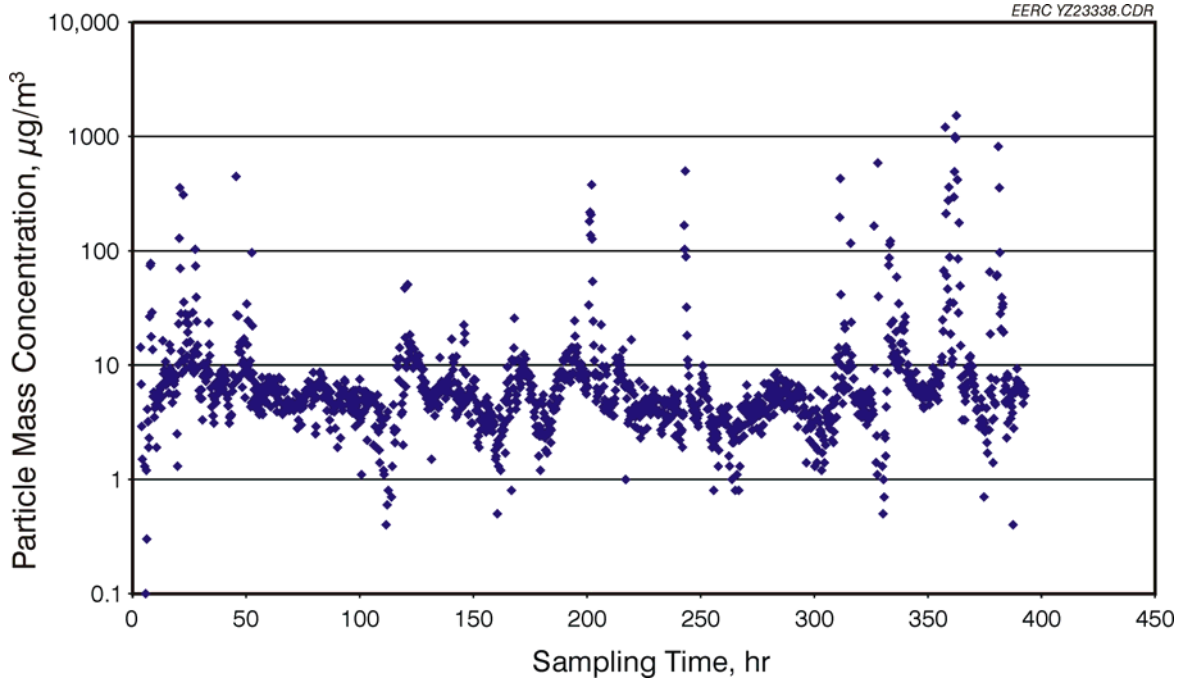


Figure III-9. Mass concentration of $PM_{1.0}$ in the welding area.

shown in Figure III-8, showing an average concentration of 4.37 μg/m$^3$, with a standard deviation of 1.80, which is lower than the $PM_{1.0}$ level obtained in the Analytical Research Laboratory. The results are somewhat surprising because the Analytical Research Laboratory had a new filtration system. The $PM_{1.0}$ mass concentration in the welding area is shown in Figure III-9, ranging from 0.4 μg/m$^3$ to 1.52 mg/m$^3$ during the 400 hour sampling period. The widely varying and high concentrations during welding indicated that the ventilation system does not protect operators from the metallic fumes generated by their welding.

*Chemical and Morphological Analyses*

The three ACCU samples were analyzed for chemical compositions. The elemental distributions are shown in Figures III-10–III-12. For the samples from the analytical laboratory and shipping/receiving room, sulfur is the dominant element, most likely in the form of sulfate. In the welding area sample, however, iron from the metallic fumes generated by welding was the dominant element. SEM analysis showed the morphology of the three samples (Figures III-13–III-15), proving that a significant number of submicron particles are presented in an indoor environment. The PM in the shipping/receiving room and analytical laboratory are single particles and probably come from the outdoor environment, while the particles in the welding area are in the nanometer range and were generated by welding.

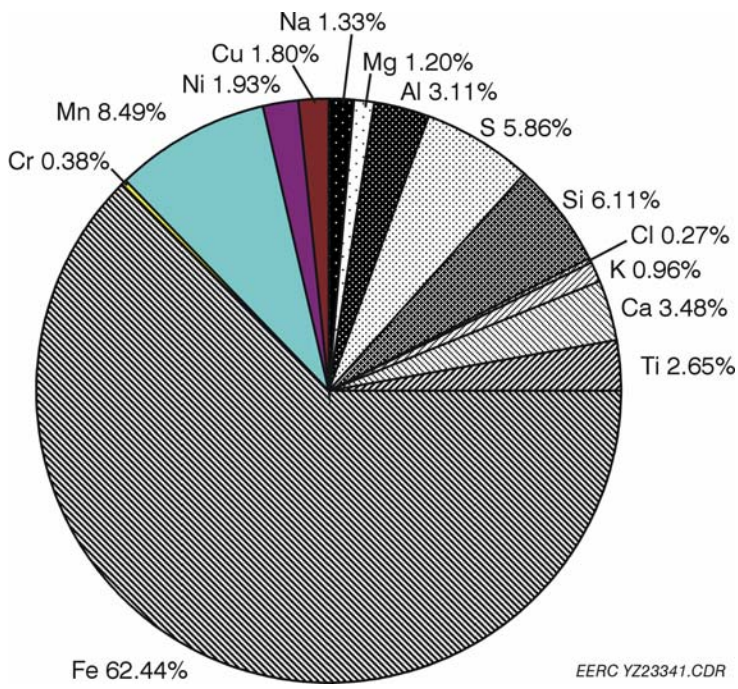


Figure III-10. Elemental distribution in the welding area.

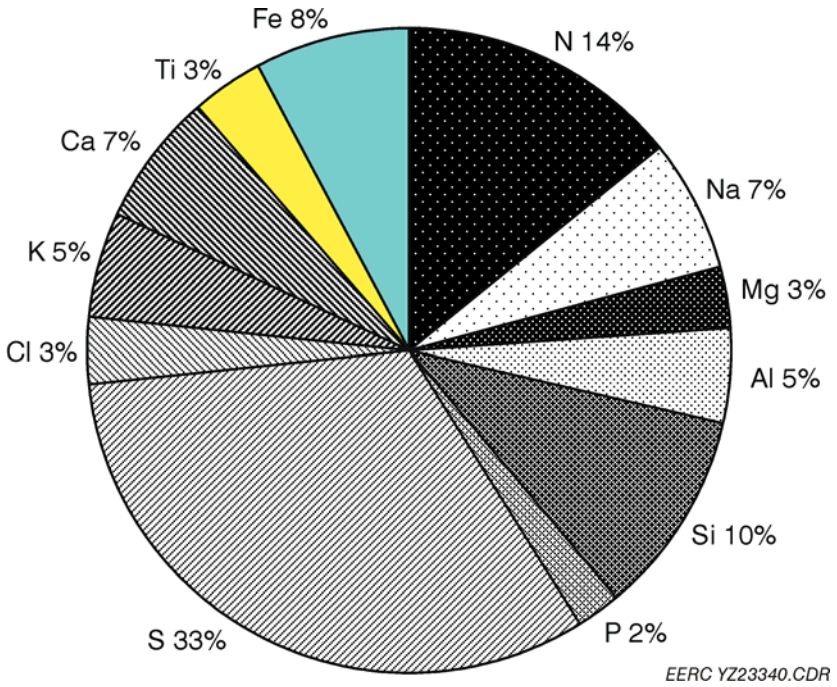


Figure III-11. Elemental distribution in the shipping/receiving room.

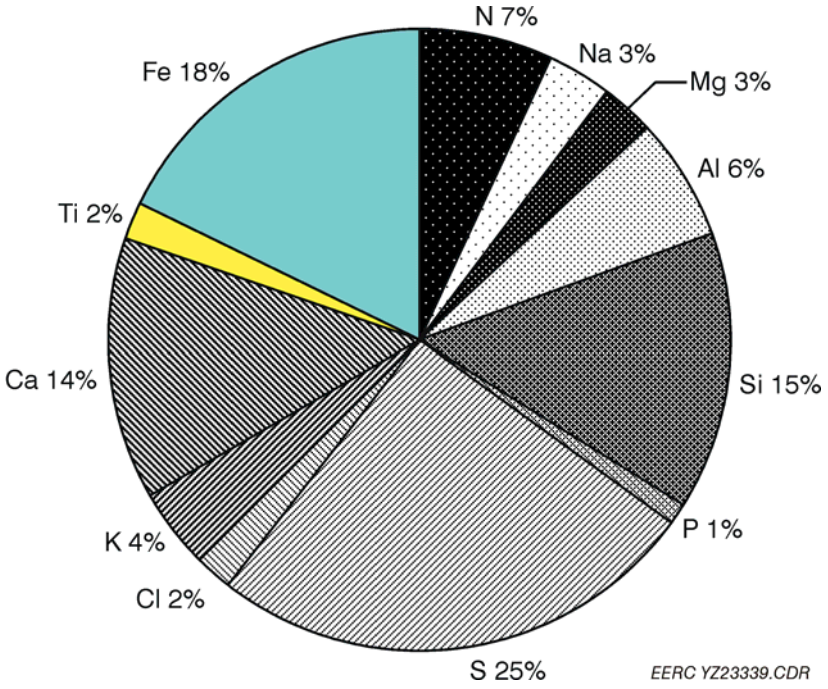


Figure III-12. Elemental distribution in the Analytical Research Laboratory.

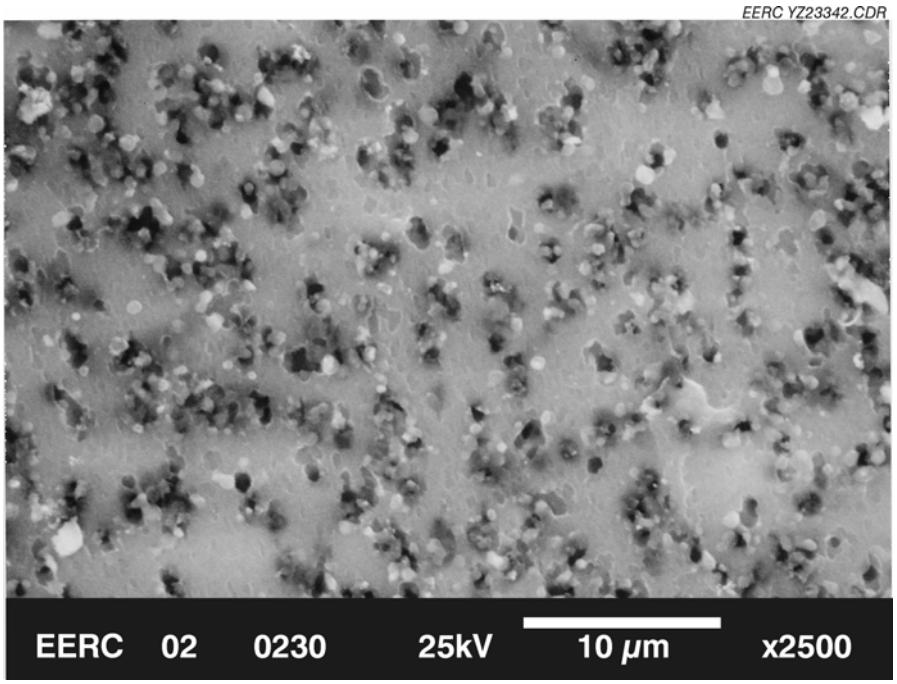


Figure III-13. SEM images of particles collected in the Analytical Research Laboratory.

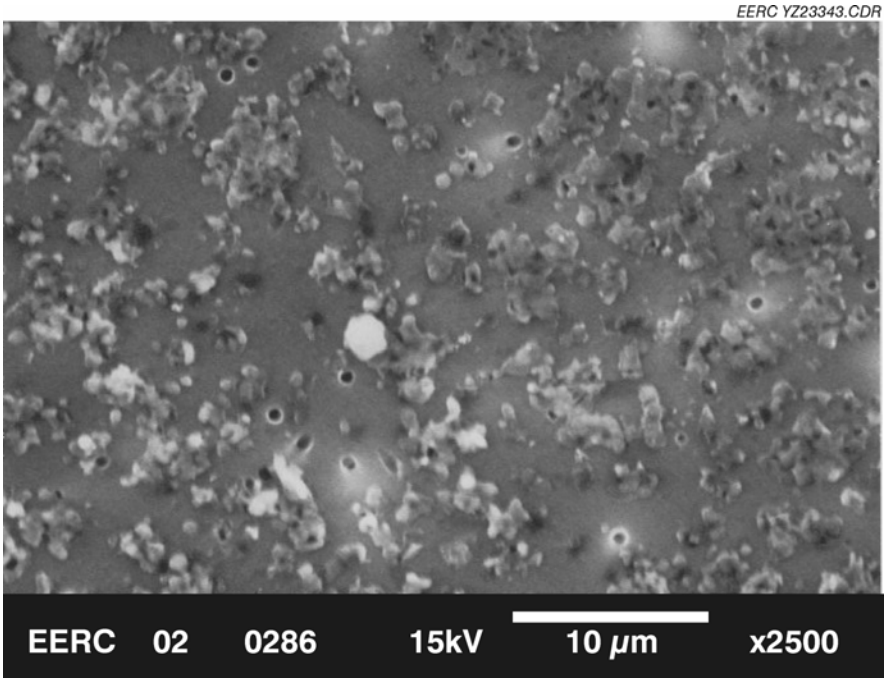


Figure III-14. SEM image of particles collected in the shipping/receiving room.

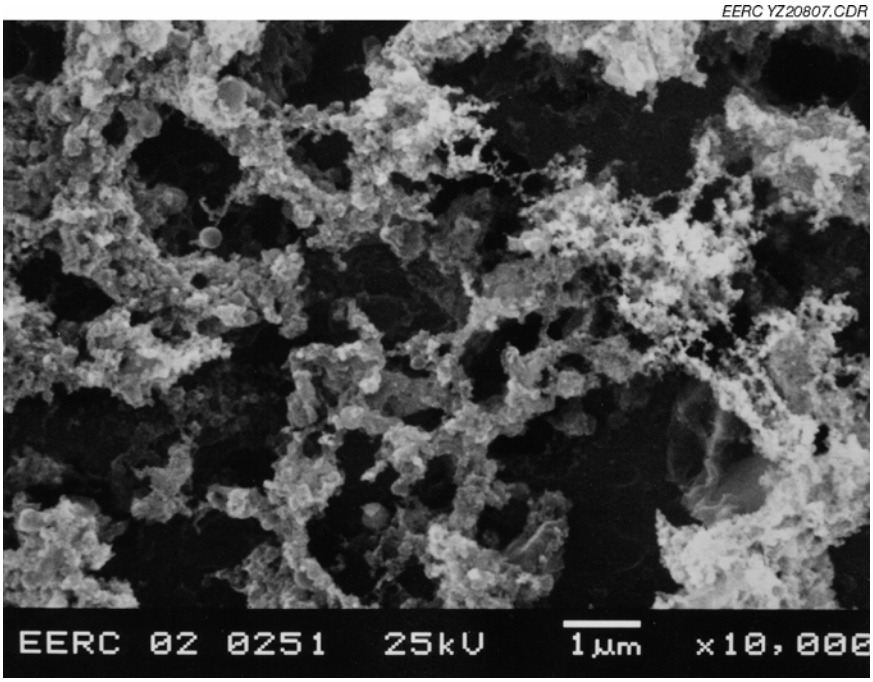


Figure III-15. SEM image of particles collected in the welding area.

### *Conclusions*

Particulate sampling shows that most particles in indoor environments are in the submicron range. High enrichments of sulfur, iron, silicon, and calcium in indoor aerosols are observed. PM levels in indoor environments are influenced by indoor activities and outdoor environment.

### *References*

1. Air Quality Criteria for Particulate Matter; Vols. I, II, and III; U.S. Environmental Protection Agency, 1996.

2. Dockery, D.W.; Schwartz, J.; Spengler, J.D. *Environ. Res*. **1992**, *59*, 362–373.

3. Long, C.M.; Suh, H.H.; Koutrakis, P. *J. Air Waste Manage. Assoc*. **2000**, *50*, 1236–1250.

4. Kamens, R.; Lee, C.T.; Weiner, R.; Leith, D. *Atmos. Environ*. **1991**, *25A.*

5. Wallace, L.A. *J. Air Waste Manage. Assoc.* **1996**, *46*, 98–126.

6. Veranth, J.M.; Smith, K.R.; Hu, A.A.; Lighty, J.S.; Aust, A.E. *Chem. Res. Toxicol.* **2000**, *13,* 382–389.

7. Tucker, W.G, *Fuel Processing Technology*, **2000**, *65*, 379–392.

## Activity 3.2 – Source of Indoor Air Pollution—Burning Candles

### *Introduction*

Epidemiological studies have shown a significant association between PM in the atmosphere and mortality (1, 2). Although there is presently nothing explaining acute effects induced by low particle concentration, it is hypothesized that inhaled singlet ultra-fine particles have a high pulmonary toxicity even at low mass concentration level because of the large numbers of particles involved (3). A related study (4) shows that, compared to large particles (>0.2 μm) of the same material, ultra-fine particles caused greater pulmonary inflammation. A human lung deposition model also showed that ultra-fine particles of ~20 nm have a 50% deposition efficiency in the alveolar region (5). The growing concerns about the health risks of fine particles have led to the promulgation of a National Ambient Air Quality $PM_{2.5}$ by EPA.

Because people spend 85% of their time indoors (6), it is widely recognized that a significant portion of total personal exposure to ambient PM occurs in indoor environments. Ambient PM is a complex mixture of particle sizes and types from many sources. Studies (7, 8) showed that the indoor particles may not only come from outside but that indoor activities, such as cooking, space heating, office machines, ventilation, etc., also can generate a significant number of submicron particles. As a result of these indoor sources, indoor particle concentrations are often higher than ambient concentrations (9).

Despite the public health implications of indoor particle exposures, few studies have characterized sources of indoor fine particles. A fast-growing industry that may have an effect on the health of the average American is candles. The National Candle Association (NCA) reports $2 billion worth of candles are sold annually. Candle manufacturer surveys show that 96% of all candles purchased are bought by women, and Kline and Company did a study that illustrated 93% of women and 7 out of 10 homes regularly burn candles. With these numbers, the potential effect on the U.S. population is significant. Most of the candles manufactured in the United States are made of paraffin, a common petroleum by-product. This wax is suitable for general candlemaking and is used in 99% of all candles manufactured in the United States. Many candles also contain dyes or pigments, fragrances, and other ingredients. Beeswax is a less common, but more highly refined wax for candlemaking. Soy wax, produced from soybean oil, is formulated with other vegetable waxes in making candles. Soy wax, which is new to the market, has been promoted as an alternative to paraffin that can be used to produce cleaner-burning candles.

Several air pollutants are released into the ambient environment during candle burning, such as metallic species (lead, zinc, or tin), volatile organic compounds (acetaldehyde, formaldehyde, polyaromatic hydrocarbons, etc.), and PM (soot). Even though the U.S. Consumer Product Safety Commission determined in 1974 that lead-core wicks did not present a health hazard, NCA members agreed to stop using lead wicks voluntarily (95% of the candle manufacturers in the United States today belong to the NCA). Most U.S.-made candles are safe from lead emissions, but imported candles may contain lead wicks. Wicks made with cotton, paper, zinc, or other nonmetallic materials are considered safe. On the other hand, candle manufacturers are not compelled to list or disclose hazardous, toxic, or carcinogenic compounds

used as ingredients in their products, but the NCA is working with the American Society for Testing and Materials to create voluntary labeling standards for the industry (10).

Lead poisoning was the initial concern with burning candles, and studies performed by Van Alphen (11) and Nriagu and Kim (12) showed high level of lead (~13.1 μg/m$^3$) while candles with metal-core wicks were burned. Several carcinogenic organic compounds have been detected in candle emissions. Experimental data by Lau et al. (13) showed that the emissions could be higher than the EPA's excess cancer-risk level under certain scenarios.

Soot emissions from burning candles are another concern for human health and have drawn increased attention in recent years. A significant amount of ultrafine soot is generated during candle burning. The generated ultrafine particles are easily deposited in the pulmonary region (5), penetrate the epithelium and reach interstitial sites (14) in the lungs. Finally, the ultrafine particles are biologically more reactive than larger sized particles and thus elicit effects at lower concentrations (15). Candle soot production increases when wicks are too long because the rate at which the candle wax is supplied to the wick is greater than can be burned effectively. Also, some candle wax compositions promote soot production. Soft wax candles and candles that contain oils and unsaturated hydrocarbons melt and vaporize faster, producing more soot when burned as compared to hard wax candles. Few studies have analyzed the composition of candle emissions or evaluated emission rates and maximum concentration.

### ***Objectives***

The goal of this study was to evaluate the impact of candle burning on indoor air quality by characterizing soot emissions from candles as a function of candle type.

### *Experimental*

#### Candle Selection

Because emissions from burning candles vary as functions of wax formulation, candle additives (pigment, fragrance), and shape of candle (jar, pillar, votive), nine different candle types were selected to test their emissions. A summary of the selected candles is listed in Table III-2. Figure III-16 shows the different shaped candles tested in this study. The diameters of the jar and pillar candles are in the range of 60–80 mm, while the votive candles usually are 35 mm in diameter.

#### Experiment Setup

A plexiglass chamber with a volume of 0.34 m$^3$ was fabricated to examine candle emissions under controlled conditions. A schematic diagram of the experimental apparatus is shown in Figure III-17. Filtered, particle-free air was introduced into the chamber, and the exhaust could be passed through two quartz-fiber filters placed in series to collect all aerosols for chemical analyses or to be sampled with a SMPS or a CPC. A pressure gauge was mounted on the chamber to ensure that the chamber was at ambient atmospheric pressure. Two gloves mounted on the chamber wall allowed manipulation of components inside the chamber while

**Table III-2. Summary of the Tested Candles and Emissions from Candle Burning**

| Formulation | Color | Fragrance | Shape | Candle Number | Particle Emission, particles/g candle | Mass Emission, mg/g candle |
|---|---|---|---|---|---|---|
| | | | Jar | 1-A | $4.0 \times 10^{11}$–$1.3 \times 10^{13}$ | 0.159–0.998 |
| Paraffin | Yes | Yes | Pillar | 1-B | $1.53 \times 10^{12}$ | NA |
| | | | Votive | 1-C | $1.6 \times 10^{12}$ | 0.203 |
| | | | Jar | 2-A | $6.4 \times 10^{11}$ | NA |
| Soy Wax | Yes | Yes | Pillar | 2-B* | NA* | NA |
| | | | Votive | 2-C | $1.9 \times 10^{12}$ | 0.145 |
| | | | Jar | 3-A* | NA* | NA |
| Paraffin | No | No | Pillar | 3-B | $2.17 \times 10^{12}$ | 0.08 |
| | | | Votive | 3-C | $4.2 \times 10^{12}$ | 0.113 |
| | | | Jar | 4-A | $4.1 \times 10^{14}$ | 0.014 |
| Soy Wax | No | No | Pillar | 4-B* | NA* | NA |
| | | | Votive | 4-C | $3.0 \times 10^{12}$ | 0.087 |

* Unavailable due to candle manufacturer limitations.

Figure III-16. Picture showing the different shaped candles tested.

maintaining a closed system. The experimental apparatus and sampling system are shown in Figure III-18.

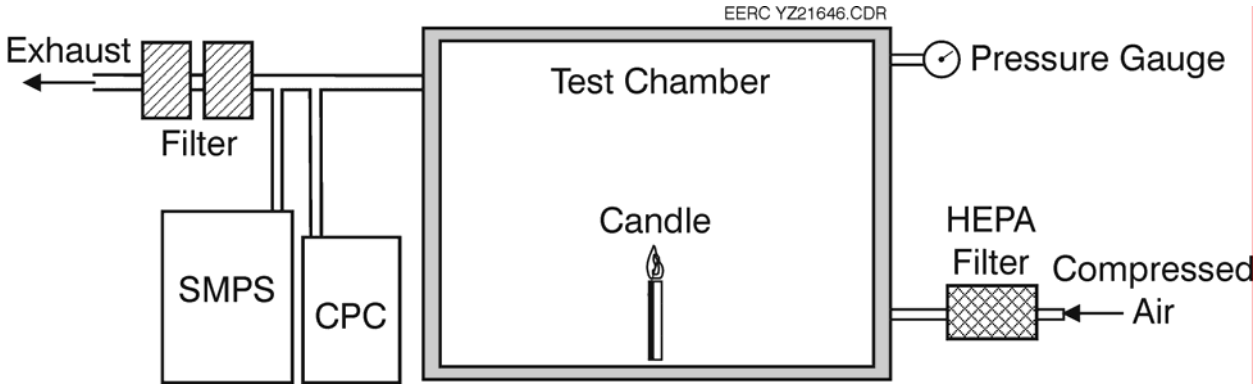


Figure III-17. Schematic of the experimental apparatus.

Figure III-18. Picture showing the experimental apparatus and sampling system.

Sampling and Chemical Analysis

The exhaust was sampled with a CPC for particle emissions as a function of time, and a SMPS to measure particle size distributions. Candle burning rates were also monitored during each candle test. Two pre-baked quartz fiber filters (heated at 500°C for 12 hours) were used in series to ensure complete capture of PM and condensable organic compounds. The front filter collected essentially 100% of the PM and some adsorbed gas-phase materials. The back-up filter was exposed to gas-phase materials, some of which adsorbed on the clean surface. The partition of condensable compounds between the gas phase and the adsorbent phases depends on temperature, available surface area for adsorption, vapor pressure, and the presence of other

competing adsorbates (16). McMurry et al. have suggested that the organic material on the backup filter was predominately adsorbed vapor (17). Both filters were extracted with hexane followed by benzene/2-propanol. The extracts were filtered and split into two fractions, the first for non-polar organic compound analysis by GC, and the second fraction was derivatized with diazomethane for polar organic compound analysis. Detailed information regarding the analysis method was reported by Fine et al. (18) and Turpin et al. (19). Morphological analysis on the samples was done by SEM.

### *Results and Discussion*

#### *Particle Emissions and Size Distributions*

Experiments were completed to examine PM emissions from various candles based on formulation, color, fragrance, and shape as listed in Table III-2. Aerosols in the candle exhaust were collected on the filters to determine the particle emission rate. The candles also were weighed before and after the tests to determine the burning rate for each specific candle. As shown in Table III-3, the burning rates for the jar and pillar candles were in the range of 0.08–0.095 g/min; rates in the range of 0.05–0.06 g/min were observed for the votive candles. Particle emissions per gram of burning candle, both number and mass basis, were calculated based on the burn rates, particle concentrations in the exhaust, and exhaust flow rates; the results are listed in Table III-2.

**Table III-3. Summary of Burning Rate of Different Candles under Stable Combustion, g/min**

| 1-A | 1-B | 1-C | 2-A | 2-C | 3-B | 3-C | 4-A | 4-C |
|---|---|---|---|---|---|---|---|---|
| 0.083 | 0.087 | 0.053 | 0.080 | 0.063 | 0.095 | 0.058 | 0.076 | 0.063 |

Temporal variations (Figures III-19–III-21) in particle number concentration in the exhaust were measured by CPC for jar, pillar, and votive candles. Figure III-19 shows particle emissions for paraffin pillar candles with and without additives (pigment and fragrance). Both candles had particulate emissions in the range of $10^{12}$–$10^{13}$ particles/g candle with time average values of $1.53 \times 10^{12}$ and $2.17 \times 10^{12}$, respectively, indicating no significant impact of candle additives (pigment and fragrance) on candle particle emissions. Totals of three paraffin jar candles I, II, and III (with color and fragrance) from different manufacturers were tested; their particle emissions are plotted in Figure III-20. Candle I had the highest particle emission of $1.34 \times 10^{13}$ particles/g candle, while $2.0 \times 10^{12}$ and $4.0 \times 10^{11}$ particles/g candle are for the candles II and III. The differences between particle emissions among the three candles are probably caused by the different wax compositions. Two soy wax jar candles (with and without additives) also were examined for their particle emissions under the same environment as the paraffin jar candle tests. The results, however, are somewhat surprising. The soy wax jar candle without any additives (pigment and fragrance), which claims to be the cleanest, started with an extremely high particle emission of $2.5 \times 10^{15}$ particles/g candle, and then gradually leveled off at $2.3 \times 10^{14}$ particles/g candle, almost 2 orders of magnitude higher than the soy wax jar candles with additives (pigment and fragrance), which had a particle emission of $4.7 \times 10^{11}$ particles/g candle.

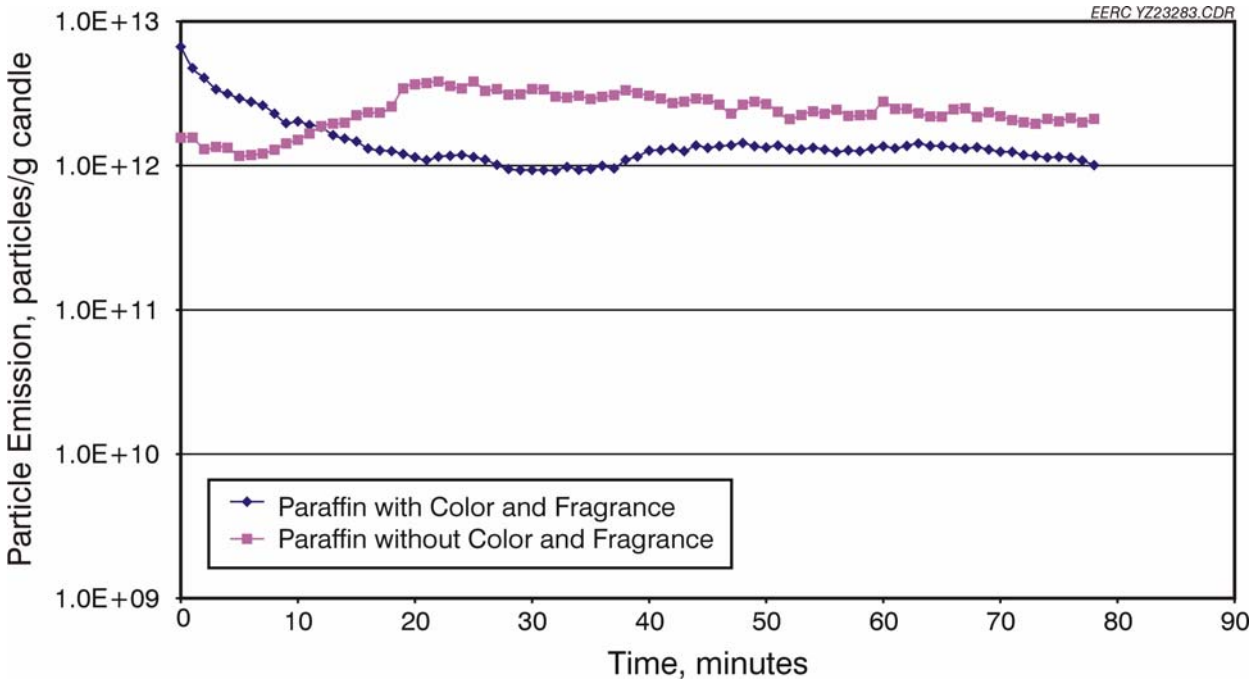


Figure III-19. Particle emissions from pillar candles.

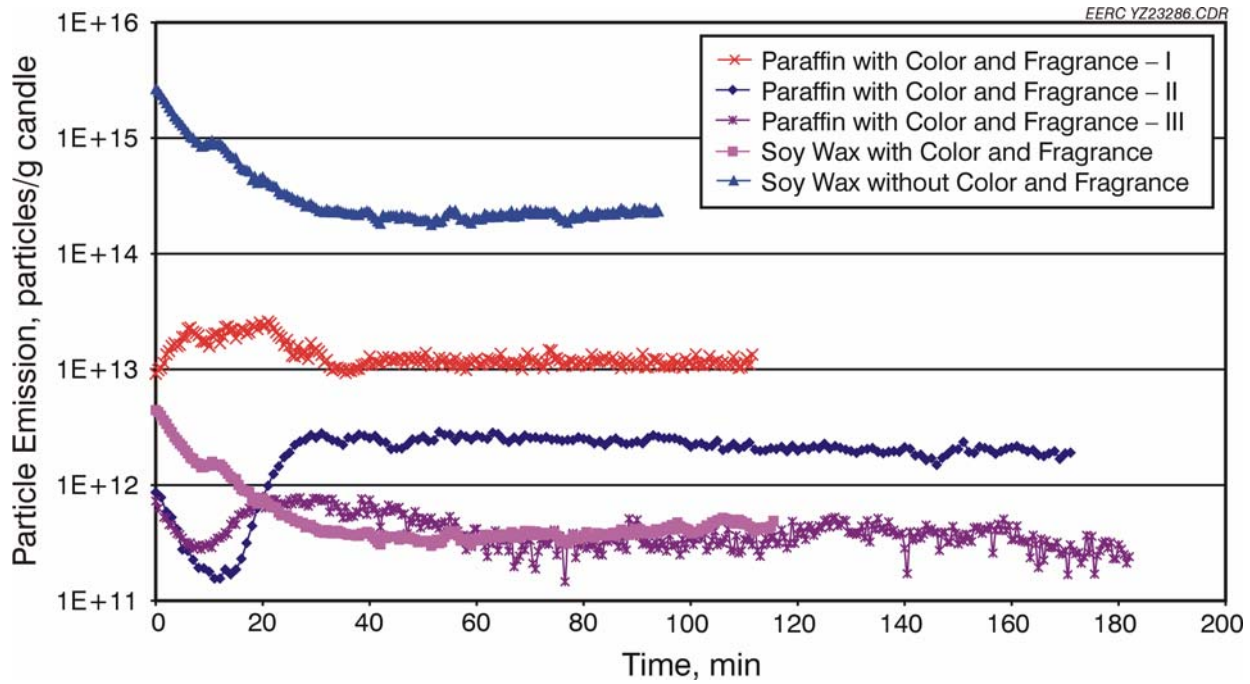


Figure III-20. Particle emissions from jar candles.

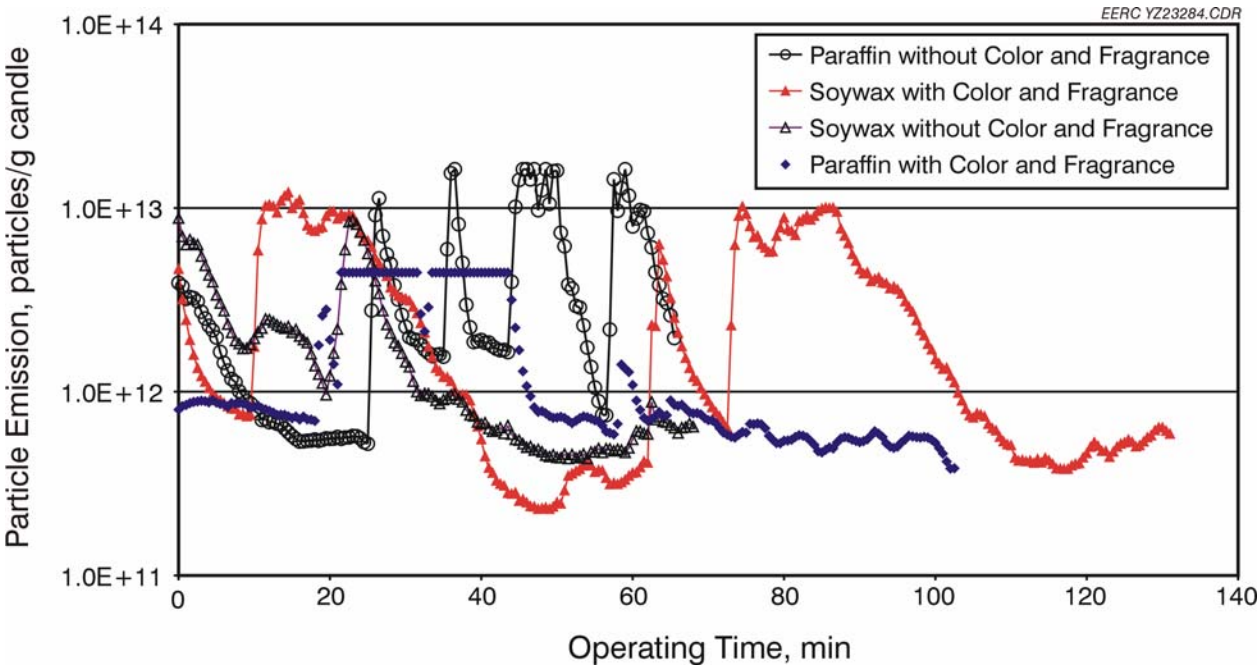


Figure III-21. Particle emissions from votive candles.

The candle additives, instead of enhancing, impeded particle emissions from the soy wax jar candles. The soft soybean wax candle probably vaporized faster and produced more soot when burned than the hard-wax paraffin candles. By comparing the mass and number concentration data for both paraffin and soy wax candles, it is clear that the particulate produced in soy wax candles either has a much smaller size or has a lighter density than the particle from paraffin candles. Paraffin jar candles appear to be as clean as, if not cleaner than, soy wax candles.

In the pillar and jar candle tests, the flames were stable, and so were the particle emissions as shown in Figures III-19 and III-20. In the votive candle tests, however, the candle flame flickered more than the pillar and jar candle flames. Initially, with a steady supply of wax to wick, the flickered flame was stable. The continuously released heat melted the votive candle to form a wax pool with a much-reduced flame, resulting in a decreased burning rate and less heat released. Also, the natural air convection surrounding the flame was disturbed when the air was drawn across the votive edge. The disturbed air had a more obvious impact on the stability of the flame with a reduced size, causing more flickering. Therefore, particle emissions from burning votive candles fluctuated. Figure III-21 shows particle emission data from four votive candles (paraffin and soy wax, with and without additives) as a function of time. All the data demonstrated periodic fluctuation patterns in the range of 1.6–4.2 × $10^{12}$ particles/g candle.

Figures III-22 and III-23 display typical particle size distributions of both paraffin and soy wax candle emissions measured by SMPS, indicating that significant amounts of nano-meter particles were generated during burning regardless of wax formulation, additive, and candle shape. Particles of this size range (20–50 nm) have been shown to have a high deposition rate in the airway tissues, and most likely cause inflammatory response (4, 5).

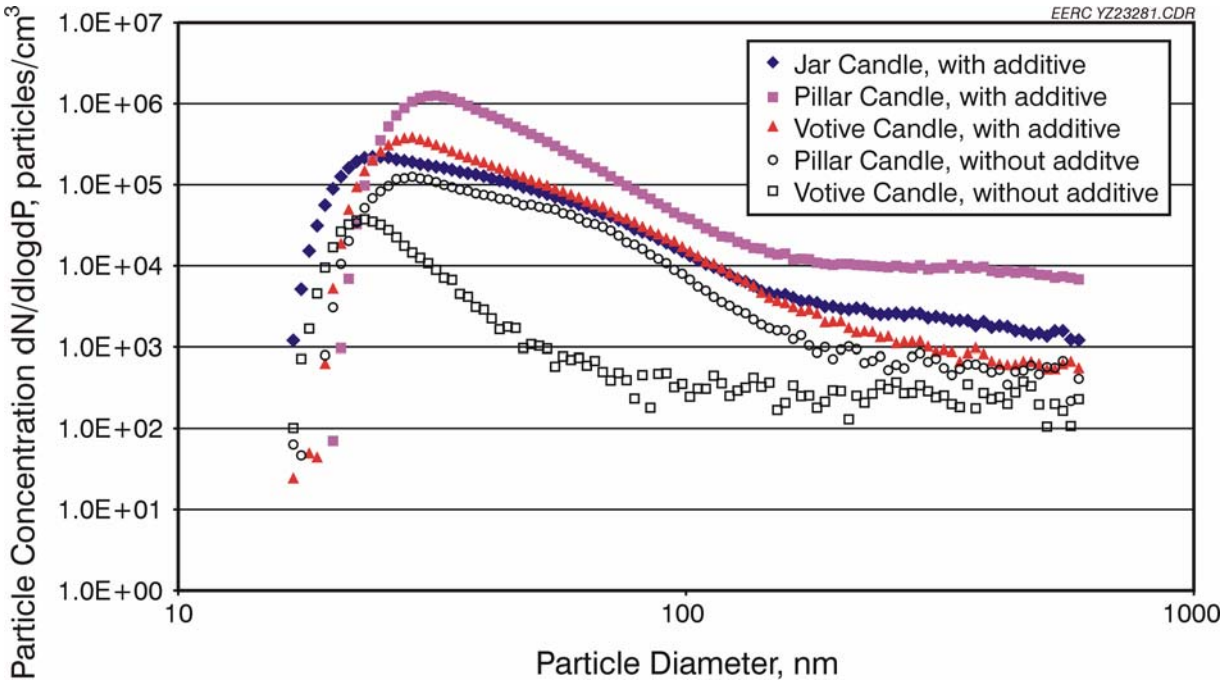


Figure III-22. Particle size distributions for paraffin wax candle emissions.

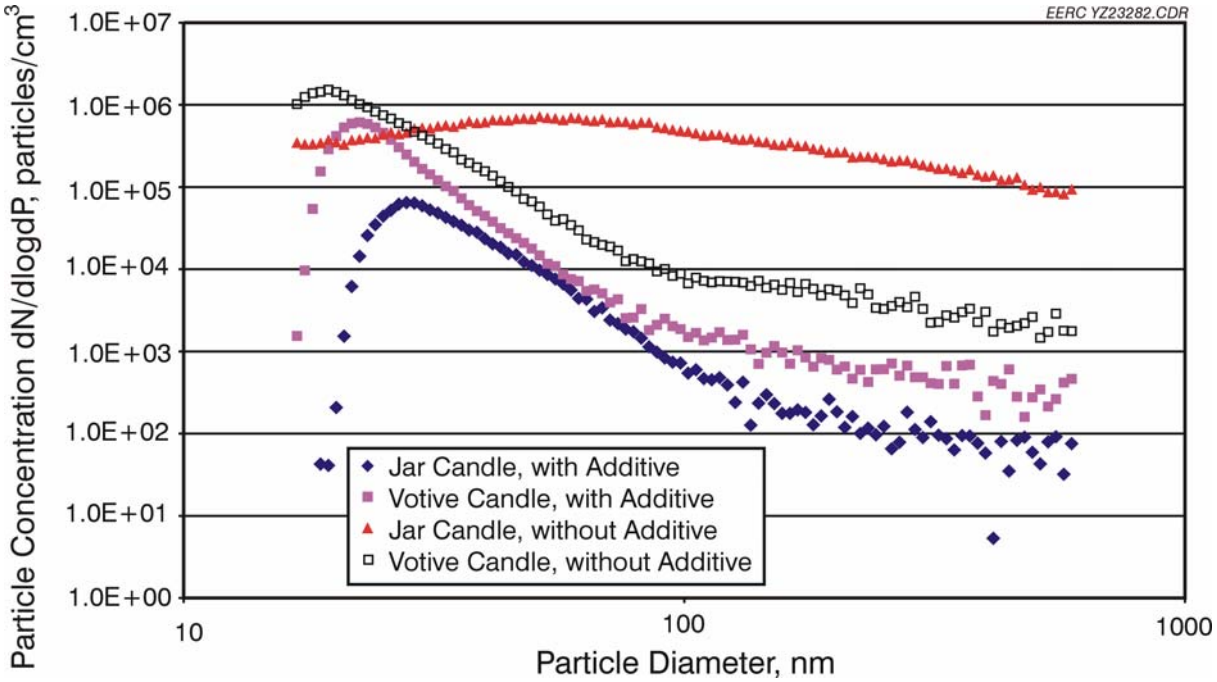


Figure III-23. Particle size distributions for soybean wax candle emissions.

Average particle emissions from the tested candles were calculated and summarized in Table III-3. Most paraffin and soy wax candles had approximately the same level of particle emissions ($10^{11}$–$10^{12}$ particles/g candle), except for the soy wax jar candles without additives, which had $4.1 \times 10^{14}$ particles/g candle. From a mass-based emission perspective, however, candles with color and fragrance have higher mass emission rates than candles without color and fragrance. Since most candles have similar particle size distributions (shown in Figures III-22 and III-23), the discrepancy between the number and mass-based particle emissions suggests that denser particulates were generated from the colored and fragranced candles than the candles without color and fragrance.

To further illustrate the impact of burning candle on PM level indoors, particle concentrations in the testing chamber under no candle burning were measured as a function of time with and without a HEPA filter, respectively (Figure III-24). Without a HEPA filter trapping particles flowing into the test chamber, particle concentration in the chamber was maintained at $5.1 \times 10^3$ particles/cm$^3$ (CPC measurement), and gradually decreased to 0 particles/cm$^3$ when the HEPA filter was used. After a particle-free environment was obtained, the candles were ignited while the particle-free air continuously flowed through the chamber. The air flow rate had to increase dramatically (an increased air-exchange rate of 36 exchanges/hr) to dilute the particle concentration in the exhaust below the CPC measurement limit. Figure III-24 shows that, even under high dilution, the particle concentration jumped to $1.1 \times 10^6$ particles/cm$^3$.

In spite of making sure that candles were burned with trimmed wicks and with a stable flame, visible black soot emissions could be seen typically coming from the flame tip. These

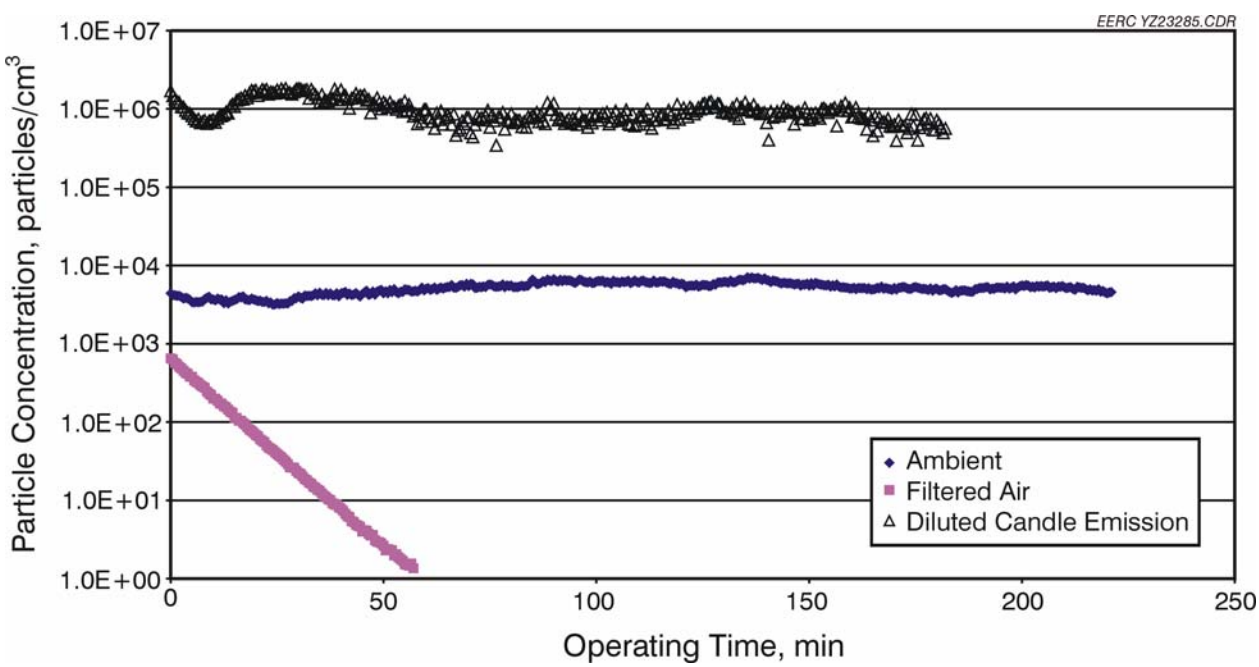


Figure III-24. Impact of burning candles on ambient environment.

visible particulate emissions are consistent with the high level of measured submicron PM. Figures III-25 and III-26 show examples of the visible black fume from the burning candles.

*Chemical Analysis on Candle Emissions*

The test candles were extracted and analyzed by GC to determine organic species present. Table III-4 summarizes the organic compound class detected in paraffin and soy wax candles.

Extractable and elutable fractions of the PM and vapor samples from candle burning also were identified and further quantified by GC–MS. The results are plotted in Figures III-27–III-29 for the emissions from the soy wax candle without additive, the soy wax candle with additive, and the paraffin candle with additive, respectively. In Figure III-27, organic compound partitions in the PM emission from the soy wax candle without color and fragrance is almost the same as the vapor sample, indicating that the particles are probably formed due to the condensation from the vapor. Approximately 77% of the extractable and elutable material was identified while the remainder was designated as an UCM of branched and cyclic hydrocarbon appearing as a broad lump in the total ion chromatogram. Long-chain esters were the dominant compounds in the emission from the soy wax candle without additive, approximately 51%–52%, followed by 14%–15% of cycloalkanes, 6%–7% of alkane, 2.5%–3% of alkenes, and 1% of branched alkanes; 0.7%–1.4% of alkanoic acid also was found in the emission from the soy wax candle without additive. No PAHs were detected. Methyl dihydrojasmonate ($C_{12}H_{22}O_3$) is the major organic compound in ester emission; it is probably a pyrolysis product of the wax ester in the soy wax candle. The alkanes in the emissions are also major constituents found in the candles. The alkanoic (carboxylic) acids in the emission were identified as the fatty acids palmitic acid ($C_{16}$) and stearic acid ($C_{18}$).

Organic compound partitions in the PM and vapor emissions from soy wax candle with additive are plotted in Figure III-28. Again, ester was the dominant species, 47% in PM and 55% in vapor phase. Cycloalkanes (14%–13%), alkane (1%–4%), alkenes (2%) and branched alkanes (1%) were also found in both PM and vapor emissions. Comparing with the analysis of the emissions from the soy wax candle without additive, higher levels of organic acid were detected in the emission from the soy wax candle with additive: 22% in PM and 11% in vapor phase, which is probably caused by the pigments and fragrances in the candles. No PAHs were detected in the emissions from the soy wax candle with additive.

Organic compound partitions in the emissions from the paraffin candle with additive (as shown in Figure III-29) are somewhat different from the emission from the soy wax candle. For the PM from paraffin candle, 76% of the extractable and elutable fraction was identified, while 24% was UCM. Alkanes became the dominant compound class in the PM emission, approximately 47.5% with smaller amounts of cycloalkanes (11.6%), ester (9.9%), branched alkanes (3.1%), and alkenes (2.6%). For the vapor-phase emission, 38% was designated as UCM. The identified organic compounds were cycloalkanes (26%), alkanes (17%), ester (12%), alkenes (5%), branched alkanes (1%). No PAH was detected in both PM and vapor emissions from paraffin wax candle with additive.

Figure III-25. Picture showing black fume from a burning candle.

Figure III-26. Picture showing black fume from a burning candle.

**Table III-4. Organic Species Detected in Paraffin and Soybean Wax Candles**

| | |
|---|---|
| Paraffin Candle with Additive | Alkane (including straight chain and branched alkanes), ester, and UCM |
| Soybean Wax Candle Without Additive | Alkane (including branched and cyclo alkanes), alkanoic acid, ester, UCM |
| Soybean Wax Candle with Additive | Alkane, alkanoic acid, ester, UCM[1] |

[1] UCM: Unidentified complex mixture.

The analysis results in Figures III-27–III-29 suggest that most of the organic compounds in the PM and vapor emissions from candle burning consist of candle component. The predominant alkanes in the paraffin candle emission are most likely the result of direct vaporization of alkane wax material and subsequent condensation into the particle phase. The presence of ester in the soy wax emission was also due to volatilization. Other compounds found in the emissions are pyrolysis products.

To further understand the formation of candle emissions, the distributions of alkanes in paraffin candles, and in both particle and vapor emissions, are plotted as a function of carbon number as shown in Figure III-30. All straight and branched alkanes are grouped by carbon number. The alkanes in paraffin candles were $C_{14}$ to $C_{40}$, with a peak at $C_{24}$. The alkanes in PM and vapor samples from burning paraffin candles have similar distributions as those in candles, except that higher concentrations of alkanes were measured at $C_{12}$. The similar distributions suggest that most alkane emissions are due to direct volatilization and recondensation of wax

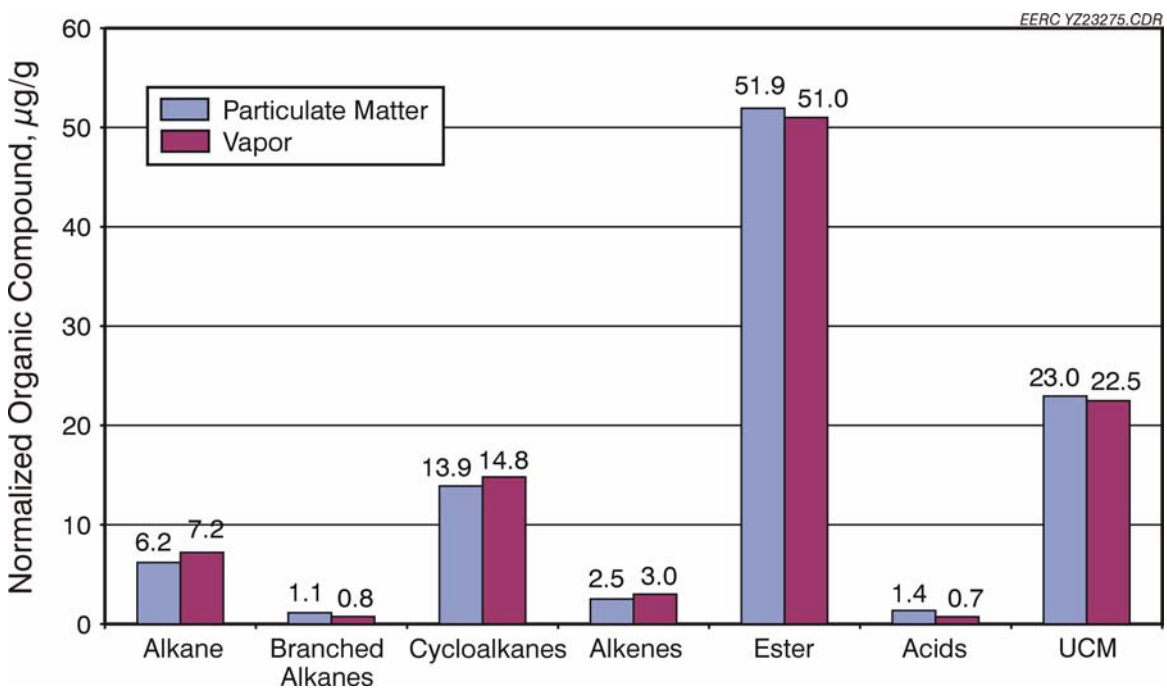


Figure III-27. Organic compound emissions from soybean wax candles without color and fragrance.

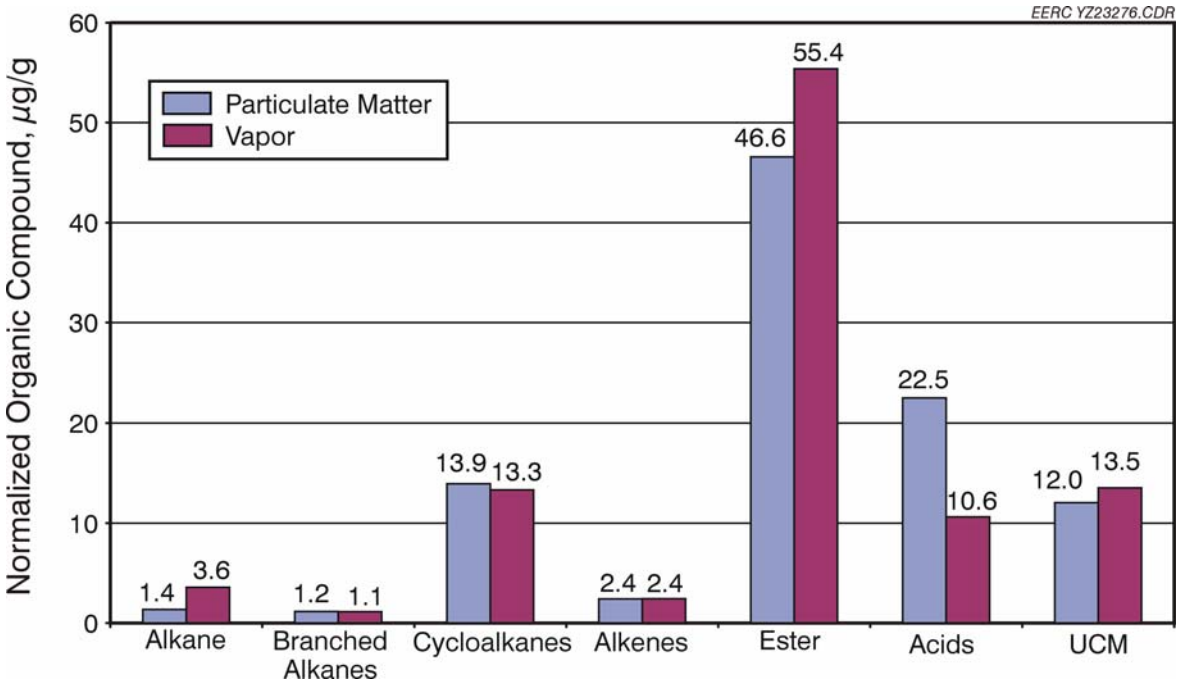


Figure III-28. Organic compound emissions from soybean wax candles with color and fragrance.

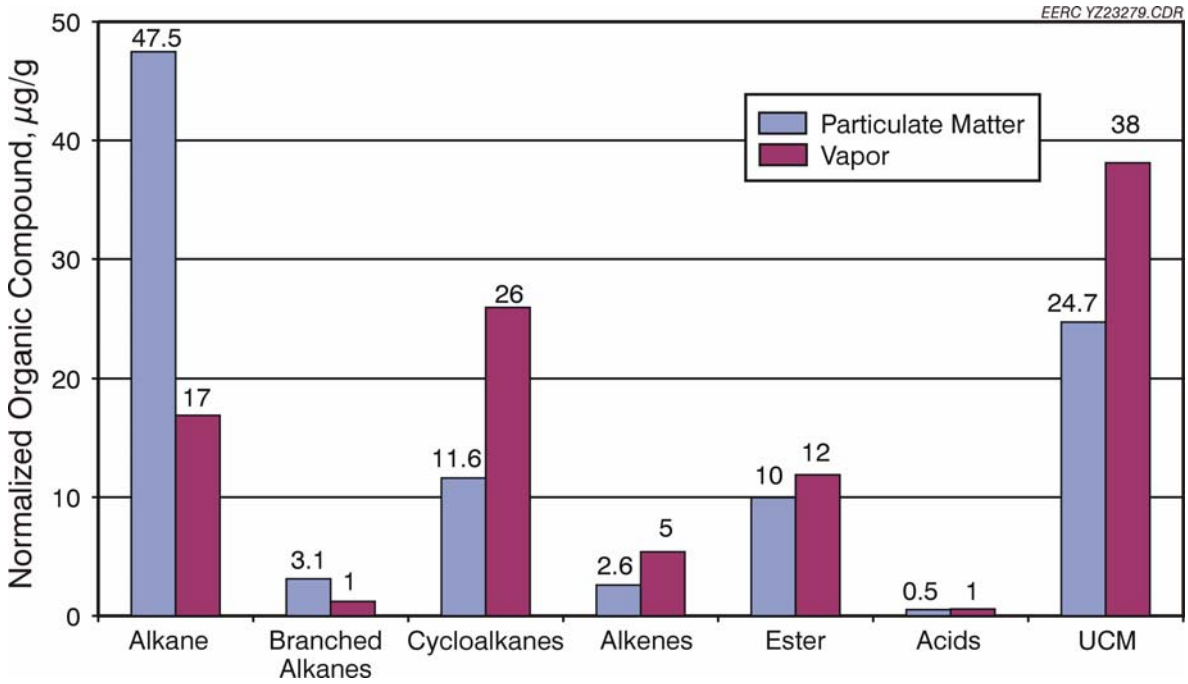


Figure III-29. Organic compound emissions from paraffin candles with color and fragrance.

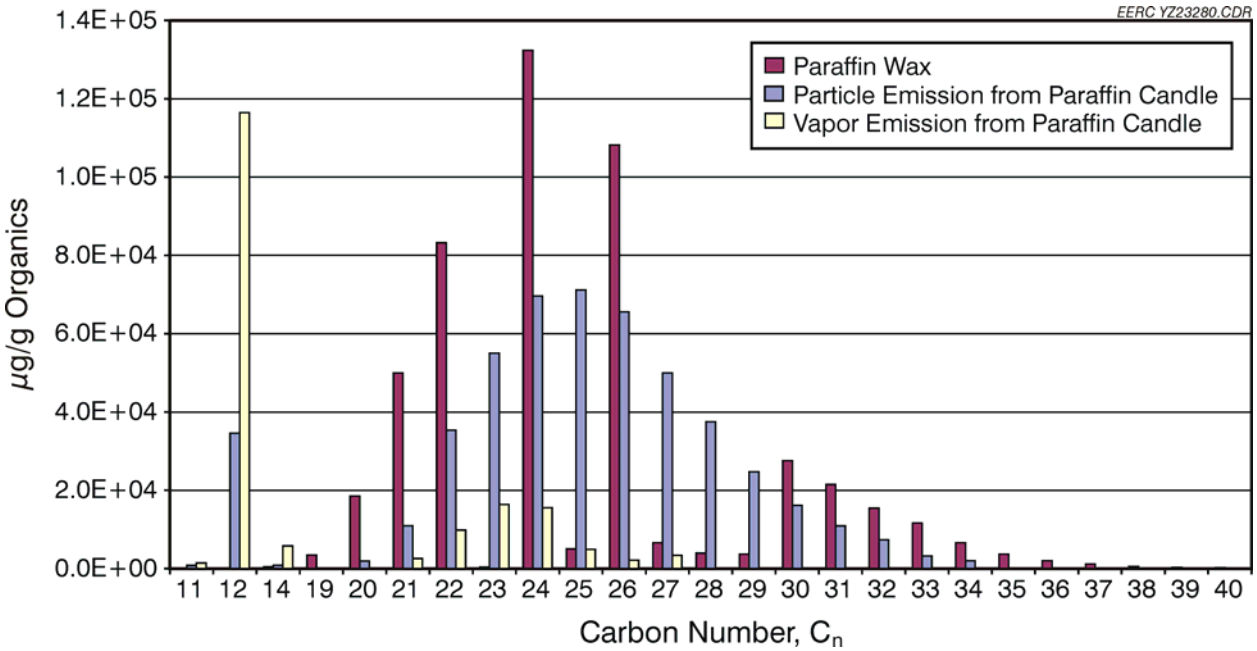


Figure III-30. Alkane distributions by carbon number for paraffin candles and their emissions.

materials. The local peaks at $C_{12}$, however, indicate that some alkanes are decomposed to low-weight molecules in candle flame. The alkane distribution in particulate emission from heavy duty diesel truck (20) is plotted in Figure III-31, showing most alkane in diesel exhaust was enriched in $C_{20}$. The differences of alkane distributions between candle and diesel emission indicated a lighter molecular structure in diesel emission than candle exhaust, and can be used as a possible trace to determine emission source.

Neither paraffin nor soy wax candles contain identified alkenes, but low levels of alkenes were found in their emissions, in the range of $C_{11}$–$C_{17}$. The distributions are shown in Figure III-32. The measured alkenes are most likely derived from alkanes that are thermally altered.

*Morphological Analysis*

A morphological analysis was conducted on the particle sample using SEM. As shown in Figure III-33, huge amounts of fine particles (much less than 1 μm) were found on the filter. These fine particles were generated from burning candles by volatilization and condensation. By comparing with the particle size distributions from SMPS measurement (Figures III-22 and III-23), it is suspected that the airborne fine particles were agglomerated with each other to form clusters when they were captured on the filter, which is a known mechanism for collecting submicron particles. A TEM image of diesel engine soot is shown in Figure III-34 (21). Both images show the same structure of chains of individual particles in nanometer size range. Although there was no significant amount of toxic materials found in the candle emissions, the ultrafine particles generated in candle burning present in high number with greater surface area than larger particles, and can reach the alveoli deep in the lungs with high deposition efficiency

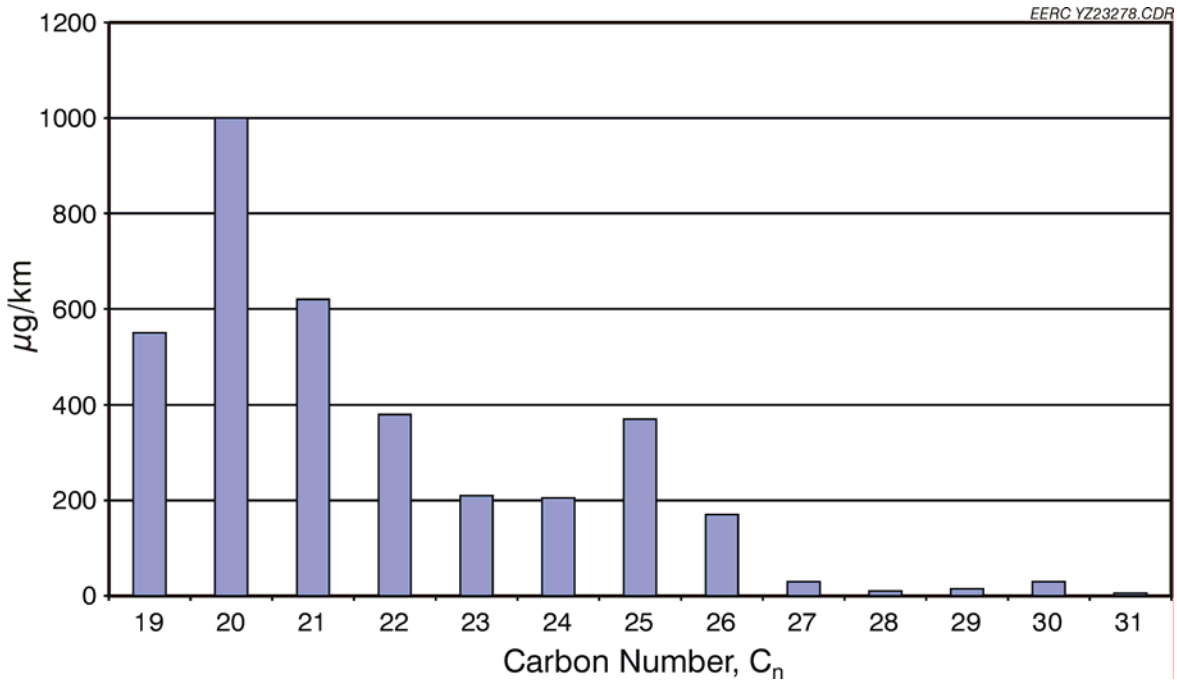


Figure III-31. Alkane distributions in particle emissions from a heavy-duty diesel truck.

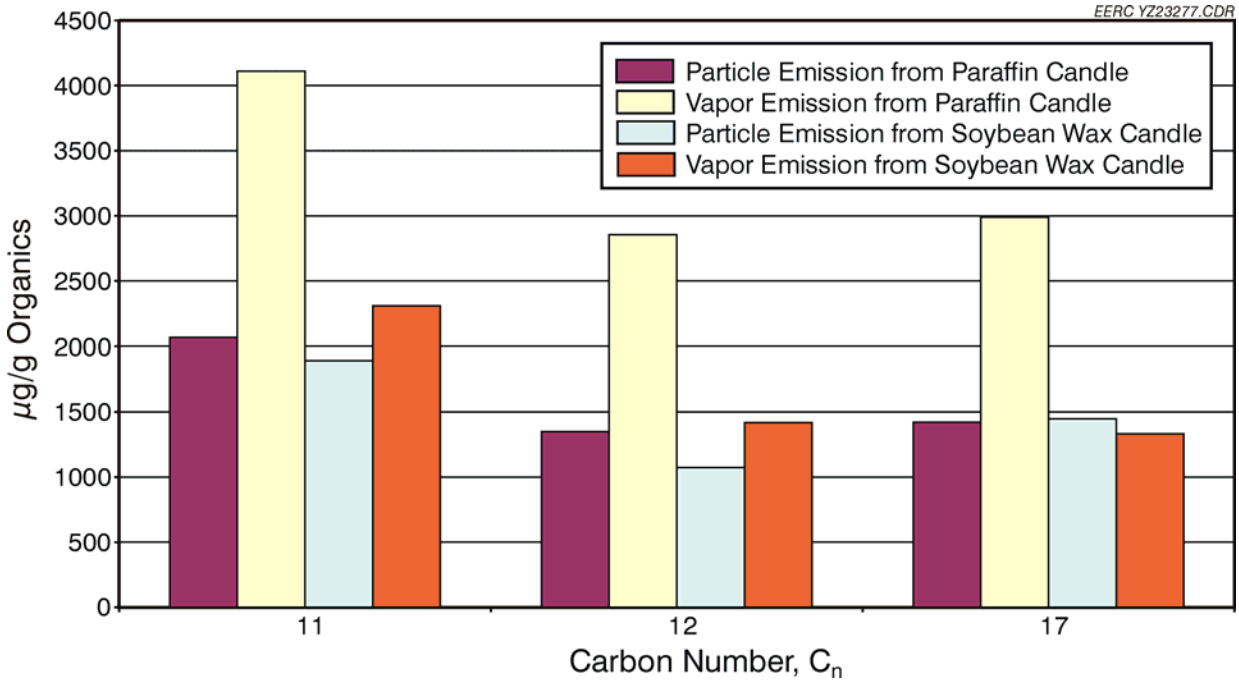


Figure III-32. Alkane distribution by carbon number for paraffin and soybean wax candle emissions.

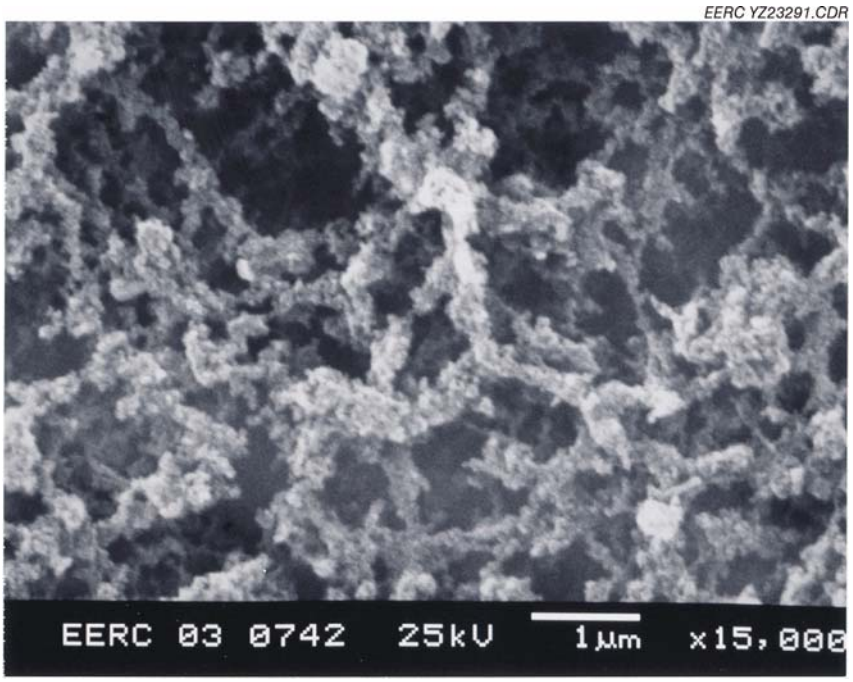


Figure III-33. SEM showing dense accumulation of fine particles on the filter.

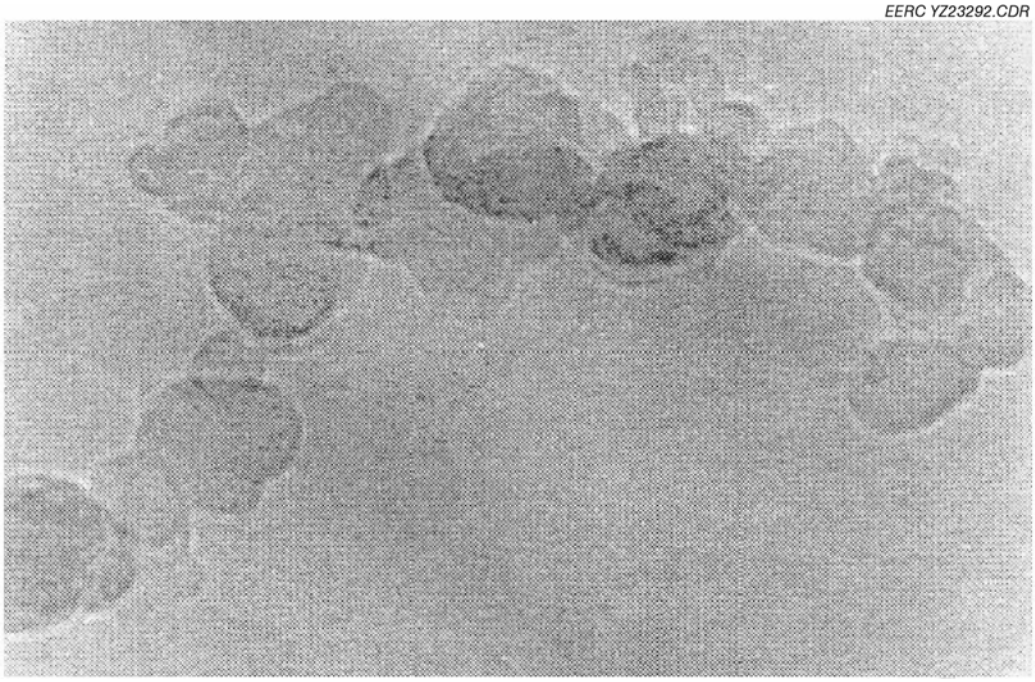


Figure III-34. TEM image (150×) of diesel soot.

of 50% (5). The deposition of ultrafine particles in airway not only induce inflammatory response which may damage tissue surface but also may move rapidly into blood stream to trigger other effects. Since ultrafine particle may be more likely to interact with cells in the lungs than those larger particles, they may be harmful regardless of specific components, or they can be a carrier to ferry toxicants deep into the lungs.

### *Conclusions*

Various candles in terms of formulation (paraffin and soy wax), additives (with and without color and fragrance), and shape (jar, pillar, and votive) were tested in a controlled environment to examine their emissions. Experimental data show burning always released significant amounts of fine particles (less than 1 μm): $10^{12}$–$10^{13}$ particles/g — paraffin candle, and $10^{11}$–$10^{14}$ particles/g — soy wax candle. Both jar and pillar type candles had stable particle emissions, while votive candles had a fluctuated pattern because of the turbulent air flow surrounding the flame.

Chemical analysis results show that most candle emissions are from vaporization and condensation of volatile wax compound combined with thermally altered by-product. Although no PAH was detected in both particle and vapor emissions from paraffin and soybean wax candles, the generated significant amounts of ultrafine particles may still be of concern to human health.

### *References*


1. Air Quality Criteria for Particulate Matter; Vols. I, II, and III; U.S. Environmental Protection Agency, 1996.

2. Dockery, D.W.; Schwartz, J.; Spengler, J.D. *Environ. Res*. **1992**, *59*, 362–373.

3. Oberdorster, G.; Gelein, R.M.; Ferin, J.; Weiss, B.; Association of Particulate Air Pollution and Acute Mortality: Involvement of Ultrafine Particles. *Inhalation Toxicology*, **7**, 111–124, 1995.

4. Oberdoster, G.; Ferin, J.; Gelein, R.; Soderholm, S.C.; Finkelstein, J.; Role of the Alveolar Macrophage in Lung Injury: Studies with Ultrafine Particles, *Environ. Health Perspect.* **1992**, *97*, 193–197,.

5. International Commission on Radiological Protection, Human Respiratory Tract Model for Radiological Protection, Report of Committee 2 of the ICRP, Oxford: Pergamon Press, 1994.

6. Long, C.M.; Suh, H.H.; Koutrakis, P. *J. Air Waste Manage. Assoc*. **2000**, *50*, 1236–1250.

7. Kamens, R.; Lee, C.T.; Weiner, R.; Leith, D. *Atmos. Environ*. **1991**, *25A*.

8. Wallace, L.A. *J. Air Waste Manage. Assoc.* **1996**, *46*, 98–126.

9. Veranth, J.M.; Smith, K.R.; Hu, A.A.; Lighty, J.S.; Aust, A.E. *Chem. Res. Toxicol.* **2000**, *13,* 382–389.

10. Knight, L.; Levin, A.; Mendenhall, C. Candles and Incense as Potential Sources of Indoor Air Pollution: Market Analysis and Literature Review. Jan 2001, EPA-600/R-01-001.

11. Van Alphen, M. Emission Testing and Inhalational Exposure-Based Risk Assessment for Candles Having Pb Metal Wick Cores. *Science of the Total Environment*, **1999,** *243/244*, 53–55.

12. Nriagu J.O.; Kim, M.J., Emission of Lead and Zinc from Candles with Metal-Core Wicks. *Science of the Total Environment* **2000,** *250*, 31–37.

13. Lau, C.; Fiedler, H.; Hutzinger, O.; Schwind, K.-H.; Hosseinpour, J. Levels of Selected Organic Compounds in Materials for Candle Production and Human Exposure to Candle Emissions. *Chemosphere* **1997**, *34*, 1623–1630.

14. Seaton, A.; MacNee, W.; Donaldson, K.; Godden, D.; Particulate Air Pollution and Acute Health Effect *Lancet* **1995**, *345*, 176–178.

15. Utell, M.J.; Frampton, M.W.; Acute Health Effects of Air Pollution: The Ultrafine Particle Hypothesis, *Journal of Aerosol Medicine*. **2000**, *13*, 4, 355–359.

16. Turpin, B.J.; Saxena, P.; and Andrews, E.; Measuring and Simulating Particulate Organics in the Atmosphere: Problems and Prospects, *Atomospheric Environment*. **2000**, *34*, 2983–3013.

17. McMurry, P.H.; Zhang, X.; Lee, C.T.; Issues in Aerosols Measurement for Optics Assessment, *Journal of Geophysical Research*. **1989**, **101**, 19189–19198.

18. Philip M. Fine, Glen R. Cass, and Bernd R.T. Simoneit, Characterization of Fine Particle Emissions from Burning Church Candles, *Environ. Sci. Technol.* **1999**, *33*, 2352–2362.

19. Barbara J. Turpin, Pradeep Saxena, Elisabeth Andrews, Measuring and Simulating Particulate Organic in the Atmosphere: Problems and Prospects, *Atmospheric Environment* **2000**, *34*, 2983–3013.

20. Rogge, W.F.; Hildemann, L.M., Mazurek, M.A., Cass, G.R., Simoneit, B.R., *Envion. Sci. Technol.* **1993**, *27*, 1892.

21. Locker, R.J.; Gunasekaran N.; Sawyer, C.; Diesel Particulate Filter Test Methods, SAE 2002 World Congress, Detroit, Michigan March 4–7, 2002.